The T cell senescence in breast cancer

Thesis Submitted in Accordance with The Requirements of The University of Liverpool and Chulalongkorn University for The Degree of Doctor in Philosophy

by

Mr. Sikrit Denariyakoon

Date 7 July 2023

The T cell senescence in breast cancer

Abstract

Background: The cancer-immune cell crosstalk is a common immune-evasion mechanism of cancer. This crosstalk can result in epigenetic changes in immune phenotypes to accelerate tumor growth and metastasis. Senescent T lymphocytes are formed during T cell differentiation, and are recently described as one of the dysfunctional T cells in cancer. In breast cancer, estrogen does not only regulate normal physiology in females, but is also involved in cancer development and cancer treatment. It may also attenuate senescent phenotypes, and increase DNA damage in several cell-lines. This thesis therefore examined for the presence of senescent T lymphocytes in breast cancer patients, the effects of breast cancer on epigenetic changes in circulating immune cells, and the effects of estrogen hormones on senescent T lymphocytes.

Methods: The in-vitro co-culture of cancer sera and normal leukocytes were examined for the methylation level by COBRA Alu technique. Senescent T cells were examined for β-galactosidase, CD28, and CD57 in breast cancer patients by flow cytometry technique. In addition, cellular senescence models were created by adding etoposide. Addition of estrogen hormones were performed in cellular senescence models, and DNA damage markers, including phospho-γH2AX, p53, and p21 were examined by flow cytometry. The statistical significance was considered as p-value < 0.05. The analysis was performed using IBM SPSS software.

Results: The breast cancer serum was found to epigenetically modify to normal leukocytes. The aging-associated epigenetic changes were correlated with cancer prognosis. In clinical samples, the non-exhausted senescent phenotypes were correlated with the progression of age, and the increase in these phenotypes was found in breast cancer patients. Moreover, these senescent phenotypes were prematurely presented in breast cancer patients. In cellular senescence models, the supplement of estrogen improved senescent phenotypes, and seemed to have DNA damage attenuation effects.

Conclusion: The Alu hypomethylation in the in-vitro models seemed to be associated with early progressive disease, and the hypomethylated PBMCs might relate to senescence phenotypes. The presence of non-exhausted senescent T cell was found in breast cancer patients, and seemed to increase in metastatic setting. The supplement of E2 could attenuate the senescent phenotypes in cellular senescence models.

ACKNOWLEDGEMENT

I would like to acknowledge my advisors, Professor Carlo Palmieri, Professor Steven Edwards, Dr Athina Giannoudis University of Liverpool, and Professor Apiwat Mutirangura, Chulalongkorn University, who helped develop the research conceptualization and insightful guidance. Their advice carried me through the accomplishment of this study. I would also like to thank Dr Athina Giannoudis, Institute of Systems, Molecular and Integrative Biology, University of Liverpool, for her constructive advices in conducting the cellular and molecular experiments. I would like to thank Dr Charoenchai Puttipanyalears, Chulalongkorn University, for his advice on molecular and protein works. I would like to thank Professor Nattiya Hirankarn and Assistant Professor Pokrath Hansasuta, Faculty of Medicine, Chulalongkorn University, for helpful advices on immunological studies.

In particular, I would like to express my sincere gratitude to Mr Kris Chatamra, Queen Sirikit Centre for Breast Cancer, King Chulalongkorn Memorial Hospital, who introduced scientific philosophy into my career pathway. This initiation develops my interest in pursuing the Ph.D. project. Moreover, I am grateful to thank my colleagues for understanding the significance of research conducting and providing their support. And I would like to give my special thanks to my family for their continuous support and understanding of my difficult time.

Importantly, I must thank the participants who contributed their data. Without these invaluable resources, the significance of this study could not be completed.

Thanks to the scholarship from Graduate School, Chulalongkorn University and Faculty of Medicine, Chulalongkorn University, and the National Science and Technology Development Agency (FDA-CO-2561-8477-TH).

Sikrit Denariyakoon

TABLE OF CONTENTS

CHAPTER 2 RESEARCH METHODOLOGY

LIST OF TABLES

Tables Page

LIST OF FIGURES

Figures Page

ABBREVIATIONS

7-AAD	: 7-amino-actinomycin D
ATM	: Ataxia-telangiectasia
CD	: Cluster of differentiation
CDK6	: Cyclin-dependent kinase 6
cDNA	: Complimentary DNA
CHK2	: Checkpoint kinase 2
CMA	: Chaperon mediated autophagy
CMV	: Cytomegalovirus
COBRA	: Quantitative combine bisulfite restriction analysis
Con A	: Concanavalin A
cPLA2α	: Cytosolic phospholipase A2α
cTECs	: Cortical thymic epithelial cells
CTL	: Cytotoxic T lymphocyte
CTLA-4	: Cytotoxic T lymphocyte associated protein 4
DAPI	: 4′,6-diamidino-2-phenylindole
DMEM	: Dulbecco's Modified Eagle's Medium
DMSO	: Dimethyl sulfoxide
DNA	: Deoxyribonucleic acid

DNMT : DNA methyltransferase

DNMT1 : DNA methyltransferase1

DNMT3a : DNA methyltransferase3a

DNMT3b : DNA methyltransferase3b

E2 : 17β-estradiol

EDSB : Endogenous DNA double-strand breaks

EDTA : Ethylenediaminetetraacetic acid

ELISA : Enzyme-linked immunosorbent assay

Eomes : Eomesodermin

Foxp3 : Forkhead box P3

FSC : Forward scatter

GFP : Green fluorescent protein

HAT : Histone acetyltransferase

HDAC : Histone deacetyltransferase

HIV : Human immunodeficiency virus

HMGB-1 : High-mobility group box-1 protein

HR : Homologous recombination

IL : Interleukin

JNK : Janus kinase

LAG-3 : Lymphocyte activation gene 3

LB : Luria-Bertani

LINE-1 : Long intersperse nucleic elements 1

lncRNAs : long non-coding RNAs

LPS : Lipopolysaccharides

MAPK : Mitogen-activated protein kinase

MDSCs : Myeloid-derived suppressor cells

MHC : Major histocompatibility complex

miRNAs : microRNAs

mRNA : messenger RNA

mTECs : Medullar thymic epithelial cells

mTOR : Mammalian target of rapamycin

NaCl : Sodium Chloride

NHEJ : Non-homologous end joining repair

NK : Natural killer

PBMC : Peripheral blood mononuclear cells

PBS : Phosphate buffered saline

PCR : Polymerase chain reaction

PD1 : Programmed cell death protein 1

PHA : Phytohemagglutinin

PMA : Phorbol myristate acetate

PTK7 : protein tyrosine kinase 7

RIND : Replication-independent

RNA : Ribonucleic acid

RPMI : Roswell Park Memorial Institute

RTEs : Recent thymic emegrants

SASP : Senescence associated secretory phenotypes

SA-β-gal : Senescence associated β-galactosidase

SINE : Short intersperse nucleic elements

SSC : Side scatter

T-bet : T-box expression in T cells

TCF-1 : T cell factor 1

TCM : Central memory T cell

TCR : T cell receptor

TEM : Effector memory T cell

TEMRA : Terminally effector memory T cells with CD45RA expression

TGF-β : Transforming growth factor β

Th1 : T helper 1

Th17 : T helper 17

Th2 : T helper 2

TIGIT : T cell immunoreceptor with immunoglobulin and ITIM domains

Tim-3 : T cell immunoglobulin domain and mucin domain protein 3

TNF-α : Tumor necrosis factor α

TRM : Tissue resilient memory T cell

TSC : Tuberous sclerosis protein

TTP : Time to progression

TVM : Virtual memory T cell

γH2AX : Members of histone H2A

CHAPTER 1 INTRODUCTION

1.1 Background

Breast cancer is the most globally prevalent cancer and the leading cause of death in females (1). After the introduction of radical mastectomy, rates of mortality and recurrence were reduced. By the 1980s, other therapeutic advances improved oncologic outcomes. These included contributions from screening protocols, the improvement of chemotherapy, targeted therapy and, radiotherapy (2). To date, the molecular understanding of cancer biology provides more specific treatments and more precise prognosis. Breast carcinoma arises in ductal epithelium or lobules of mammary glands, and intraductal growth of atypical cancerous cells increases capability for invasion and metastasis (3). Sometimes, this adaptation occurs rapidly and leads to an aggressive clinical presentation. This diversity of cancer biology results in different disease prognoses. Recently, there have been attempts to classify breast cancer subtypes in terms of biology and treatment direction. Commonly, there are 4 subtypes of breast cancer used as prognostic factors and predictive factors. The subtypes include luminal-A; luminal-B; Her-2 enriched and triple negative breast cancer (4). These classifications predict the responses of antihormonal treatment and targeted therapy (3, 5, 6).

Breast cancer-associated immune cells are considered to be important cells in tumor biology. The infiltrating immune cells result from self-immune responses to the transformed cells. In breast cancer, there are immune cell-enriched tumors and immune cell-deserted tumors, which demonstrate different biologies (7). Hence, the presence of tumor-infiltrating immune cells is also used to classify breast cancer biology. Many researchers use the presence of tumor infiltrating immune cells to classify triple-negative cancer subtypes (8). Lehmann et al. characterized the triple-

negative subtype into six further subtypes (9). One of those subtypes was an immunomodulatory subtype which had lymphocyte and immune signaling-enriched features. This subtype had favorable prognostic outcome and was predicted to respond to immune checkpoint inhibitors (9). Moreover, increased infiltrating immune cells may benefit survival outcomes and complete pathological responses (10). Recently, a study reported that above 10% of infiltrating immune cells indicated increased overall survival rates (11). Moreover, the increase of tumor infiltrating lymphocytes after neoadjuvant chemotherapy elicited better survival outcomes (12). However, previous results demonstrated heterogeneity of these associations, and the infiltration of suppressive immune cells was found to impair the survival outcome (13). These observations indicate cancer immune cell crosstalk. Moreover, this crosstalk affects the circulating immune cell changes in breast cancer (14). The discovery of dysfunctional T cells may help explain the occurrence of cancer immune evasion (15, 16). The inducible dysfunctional immune cells arise because of the plasticity of immune cells which is dependent on epigenetic machinery (17). As a result, changes in genome-wide hypomethylation of blood cells were found prior to the symptoms developed in a nested case-control study (18). From this, cancer-induced epigenetic changes of immune cells may occur via cell-cell contact or by non-cell contact mechanisms (19). Eventually, the expansion of suppressive immune cells and dysfunctional immune cells worsens oncological outcomes of breast cancer (20).

1.2 Cancer immunology and cancer-immune cell crosstalk

Self-immune responses are the self-protective systems that recognize and respond to cancer development. Innate and adaptive immune responses eliminate the tumor cells collaboratively. Dendritic cells are the important players in connecting between innate and adaptive immune responses. The most effective killer cells are cytotoxic T cells. The endeavor to prime cancer-specific T cells is the ultimate key to eliminate cancer cells. After dendritic cells recognize the foreign antigens, the naïve T cells which locate in secondary lymphoid organs are selectively primed from activated dendritic cells. The cancer-specific T cells are activated and the antigen-containing tumor MHC class I molecules are subsequently targeted by antigen-specific T cells (21, 22). Although cancer-specific T cells work extensively, some immune cells were blinded from tumor cells. The remaining cancer cells develop immune tolerance, which is the major cause of cancer development and metastasis. Several immune evasion mechanisms have been studied, such as immune checkpoint molecule expression, immune suppressive cells accumulation, and immune suppressive molecules secretion (23, 24). These consequences are resulted from cancer-stromal cell and immune cell crosstalk which introduce effector immune cell dysfunction, and lead to cancer growth (25, 26).

Growing cancer cells can produce a compatible microenvironment and tolerate immune systems. These interactions are used as cancer-immune cell crosstalk. Tumor microenvironments are organized differently from normal tissues. Neovascular structures are disorganized and impaired autonomic responses to fully feed tumor cells and support tumor survival. After the tumor cells grow, they produce mediators to gather several cell types to facilitate tumor viability. These stromal cells consist of mesenchymal stem cells, cancer-associated fibroblasts, neurons, and adipose tissue, etc., which have been found to promote cancer survival

(27). Moreover, immune cells and tumor cells interact with complex relationships, which are both pro-tumor and anti-tumor roles (28-30). In pro-tumor roles, these suppressive immune cells or inhibitory immune cells are trapped in cancer stroma, and were found to counteract or blind immune systems by releasing several mediators to impair circulating immune cells (29, 31).

1.3 Breast cancer and immune crosstalk result in global methylation changes in peripheral immune cells

According to cancer-specific T cells activation, after T cell priming in secondary lymphoid organs, the effector T cells target to eradicate tumor cells (21). A study showed that cancer cells and cancer-associated stromal cells produced mediators that promote immune evasion (32). Some of these mediators epigenetically modified gene expression in T cells and caused alteration of T cell phenotypes. Epigenetic changes of immune cells can result in immune plasticity and differentiation (17). As a result, the global methylation changes in blood or breast cancer-associated immune cells has been studied as cancer signatures in terms of cancer detection (19), however, the association of global DNA methylation levels and breast cancer risk were inconclusive because of heterogenous measurement techniques, sample types, and study designs (19, 33). The co-culture of breast cancer cell line demonstrated the global methylation changes in peripheral immune cells, but in cancer, circulating mediators from breast cancer cells may cause complex methylation changes of immune cells in breast cancer patients. Changes in immune cells after exposure to breast cancer serum has not been investigated, and so this is one aim of the study in this thesis, whose details are described in chapter 3.

1.4 DNA damage accumulation causing epigenetic changes and immune senescence in breast cancer

After DNA damage occurs, cell cycle checkpoints are activated to allow the completion of DNA repair, and the remaining steps in the cell cycle will continue (34). However, demethylation and deacetylation occur during the DNA damage. Sometimes, apoptosis is not triggered by incorrect DNA repair or concealed DNA damage, and the accumulated mutant DNA lesions lead to oncogenesis or genomic instability (35-37). Genomic instability is one of the hallmarks of cellular senescence, which results from the accumulation of DNA lesions and global hypomethylation (35-37). Moreover, global hypomethylation has been used to describe the normal aging pattern (35, 36). For decades, the methylation level of transposons, which intersperse among human chromosomes, has been used as surrogate markers of global methylation. For instance, the *Alu* elements, active elements of short intersperse nucleic elements (SINE), were found to be hypomethylated in the elderly (38). Concomitantly, studies have shown that Alu elements hypomethylation was related to aging and some chronic diseases (39, 40). Furthermore, the increase of methylation of Alu elements was found to protect genomes from DNA damaging agents (41). Cellular senescence is associated with the accumulation of DNA damage and genomic instability, and the senescent T cells are also prematurely generated by the DNA damage mechanism (42). Premature senescent T cells are found in autoimmune diseases and cancer (43, 44) In cancer, previous studies supported the evidence of cancer-inducing senescent phenotypes of T cells, including lung, head and neck, multiple myeloma, and breast cancer, but the senescent T cells and exhausted T cells were intertwined, and checkpoint inhibitors can restore the exhausted T cell function, but not senescent T cells (45, 46). Furthermore, the presence of these T cells was associated with poor survival

outcomes, but the characterization of non-exhausted T cells senescence, which exclude exhausted T cell lineage, is not well understood in breast cancer patients. A second aim of this thesis was to characterize these cells and these experiments are described in chapter 4.

1.5 Anti-senescence treatments

Several approaches have shown convincing data to induce anti-senescence effects (47, 48). There are common pathways that may be targeted to alleviate senescence phenotypes and genetic instability including insulin-like signaling pathway, target of rapamycin (mTOR), sirtruin, and antioxidants (49). In animal models, there were few compounds shown to increase the lifespan including rapamycin, estradiol, metformin, and sirtuin activators (50). However, estradiol seemed to have antisenescence effects and immune modulation effects (47). Therefore, the use of estradiol to alleviate the T cell senescence was another aim in this thesis, and details of this approach are described in chapter 5.

1.6 Overall aims of this thesis:

Cancer-immune cell crosstalk is an important factor that may result in immune-evasion in cancer, and support cancer spreading. Changes in the functions of immune cells, perhaps as a result of epigenetic changes induced via factor(s) released by cancer cells to provide phenotypic plasticity, may include: T cell anergy; T cell exhaustion and T cell senescence. The overall aim of this thesis is to determine the proportion of non-exhausted T cell senescence in breast cancer patients and to improve the senescence phenotypes of senescent T cells.

1.7 The specific aims and hypothesis:

1. Explore if cancer serum, which may contain systemic factors originating from the tumor, can change the global methylation profile of PBMCs using Alu element as a marker: previous studies have shown the association of this feature with cancer and ageing. Therefore, our hypothesis is that breast cancer serum can alter Alu elements methylation profile of PBMCs.
2. Characterize non-exhausted senescent T cells in breast cancer patients. Senescent T cells are found to be increased in breast cancer patients and further elevated with advanced age. Since these cells differ from exhausted T cells, our focus is on non-exhausted senescent T cells. Our hypothesis is that non-exhausted senescent T cells are a different entity from exhausted T cells lineage, and are increased in breast cancer patients.
3. Explore the role of estradiol to experimentally attenuate T cell senescence *in-vitro*. We hypothesize that estradiol can improve DNA damage levels and senescent phenotypes in senescent T cell model.

1.8 Objectives

1. Measure the levels of Alu element methylation in healthy PBMCs after incubation with bovine, normal or cancer serum for 48 h.
2. Determine the proportions of CD28-, CD28-CD57-, CD28-CD57+ and β-galactosidase hi+ cells by flow cytometry in PBMCs with PD1- of breast cancer patients that are stratified by age compared to healthy volunteers.
3. Measure DNA damage markers, senescent phenotypes, and function in the senescent T cell model after incubation with estradiol following the exposure to DNA damaging agent.

1.9 Experimental design

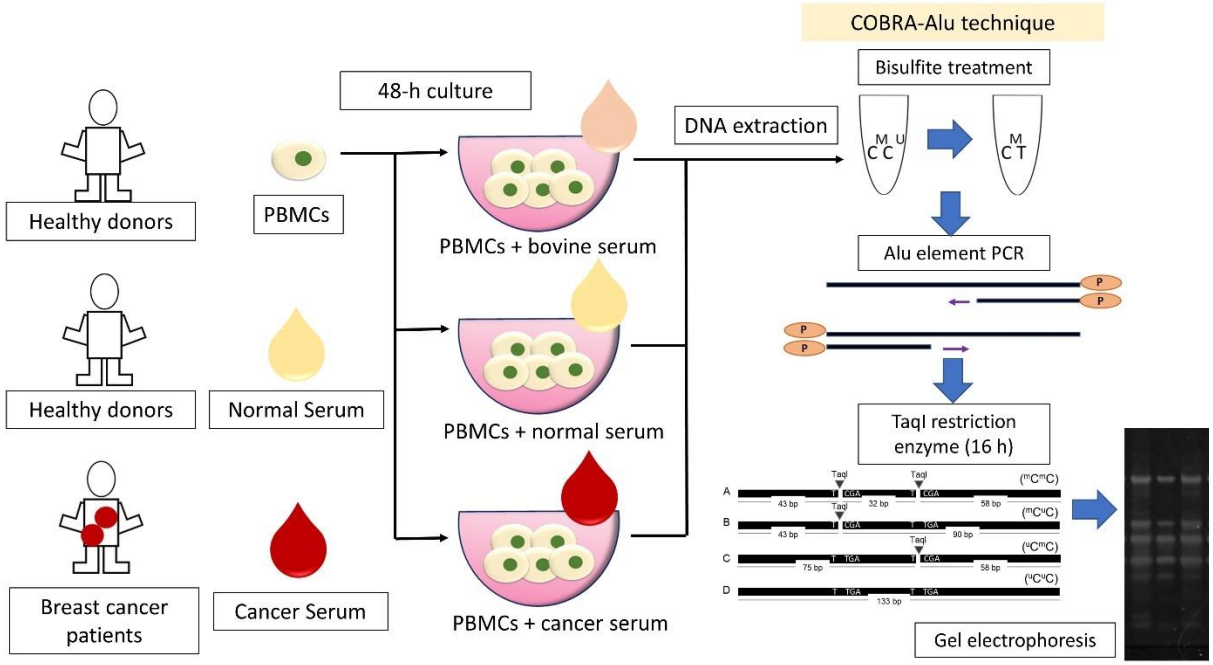

Figure 1.1 The experiment to measure the levels of Alu element methylation in healthy PBMCs after incubation with bovine, normal or cancer serum for 48 h. The figure shows 3 experimental conditions including healthy PBMCs incubated with bovine serum, healthy PBMCs incubated with normal serum and PBMC incubated with cancer serum, then these PBMCs were extracted for DNA at 48-h after the incubation. These DNA pellets were subjected to bisulfite conversion, Alu element amplification by PCR, and Taq1 restriction enzyme incubation, respectively. Finally gel electrophoresis was performed to identify DNA bands and measure band intensity.

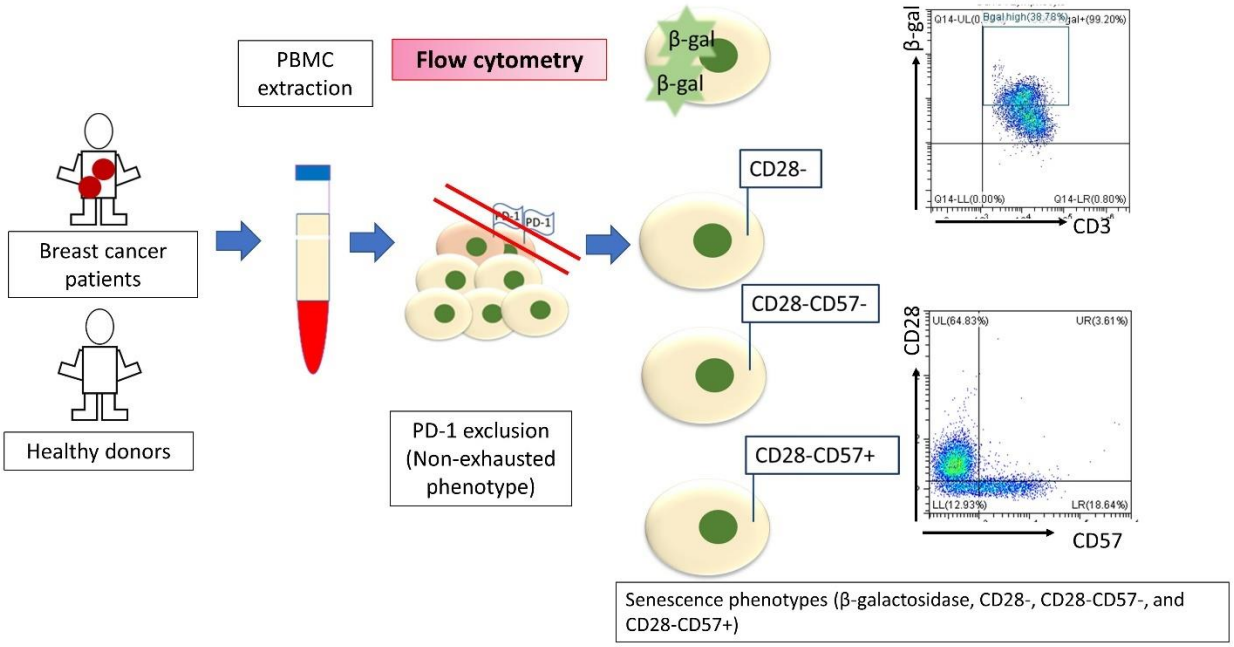

Figure 1.2 The experiment to determine proportions of CD28- and β-galactosidase hi+ cells by flow cytometry in PBMCs with PD1- of breast cancer patients that are stratified by age compared to healthy volunteers. The figure shows 2 groups of samples: PBMCs from breast cancer patients and healthy participants, and these samples were subjected to exclude exhausted phenotype by PD-1 staining. The non-exhausted T cells were determined their senescence phenotypes by markers including β-galactosidase signals, CD28-, CD28-CD57-, and CD28-CD57+, and flow cytometry was performed to determine these population.

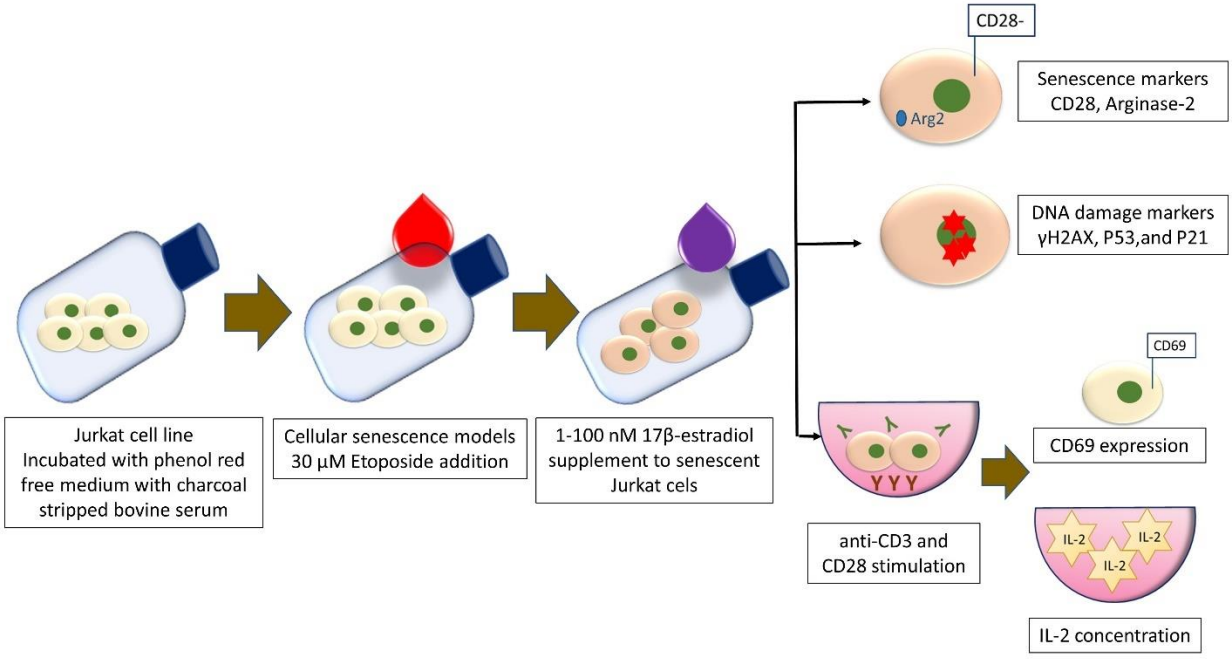

Figure 1.3 The experiment to measure DNA damage markers, senescent phenotypes, and function in the senescent T cell model after incubation with estradiol following exposure to DNA damaging agent. The figure shows phenol-free media incubation of Jurkat cells before addition of 30 μM etopositde, and the supplement of 17β-estradiol was performed. These Jurkat cells were measured for CD28 expression and arginase-2 expression regarding senescence phenotypes, and γH2AX, p53, and p21 expression regarding DNA damage levels. Moreover, these Jurkat cells were subjected to antiCD3 and antiCD28 stimulation to measure CD69 expression in Jurkat cells, and the supernatants were measured for IL-2 concentration.

CHAPTER 2 RESEARCH METHODOLOGY

2.1 Cell lines and their characteristics

1. Jurkat cell line

The human leukemic cell line or Jurkat E6.1 cell line was kindly provided by hematology and leukemia research group, University of Liverpool, UK. The Jurkat cells were regularly evaluated their phenotypes and bacterial contamination. These cell lines are clones of the Jurkat-FHCRC cell line which was originally isolated from the peripheral blood of a 14-year-old male with acute T-cell leukemia. They are used as models for the biology of peripheral T lymphocytes and Jurkat cells E6.1 express CD3, CD4, CXCR4 (51).

2. T47D cell line

The T-47D cell-line was purchased from ATCC, USA. The T47D cells were regularly evaluated bacterial contamination. T-47D cells are cell lines of invasive ductal carcinoma originating from the pleural effusion of 54-year-old female patient with pleural metastasis. Their phenotypic characteristics include expression of androgen receptor, estrogen receptor and progesterone receptor (52).

2.2 Methods

2.2.1 Cell culture

Jurkat cells were cultured in Roswell Park Memorial Institute (RPMI) 1640 medium supplemented with 10% fetal bovine serum, 2mM L-glutamine, plus 100 U/ml penicillin and 100 μg/ml streptomycin. The medium was replaced every 48-72 h. The viability was assessed by trypan blue staining and usually > 90%.

T47D cells were cultured in RPMI 1640 medium supplemented with 10% fetal bovine serum, 2mM L-glutamine, plus 100 U/ml penicillin and 100 μg/ml streptomycin. The medium was changed every 48-72 h. Warm 1X phosphate buffered saline (PBS) was used to wash the cells twice. The incubation with 0.25% Trypsin-EDTA for 2 min was used to detach these adherent cells when confluency reached 85-100 %.

Peripheral blood mononuclear cells (PBMCs) were cultured in RPMI 1640 medium supplemented with 10% fetal bovine serum or human serum as described in the text.

2.2.2 Cancer sera induced changes in Alu element methylation of normal PBMCs

2.2.2.1 Participants

Sample size calculation

The pilot study of 4 cases of Alu elements methylation in cancer group and 2 cases of normal group. The mean of Alu element methylation is higher in normal serum group as shown in Figure 2.1.

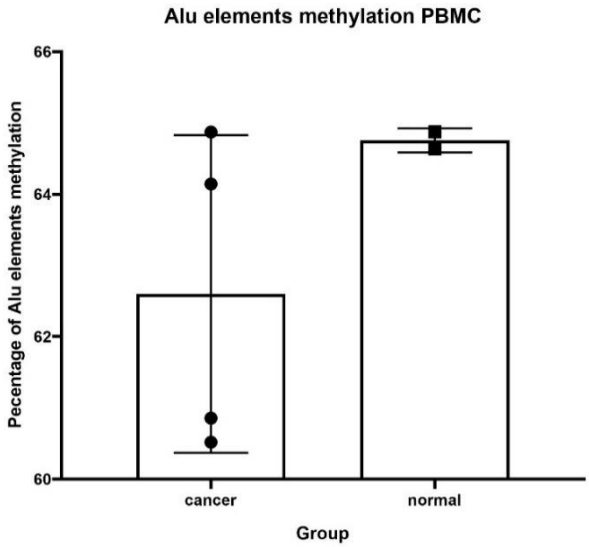

Figure 2.1 This bar shows the percentage of Alu element methylation between normal and cancer PBMCs.

The mean Alu element methylation in cancer serum group = 62.6%, while in normal serum group =64.76%. The standard deviation = 2.23 and 0.17 respectively. Sample size calculation formula:

N $= (\sigma^2_A + \sigma^2_B)(\frac{z1-\alpha+z1-\beta}{\mu A-\mu B})^2$

σ = standard deviation

μ = mean

Z1-α = type I error, α = 0.05

Z1-β = power , 1-β = 0.80

N = 7 each group

The sample size calculation was 7 samples.

The recruitment of 16 metastatic breast cancer participants and 16 healthy participants with normal mammographic results was performed at Queen Sirikit Centre for Breast Cancer from December 2020-May 2021. The follow-up data were updated until the progressive disease was noted radiographically or the 90-day follow-up duration was reached because the 90-day duration was the recommended duration as expert consensus to evaluate clinical responses (53, 54). Time to progression was calculated from the sample retrieval date to the disease progression date. The exclusion criteria included other chronic medical diseases, other malignancies, and a history of blood transfusion within 3 months. A written informed consent was obtained from each participant. The demographic data and medical records were retrieved from King Chulalongkorn Memorial Hospital database. The study was approved by the Ethics Committee of the Faculty of Medicine, Chulalongkorn University (IRB no. 789/63).

2.2.2.2 Preparation of peripheral blood mononuclear cells (PBMCs)

Blood was collected be venipuncture from patients or healthy controls into tubes with EDTA as anti-coagulant and kept at 4^{o}C until cell isolation (usually 6 h). The blood was diluted with RPMI 1640 medium in a ratio of 1:1 in 15 ml conical tubes and gently mixed, layered onto Lymphoprep™ (Stemcell™, UK) in 15 ml conical tubes and then centrifuged at 500g for 30 min with the brake-off. The interface PBMC layer was carefully collected and placed in 15 ml conical tubes containing 5 ml of 37°C RPMI 1640 medium and centrifuged at 500g for 10 min. RPMI 1640 medium was used to wash the cells twice and 0.4% trypan blue was used when manually determining cell counts in hemocytometer. A total of four corner squares was counted and calculated as the following formula. Cell concentration(cells/ml) = total viable cells x $10^4/2$. The isolated PBMCs were

maintained in a 6-well-plate containing RPMI 1640 medium in a humidified 5%CO_2 incubator at 37^{o}C.

2.2.2.3 Preparation of human sera

Blood was collected by venipuncture into clot blood tubes After collecting, samples were incubated at room temperature for 30 min, and kept at 4°C until processing. The samples were centrifuged at 500g for 5 min, and the serum was harvested and stored at -20^{o}C until use.

2.2.2.4 Culture of PBMCs and cancer serum

PBMCs were cultured with cancer serum to determine if this resulted in methylation changes in Alu elements. One triplicated experiment used samples from a single volunteer and experimental conditions. Three experimental systems were set up. The first condition was PBMCs and bovine serum, the second was PBMCs and normal serum and the third was PBMCs and cancer serum. RPMI 1640 medium supplemented with 20% serum was placed in a 6-well plate and 5 x 10^5 PBMCs (2.5 x 10^5 cells/ml) were added to triplicate wells. The culture well plates were maintained at 37^{o}C in a humidified atmosphere with 5% CO_2 incubator for 48 h.

After 48-h culture, the PBMCs were enumerated and assessed for viability by trypan blue exclusion assay under light microscope. The cells were collected in 1.5 ml Eppendorf tubes and centrifuged 500g at 16^{o}C for 10 min. The supernatant was discarded and the cell pellets were subjected to DNA extraction.

2.2.2.5 Measurement of methylation of Alu elements

The PBMC pellets from above were lysed by cell lysis buffer II (0.75 M NaCl, 0.024M EDTA at pH 8) with 10% sodium dodecyl sulfate (Sigma-Aldrich, USA) and 20 mg/ml proteinase K (Usbio, USA). Cell lysates were incubated in a 37°C water bath overnight. Subsequently, 0.5 ml of phenol-chloroform was added and samples were vortexed and centrifuged at 10,000 g for 5 min. The samples separated into 3 layers and the top layer fluid was collected carefully and added to 0.5 ml of 100% ethanol and 0.25 ml of 10M ammonium acetate. The samples were mixed and centrifuged at 10,000 g for 5 min. The supernatant was discarded and the pellet was washed with 0.5 ml of 70% ethanol, centrifuged at 10,000 g for 5 min and the supernatant was discarded. The pellet was air dried and then dissolved by 30-50 µl of distilled water. The DNA concentration was measured by Nanodrop spectrophotometer.

DNA methylation was determined in 500 ng of DNA samples using the EZ DNA methylation GoldTM kit (Zymo Research, USA) and the manufacturer's instructions. Briefly, CT conversion reagent and washing buffer were prepared and 130 µl CT conversion reagent was added to 20 µl DNA and mixed. The tube was placed in a thermal cycler and incubated at 98°C for 10 min, 64°C for 2.5 h and held at 4°C for up to 20 h. Afterwards, 600 µl M-binding buffer was added and washed through Zymo-Spin™ IC column. Subsequently, the samples were added to 200 µl M-desulphonation buffer and washed through the column. Finally, the samples were eluted with 10 µl M-Elution Buffer and stored at -20°C until use.

Quantitative Combined Bisulfite Restriction Analysis for Alu elements (COBRA Alu)

One microliter of bisulfited DNA was subjected to 45 cycles of PCR using Alu elements forward primer (5'-GGYGYGGTGGTTTAYGTTTGTAA-3') and Alu-Reverse primer (5'-CTAACTTTTTATATTTTTAATAAAAACRAAATTTC ACCA-3') at an annealing temperature of 57 ^{o}C to generate 133 bp amplicons. The amplified PCR was digested by 2 units of Taq1 (Thermo Scientific, USA) endonuclease in NE bufferIII at 65 ^{o}C overnight (12-16 h). The PCR products were visualized by 8% polyacrylamide gel electrophoresis and stained with SYBR green (SYBR® Green JumpStart™ *Taq*ReadyMix™, Sigma-Aldrich, USA). After incubation with SYBR solution, the gels were visualised with epiblue light. Five bands were identified intensity analysis by performed using a phosphor imager and Image Quant Software (Molecular Dynamics, GE Healthcare®, Slough, UK)

Figure 2.2 The restriction sites of methylated CpG in COBRA Alu. The figure shows methylated restriction sites which were cut by Taq-I enzyme: 2 unmethylated sites (A), one unmethylated site (B, C) and 2 methylated sites (D).

The percentage of methylated Alu elements detected by the COBRA Alu technique, was calculated after measuring the intensities of PCR products generated after addition of Taq1 restriction enzyme, which cuts methylated cytosines, as shown

in Figure 2.2. The intensity of each band determined the abundance of amplicons. The intensity was divided by the length of DNA base pair fragments to become the amount of each amplicon: 133/133=V($^{u}C^{u}C$), 58/58=W($^{m}C^{m}C$ and $^{u}C^{m}C$), 75/73=X($^{u}C^{m}C$), 90/90=Y($^{m}C^{u}C$), and 43/41=Z($^{m}C^{m}C$ and $^{m}C^{u}C$). The percentage of Alu element methylation was then calculated as %Total methylation = {(Z + W) / (Z +W + 2V + X +Y)}×100.

2.2.3 Premature T cell senescence in breast cancer patients

2.2.3.1 Participants

Sample size calculation

The previous study examined for the presence of senescent T cells in breast cancer patients and found that there were 303 cells/μL of CD28+CD8+ T cells in breast cancer group (SD = 125), and 229 cells/μL of CD28+CD8+ T cells in healthy participants (SD = 113) (43).

$$N = (\sigma^2_A + \sigma^2_B)\left(\frac{z1-\alpha+z1-\beta}{\mu A-\mu B}\right)^2$$

σ = standard deviation

μ = mean

Z1-α = type I error, α = 0.05

Z1-β = power , 1-β = 0.80

N = 25 each group

A total of 47 breast cancer patients and 41 healthy women were recruited in this study from December 2020 to September 2021. The recruitment and sample retrieval were performed before all therapeutic modalities were given. The healthy volunteers were defined as the presence of negative annual mammographic results or surgical patients with non-cancerous pathological results. Both groups were stratified every ten years of age from 30-69 years. Moreover, the medical history

was assessed. The presence of underlying medical disease, any autoimmune disease, immunodeficiency, and previous chemotherapy was the exclusion of this study. The pathological results were assessed after sample retrieval. The staging was recorded according to the 7th Edition of American Joint Committee on Cancer Staging System for Breast Cancer. The surrogate subtypes were categorized from the result of immunohistochemistry staining. Ki67 > 20% was used as a marker for Luminal B subtype. A written informed consent was obtained from each participant. All clinical assessments were conducted according to the principles of the Declaration of Helsinki. The Institutional Review Board of Faculty of Medicine, Chulalongkorn University approved the study (IRB no. 789/63).

2.2.3.2 Preparation of peripheral blood mononuclear cells (PBMCs)

Venipuncture blood was collected in 6 ml EDTA tubes and placed at 4^{o}C until diluted with RPMI 1640 medium at a ratio of 1:1 in 15 ml. conical tubes. The blood samples were gently layered on Lymphoprep™ (Stemcell™, UK) in 15 ml conical tubes and centrifuged at 500g for 30 min with brake-off. The interface of PBMCs layer was gently collected and placed in new 15 ml conical tubes containing 5 ml of 37°C RPMI 1640 medium and centrifuged at 500g for 10 min, and washed twice in RPMI 1640 medium. 0.4% trypan blue was used when manually determining cell counts in hemocytometer. A total of four corner squares was counted and calculated as the following formula: Cell concentration(cells/ml)=total viable cells x $10^4/2$, and cells were analyzed by flow cytometry.

2.2.3.3 T cell senescence flow cytometry panels

PBMCs were collected up to $1x10^6$ cells/tube and centrifuged at 500g for 5 min. The cell pellets were washed twice with 500 µl of 1X PBS, and resuspended in 100 µl of PBS for cell staining. Apoptotic PBMC were measured after addition of 0.5 µl Zombie Aqua (Biolegend, USA). Firstly, the samples were incubated with Zombie Aqua on ice for 15 min, centrifuged, and the supernatant was discarded. The samples were then incubated with 0.5 µl Senescence-Associated β-galactosidase reagent (SA-β-gal) in 500 µl Hanks' Balanced Salt Solution (Gibco, USA) for 15 min at room temperature. The samples were centrifuged and discarded supernatant. Thereafter, the samples were incubated with fluorophore-labelled antibodies including: phycoerythrin-cyanin 5.5 labelled antihuman CD3; phycoerythrin-cyanin7 labelled antihuman CD57; Alexa Fluor®647 labelled antihuman CD45; Alexa Fluor®700 labelled antihuman CD279(PD-1); allophycocyanin-cyanine7 labelled antihuman CD28; brilliant violet 421 labelled antihuman CD4 and brilliant violet 650 labelled antihuman CD8 for 15 min at 4°C in the dark. The samples were analyzed by flow cytometry. All antibodies were purchased from Biolegend, USA.

2.2.3.4 Activation of peripheral blood mononuclear cells

After isolating, the PBMCs were incubated in complete RPMI 1640 medium supplemented with 10% fetal bovine serum in a 6-well plate overnight. Two µg/ml purified antihuman CD3 in 1X PBS was coated in a 24-well plate at 37°C for 2 h and the plate was washed twice with warm (37°C) 1X PBS. Trypan blue was used to enumerate the cells in hemocytometer. $5x10^5$ PBMCs were placed in 500 µl complete RPMI 1640 medium in the antihuman CD3 coated 24-well plate. 2 µg/ml of purified antihuman CD28 and recombinant IL-2 50U/ml were added and incubated in a humidified 5%CO_2 incubator at 37°C for 16 h. The samples were then harvested for activation marker staining.

2.2.3.5 Activated T cell flow cytometry panels

Apoptotic PBMC were measured after addition of 0.5 μl Zombie Aqua (Biolegend) staining. Firstly, the samples were incubated with Zombie Aqua on ice for 15 min and then incubated with fluorophore-labelled antibody panels, including: phycoerythrin antihuman CD69 and phycoerythrin-cyanin 5.5 labelled antihuman CD3, for 15 min. The stained cells were transferred into 5 ml flow cytometric tubes, placed on ice in the dark until flow cytometry was performed. Antibodies were purchased from Biolegend, USA.

2.2.4 The effects of 17β-estradiol on cell models of cellular senescence

2.2.4.1 Cell maintenance

Jurkat cells were initially grown in complete RPMI 1640 medium and washed twice and subsequently were maintained in phenol red-free DMEM (Invitrogen, USA) supplemented with 10% charcoal-stripped fetal bovine serum (Sigma–Aldrich, USA), 2mM L-glutamine, 100 U/ml penicillin plus 100 μg/ml streptomycin for 48-72 h.

T47D cells were initially grown in complete RPMI 1640 medium and washed twice. They were then plated and maintained in phenol-red free DMEM (Invitrogen, USA) supplemented with 10% charcoal-stripped fetal bovine serum (Sigma–Aldrich, USA), 2mM L-glutamine, 100 U/ml penicillin plus 100 μg/ml streptomycin for 48 h.

2.2.4.2 Jurkat cell senescence model

Etoposide (Cayman Chemical, USA) was dissolved in DMSO for a 100mM etoposide stock solution and kept in -20^{o}C until use. The stock was then diluted in complete medium to give a 10 mM solution. Jurkat cells were plated at 1 x 10^6 cells in a 6-well plate of complete phenol red-free DMEM. 6 μl etoposide was added to give a final concentration of 30μM etoposide. The samples were mixed and incubated for 1 h, washed twice and these senescent Jurkat cells were subjected to further experiments.

2.2.4.3 T47D cell senescence model

T47D cells were harvested and plated in phenol red-free complete DMEM for 48h prior to the performance of the senescence assay. The medium was subsequently removed and cells were washed twice. 100mM Etoposide was diluted in phenol red-free complete DMEM and added to the cells at a 7.5 μM final solution, for 24 h. The senescent T47D cells were subjected to further experiments.

2.2.4.4 17β-estradiol treatment

After etoposide treatment, Jurkat cells were seeded at the concentration of 5 x 10^5 cells/ml in complete phenol red-free DMEM (Invitrogen, USA). E2 was added at concentrations of 1 nM, 10 nM, and 100 nM, and 1 μl of 100% ethanol was added as a vehicle control. The treated Jurkat cells were harvested at 24- , 48-, and 72- h.

This treatment regimen was also performed on senescent T47D cells. After 24-h incubation with etoposide, the senescent T47D cells were washed with warm

1X PBS twice. Subsequently, vehicle control plus 1 nM, 10 nM, and 100 nM of E2 were added to samples and incubated for 24- and 48 h.

2.2.4.5 DNA damage assays

DNA damage assay: γH2AX flow cytometry assay

Jurkat cells or T47D cells were harvested and washed with 1X PBS and centrifuged at 300g for 5 min. The supernatants were discarded, and the samples vortexed to loosen cell pellets. One ml of pre-cooled 70% ethanol was added drop by drop while vortexing. The samples were incubated at -20°C for at least 60 min and after fixation 100 µl of 1% (v/v) TritonX-100 was added for 5 min and washed with 1X PBS. All samples were incubated with 0.5 µg/ml (1:200) rabbit antihuman phosphorylated γH2AX (Ser139, Cell Signaling Technologies) antibody for 30 min. and then incubated with 0.2 µg/ml (1:500) Alexa fluor® 647 conjugated goat anti-rabbit antibody (Thermofisher, USA) for 30 min. The samples were resuspended in 1X PBS before analysis by flow cytometry.

DNA damage assay: p21 flow cytometry assay

Jurkat cells or T47D cells were harvested and washed by 1X PBS. The samples were centrifuged at 300g for 5 min, and the supernatants discarded. 500 µl of 1%(v/v) formaldehyde was added and vortexed and incubated on ice for 20 min. After fixation, 100 µl 1% (v/v) TritonX-100 was added for 10 min and washed with 1X PBS. After the cell pellets were loosened, the samples were incubated in 0.5 µg/ml (1:200) rabbit anti-human p21 polyclonal antibody (Sigma–Aldrich, USA) for 30 min. Subsequently, the samples were incubated in 0.2 µg/ml (1:500) Alexa fluor® 488-conjugated goat anti-rabbit antibody (Thermofisher, USA) for 30 min. Finally, 500 µl of PBS was used to resuspend the cells and flow cytometry was

performed. The Overton function (FlowJo, BD. USA) was used to determinate the proportions of positive cells.

DNA damage assay: p53 flow cytometry assay

Jurkat cells or T47D cells were harvested, fixed and permeabilized as in p21 flow cytometry assay. Next, 0.5 μg/ml (1:200) mouse antihuman p53 monoclonal antibody clone DO-1 (Sigma–Aldrich, USA) was added for 30 min. Subsequently, the samples were incubated with 0.2ug/ml (1:500) allophycocyanin conjugated goat antimouse antibody (Thermofisher, USA) for 30 min and resuspended. The flow cytometry was performed, and Overton function (FlowJo, BD. USA) was used to determinate proportions of positive cells.

2.2.4.6 Cellular senescence assays

1. Senescence panels for Jurkat cells

Apoptotic PBMC were measured using 1 μl of 7-AAD (Biolegend, USA). Samples were then incubated with antibody panels, including phycoerythrin labelled antihuman CD28 (Thermofisher, USA) and allophycocyanin-cyanine7 conjugated antihuman CD45 (Biolegend, USA) for 15 min in the dark. After cell staining, 1%(v/v) formaldehyde was added for 20 min and the cells were washed. Finally, the cell samples were resuspended in 500 μl of PBS and analysed by flow cytometry.

2. Arginase-2 flow cytometry assay

Jurkat cells or T47D cells were harvest, fixed and permeabilized as in p21 flow cytometry assay. Next, the samples were incubated in 0.5 μg/ml (1:200) rabbit antihuman arginase-2 monoclonal antibody (Abcam, USA) for 30 min. 0.2 μg/ml Alexa fluor® 488 conjugated goat antirabbit antibody (Thermofisher, USA) was

added for 30 min. Finally, 500 µl of PBS was used to resuspend the cells and flow cytometry was performed. The Overton function (FlowJo, BD. USA) was used to determinate the proportions of positive cells.

3. Arginase-2 immunofluorescent staining

Jurkat cells or T47D cells were harvested, fixed and permeabilized as in γH2AX staining. Next, 0.5 µg/ml (1:200) rabbit antihuman arginase-2 monoclonal antibody (Abcam, USA) was added at 4°C overnight. Then, 0.2 µg/ml (1:500) Alexa fluor® 488 conjugated goat anti-rabbit antibody (Thermofisher, USA) was added for 2 h at room temperature. The samples were washed and incubated in 1:50,000 (100 ng/ml) DAPI (Thermofisher, USA) for 10 min. Coverslips were added and immunofluorescence microscopy was performed.

2.2.4.7 Activation of Jurkat cells

10 µg/ml purified antihuman CD3 in PBS was added to a 96-well plate at 37°C for 2 h and washed twice with 1X PBS. $1x10^5$ Jurkat cells were seeded in 200 µl complete phenol red-free DMEM with E2 supplemented at the concentration indicated in the text. 10 µg/ml purified antihuman CD28 was added, and the samples were incubated in a humidified 5%CO_2 chamber at 37°C incubator for 24 h. The cells were harvested for staining, while the supernatants were collected in Eppendorf tubes and stored at -20°C for IL-2 assays.

2.2.4.8 Activation markers for Jurkat cells

Apoptotic PBMC were measured by adding 1 µl of 7-AAD (Biolegend, USA) and then incubated with fluorophore-labelled antibody panels, including

phycoerythrin-labelled antihuman CD69 (Thermofisher, USA) and allophycocyanin-cyanine 7-conjugated antihuman CD45 (Biolegend, USA) for 15 min in the dark. Finally, the samples were resuspended in 500 µl of PBS and analyzed by flow cytometry.

2.2.4.9 IL-2 concentration assay

IL-2 levels were determined by ELISA according to the manufacturer's instructions (Thermofisher). The range of detection was 2 pg/ml – 250 pg/ml. A 96-well plate was firstly coated by the antibody overnight. Then 100 µl of supernatant was added to the plate. Concomitantly, a standard solution was added to make the standard curve. After incubation, the 96-well plate was washed and the detection antibody and Avidin-HRP were added. TMB solution and Stop solution were then added. Absorbance was measured at 450 nm using aThermo Scientific™ Multiskan™ FC Microplate Photometer (Thermo Fisher Scientific, USA). The standard curve was generated and IL-2 concentrations in the samples were calculated

2.3 Data and statistical analysis

In this study, the unpaired t-test and student t-test were used to compare quantitative data. The Pearson correlation and the linear regression models were used in clinical study. The statistical analysis was performed by SPSS v22.0. The figures were produced by GraphPad Prism, version 8.0. The statistical significance was considered when p value was <0.05

2.4 Ethical consideration

All clinical assessments were conducted according to the principles of the Declaration of Helsinki. The Institutional Review Board of Faculty of Medicine, Chulalongkorn University, approved the study for clinical and *in-vitro* study (No.789/2563 Date 30 November 2020). Written informed consent was obtained from all individual participants

CHAPTER 3 CANCER SERA INDUCED CHANGES IN ALU ELEMENT METHYLATION OF NORMAL PBMCS

3.1 Introduction

3.1.1 Cancer development and global methylation changes in peripheral immune cells

DNA methylation is the addition of methyl groups to CpG sites in eukaryotic genomes. Approximately 80% of CpG sites are methylated in normal human somatic cells (55). The hypermethylated promoters result in transcriptional factor blockages, leading to gene silencing. Many DNA methyltransferase (DNMT) family members are responsible for DNA methylation, and all contain the conserved catalytic region, which uses S-adenosylmethionine to transfer the methyl group. There are three crucial DNMT which methylate human genomes, including DNA methyltransferase1 (DNMT1), DNA methyltransferase3a (DNMT3a), and DNA methyltransferase3b (DNMT3b) (56). The DNMT1 preferentially binds to hypomethylated CpG sites together with a protein complex known as UHRF1. This mechanism is described as "maintenance methylation". This is also important in the DNA replication process in terms of methylation of daughter strands. Recently, a study found that *de novo* methylation is also slowly exhibited by DNMT1 (57). However, DNMT3a and DNMT3b are mainly accountable for *de novo* methylation of the unmethylated CpG sites (58-60). There are two major approaches to access DNA methylation including global DNA methylation and site-specific DNA methylation. The global DNA methylation is to access the signature or landscape of target cells, but the site-specific DNA methylation is to access the specific gene signature. Currently, the global DNA methylation changes in cancer-associated immune cells have been used as cancer signature and landscape of immune function changes (61).

Global DNA methylation is the level of methylated cytosines in human's genomes or human's exomes (62). Apart from genomes and exomes, human genomes contain 30-40% of transposon elements which distribute throughout the genomes (63). These repetitive sequences are able to integrate any parts of human genomes (63). There are two types of transposons which transpose with and without reverse transcriptase. The retrotransposons which depend on reverse transcriptase enzyme are classified into 3 subtypes including long terminal repeat retrotransposon (LTR), long interspersed nuclear elements (LINE) and short interspersed nuclear elements (SINE) (63). LINE-1 is the most active elements in LINE subgroup. There are approximately 500,000 copies contained in the human genomes. There are 3,000 copies consisted at least 4,500 base pairs which classified as full length LINE-1 (64). Alu elements are contributing million copies or 11% throughout human genomes. Alu elements are approximately 300 base pairs. Many studies used DNA methylation in transposons as global methylation levels (65-67).

According to cancer-specific T cells activation, after T cell priming in secondary lymphoid organs, the effector T cells target to eradicate tumor cells (21). However, cancer cells and cancer-associated stromal cells could promote immune evasion by producing mediators to epigenetically modify gene expressions in T cells and lead to the plasticity of T cell phenotypes (32). A previous study showed that global hypomethylation of T cells was found after antigen exposure, and the subsequent de novo methylation was accountable for an exhausted phenotype (61). Some researchers hypothesized that blood DNA methylation could demonstrate the consequences of cancer-immune cell interactions. Therefore, blood DNA methylation could early detect carcinogenesis (68). For decades, blood DNA methylation level has been studied as a non-invasive biomarker (33). The recent meta-analysis of prospective trials showed non-significant association of specific

site DNA methylation and breast cancer risk (68). However, most cancer types showed genome-wide global hypomethylation (69-71). As we know, transposons contain repetitive sequences and CpG rich elements which intersperse in whole genomes. Many researchers used the methylation levels of transposons as global methylation surrogates (72, 73). A prospective study showed the association of the increased of LINE-1 methylation and shorter interval of cancer development especially prostate cancer (74). Furthermore, the methylation of Alu elements tended to decrease at the shorter intervals of all cancer diagnoses (74).

3.1.2 Breast cancer and methylation changes in peripheral immune cells

The global methylation changes in blood or breast cancer-associated immune cells had been studied as cancer signatures for decades (19). As we know, blood DNA hypomethylation might associate to higher BMI, and familial breast cancer risk (68). Moreover, blood-based methylation changes had been studied as breast cancer screening biomarkers in average-risk population and high-risk population (19, 33). In recent meta-analysis, there were inconclusive results regarding global DNA methylation levels and breast cancer risk due to heterogenous measurement techniques, sample types, and study designs (19, 33), but many studies showed blood hypomethylation in breast cancer patients (68, 72, 75) as shown in Table 3.1–3.2. Intriguingly, there was a study showed promoter hypermethylation in the patients (76). In high familial risk studies, two studies could demonstrate significant hypomethylation in breast cancer patients, while most studies could not demonstrate significant differences as shown in Table 3.2. In addition, hormonal receptor positive breast cancer and HER2 positive breast cancer were associated with blood hypomethylation in two cohorts (77, 78), but triple negative breast cancer was related to hypomethylation of lymphocytes in one cohorts (79) as shown in Table

3.3. These seemed to be no differences in terms of breast cancer subtypes. Collectively, blood global hypomethylation seemed to be signature related to breast cancer irrespective of subtypes.

Blood DNA was derived from leukocytes and circulating DNA, and these could not address the methylation status of peripheral lymphocytes in breast cancer patients. In a recent study, peripheral T lymphocytes from breast cancer patients showed global hypomethylation compared to heathy volunteers, and those cells showed further hypomethylation in advanced stage breast cancer (75). Furthermore, the study showed the significant prognostic value of the selected CpG clusters in terms of disease recurrences, therefore, the hypomethylated T cells possibly promoted breast cancer progression (75). These features were the evidence of non-contact fashion of cancer cells and immune cells interrogation, which perhaps related to the secretion of breast cancer cells (75). In *in-vitro* studies, breast cancer cell-lines and colon cancer cell-lines could methylate long interspersed nucleic elements 1 (LINE-1) in healthy immune cells after co-culture with non-contact fashion (80, 81). However, circulating cancer secretion consisted of several mediators rather than the presence of breast cancer cells that could result in complex methylation changes of immune cells in breast cancer patients. The hypermethylation changes from co-culture experiments seemed to be different from the blood-based global methylation, in which hypomethylation seemed to be reported, and the early changes after exposure were not well understood. These gap knowledges might connect the findings of global methylation changes in the presence of breast cancer and the clinical relevance.

Table 3.1 Global DNA methylation in peripheral blood of breast cancer patients and healthy controls in average-risk population in individual cohorts.

Study design	Samples	Measurement	Sample size (case/control)	Main findings	References
Case-control	Blood DNA	Pyrosequencing (mean LINE-1 met)	19/18	No significant differences	Choi JY, 2009(72)
Case-control	Blood DNA	LC-MS (mean 5-mdC)	176/173	Hypomethylation of 5-mdC in cases (4.18 VS 4.38 p<0.001 in validation set)	Choi JY, 2009(72)
Case-control	Blood DNA	MethyLight (%Sat2 met)	40/40	Sat2 hypomethylation in cases (125 VS 150 P=0.01)	Cho YH, 2010(67)
Case-control	Blood DNA	MethyLight (%LINE-1 met)	40/40	No significant differences	Cho YH, 2010(67)
Case-control	Blood DNA	MethyLight (%Alu met)	40/40	No significant differences	Cho YH, 2010(67)
Case-control	Blood DNA	MethyLight (%Alu met)	40/40	No significant differences	Cho YH, 2010(67)
Case-control	PBMC	COBRA-LINE-1 (%met)	36/144	No significant differences	Kitkumthorn N, 2012(82)
Case-control	Blood DNA	Pyrosequencing (mean LINE-1 met)	1064/1100	No significant differences	Xu X, 2012(76)
Case-control	Blood DNA	LUMA (%met)	1055/1101	Global promoter hypermethylation in cases (57.3% VS 52.4% p<0.001)	Xu X, 2012(76)
Case-control	Blood DNA	LUMA (%met)	384/384	Global genomic hypomethylation in cases (68.9% VS 70.2% p<0.01)	Kuchiba A, 2014(83)
Nested case-control (NOWAC)	Blood DNA	Methylation array (β value	168/168	Unchanged epigenome-wide methylation	Van Veldhoven K, 2015(18)
Case-control (PLCO)	WBC (buffy coat)	LC-MS (mean 5-mdC)	428/419	No significant differences	Sturgeon, 2017
Case-control	PBMCs	Pyrosequencing	28/9	8283 hypomethylated genes and 2489 hypermethylated genes	Parashar, 2018(75)
4 prospective cohort studies	Blood DNA	Meta-analysis (Methylation array and pyrosequencing)	1926/1703	May relate to late stage breast cancer (OR of average methylation 0.83, p=0.02)	Bodelon, 2019(68)

Table 3.2 Global DNA methylation in peripheral blood of breast cancer patients and healthy controls in high-risk population in individual cohorts.

Study design	Samples	Measurement	Sample size (case/control)	Main findings	References
Case-control (BGS)	WBC (buffy coat) from familial high-risk of breast cancer	Pyrosequencing (mean LINE-1 met)	241/242	No significant differences	Brennan K, 2012(84)
Case-control (EPIC)	WBC (buffy coat) from familial high-risk of breast cancer	Pyrosequencing (mean LINE-1 met)	232/263	No significant differences	Brennan K, 2012(84)
Case-control (KconFab)	Blood DNA from familial high-risk of breast cancer	Pyrosequencing (mean LINE-1 met)	153/218	No significant differences	Brennan K, 2012(84)
Case-control	Blood DNA from familial high-risk breast and/or ovarian cancer	LUMA (%met)	263/321	No significant differences	Delgado-Cruzata L, 2012(85)
Case-control	Blood DNA from high-risk breast and/or ovarian cancer families	[3H]-Methyl acceptance assay	233/295	Global genomic hypomethylation in cases (97,111 VS 88,030 $p<0.05$)	Delgado-Cruzata L, 2012(85)
Case-control	WBC or granulocytes from familial high-risk of breast cancer	MethyLight (%Sat2 met)	266/333	No significant differences	Wu HC, 2012(73)
Case-control	WBC or granulocytes from familial high-risk of breast cancer	MethyLight (%Alu met)	266/334	No significant differences	Wu HC, 2012(73)
Case-control (BCFR)	WBC or granulocytes from familial high-risk of breast cancer	Pyrosequencing (mean LINE-1 met)	279/340	No significant differences	Wu HC, 2012(73)
Case-control (BCFR)	WBC or granulocytes from familial high-risk of breast cancer	MethyLight (%LINE-1 met)	265/333	No significant differences	Wu HC, 2012(73)
Nested case-control	Blood DNA or Serum DNA from familial high-risk of breast cancer	Pyrosequencing (mean LINE-1 met)	294/646	No significant differences	Deroo LA, 2014(86)
Nested case-control (BGS)	WBC (buffy coat) from familial high-risk of breast cancer	WGBS (β value	548/548	Unchanged epigenome-wide methylation	Van Veldhoven K, 2015(18)
Nested case-control (EPIC)	Blood DNA from familial high-risk of breast cancer	Methylation array (β value)	162/162	Epigenome-wide hypomethylation in cases (53% VS 53.18% $p<0.001$)	Van Veldhoven K, 2015(18)

Table 3.3 Global DNA methylation in peripheral blood with breast cancer subtype stratification in individual cohorts.

Study design	**Samples**	**Measurement**	**Sample size (case/control)**	**Main findings**	**References**
Case-control	Blood DNA	Pyrosequencing (mean LINE-1 met)	109 HR+ 63 HR-	No significant different among HR status	Choi JY, 2009(72)
Case-control	Blood DNA	LUMA (%met)	419 ER+	Promoter hypermethylation irrespective ER/PR status	Xu X, 2012(76)
Nested case-control	WBC or lymphocytes	Microarray (β value)	297 ER+ 217 PR+ 109 HER2+	HER2 (OR =0.28 p=0.002) No significant difference in ER and PR	Severi G, 2014(77)
Nested case-control (EPIC)	Blood DNA from familial high-risk of breast cancer	Methylation array (β value)	56 ER+ 18 ER -	ER+ (OR 0.59 p=0.03) ER- (OR 0.49 p=0.13)	Van Veldhoven K, 2015(18)
Nested case-control (NOWAC)	Blood DNA	Methylation array (β value	130 ER+ 28 ER-	ER+ (OR 1.10 p=0.50) ER- (OR 0.80 p=0.38)	Van Veldhoven K, 2015(18)
Case-control	Pan-lymphocyte	Mehylation arrays ((β value)	231 TNBC/231	Hypomethylation in TNBC (OR=0.56–0.61 p<0.0001)	Manoochehri, 2021(79)
Case-control	Neutrophil	Mehylation arrays ((β value)	231 TNBC/231	Hypermethylation in TNBC (OR =2.07–3.02 p<0.0001)	Manoochehri, 2021(79)

3.2 Results

3.2.1 Participant demographics

Sixteen healthy participants from the breast cancer screening clinic took part in this study and their mean age was 53.06 years old (range 37-62). In the breast cancer group, 16 sera were obtained from metastatic breast cancer patients, with a mean age of 50.5 years old (range 33-62). The ECOG score was determined and found that 75% of patients were ECOG 0-1 and 25% of those were ECOG 2 as in Table 3.4. The most common metastatic sites were liver (56.5%) and lung (50%). All cancer participants received systemic treatment, including chemotherapy, targeted therapy and hormonal treatment for their disseminated diseases, while 7 patients of those received chemotherapy intravenously at the median duration of 7 days prior to the recruitment. The median follow-up time was 140.5 days in breast cancer group, and at least 90 days in the non-progression group. The clinico-pathological characteristics are categorized in Table 3.4 and disease progression was determined by radiographic evidence. The time to progression was calculated from the sample retrieval date to the disease progression date.

Table 3.4 Patients characteristics and clinico-pathological characteristics in metastatic breast cancer patients.

Factors	N (%)	Factors	N (%)
ECOG score		**Estrogen receptor**	
0	4 (25%)	**Positive**	10 (62.5%)
1	8 (50%)	**Negative**	6 (37.5%)
2	4 (25%)		
Comorbidity		**Progesterone**	
DM	2 (12.5%)	**receptor**	6 (37.5%)
Others (hypothyroid)	1 (6.25%)	**Positive**	10 (62.5%)
		Negative	
Metastatic site		**HER2**	
Liver	9 (56.25%)	**Positive**	3 (18.75%)
Lung	8 (50%)	**Negative**	13 (81.25%)
Bone	3 (18.75%)		
Others	2 (12.5%)		
Grade		**Treatment**	
1-2	6 (37.5%)	**Chemotherapy**	9 (56.25%)
3	10 (62.5%)	**Targeted therapy**	9 (56.25%)
		Anti-hormone	7 (43.75%)
Subtypes		**Time since previous**	Median 7 days
Luminal B	10 (62.5%)	**Intravenous**	(range 1-19 days)
HER2	1 (6.25%)	**chemotherapy (N=7)**	
TNBC	5 (31.25%)		
Time to progression			
≤ 90 days	7 (43.75)		
> 90 days	9 (56.25%)		

3.2.2 Quantitative Combined Bisulfite Restriction Analysis for Alu elements

After DNA extraction and bisulfite treatment, Alu elements in DNA were amplified by PCR. The amplicons were treated with restriction enzymes which were specified to methylated cytosines to detect the methylation status of restriction sites on Alu elements amplicons. Samples were analyzed on 8% acrylamide gels to quantify bands and calculate the percentages of methylation of Alu elements as shown in Figure 3.1.

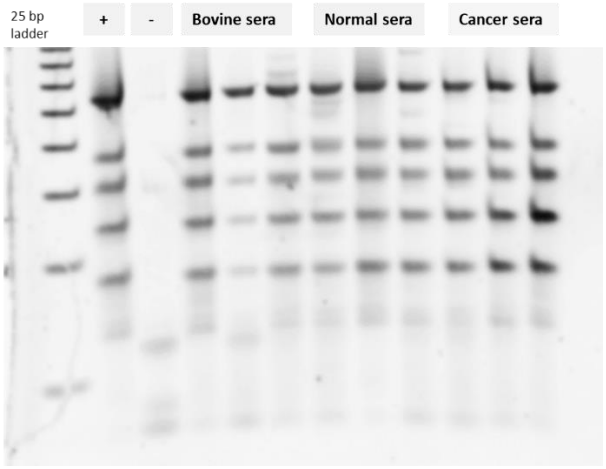

Figure 3.1 Bands detected after 16-h restriction enzyme incubation. The figures show band detection on 8% acrylamide gel with 25bp ladder including positive control(+), negative control(-), bovine sera culture, normal sera culture, and cancer sera culture.

3.2.3 Changes in Alu element methylation of PBMCs after incubation with cancer or normal serum

After 48-h culture, the mean percentages of Alu element methylation were 67.61%, 66.17%, and 66.87% after incubation with bovine serum, normal serum, and cancer serum, respectively (Figure 3.2). The paired t-test was performed between groups, but no statistical significance was observed (p=0.54 in cancer vs normal serum, and p=0.41 in cancer vs bovine serum).

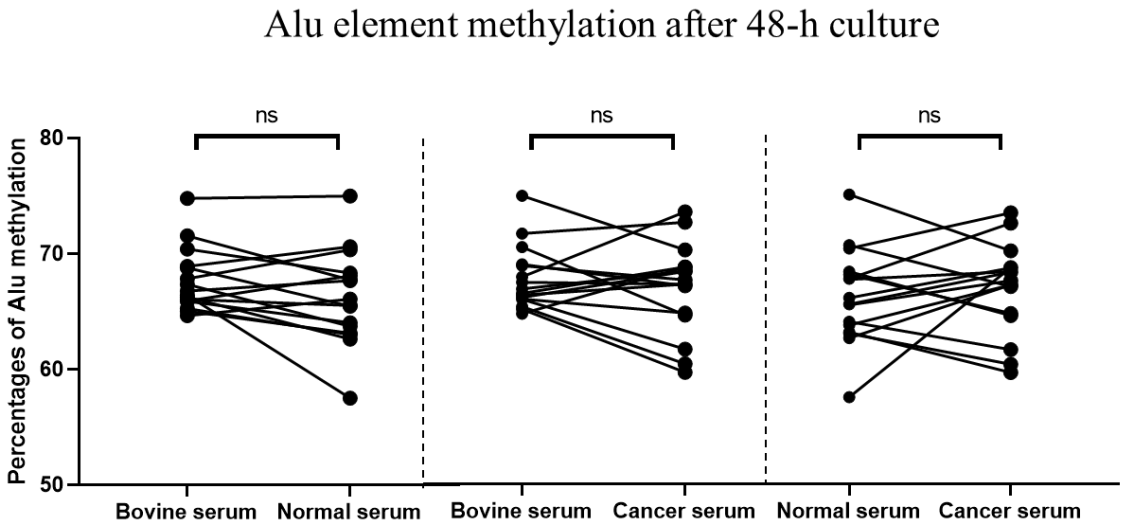

Figure 3.2 Percentages of Alu element methylation in the individual group. The figure shows scatter plots with connected lines of percentages of Alu element methylation after 24-hour incubation with bovine serum, normal serum or cancer serum in pairs. (N=16)

3.2.4 The Alu element methylation changes related with progression of age

To clarify the effects of ageing on DNA methylation, changes in percentages of Alu element methylation were calculated from the differences between incubation with cancer serum or normal serum compared to incubation with bovine serum. The

percentage changes of normal serum group and cancer serum group were correlated with age of the participant. In the normal serum group, the Pearson correlation was -0.203, and p-value was 0.452, while the Pearson correlation was -0.624, and the p-value was 0.0098 in cancer group as shown in Figure 3.3. There was a trend that the Alu elements hypomethylation was correlated with progression of age in both normal serum and cancer serum group, but no statistical significance was found in normal serum group.

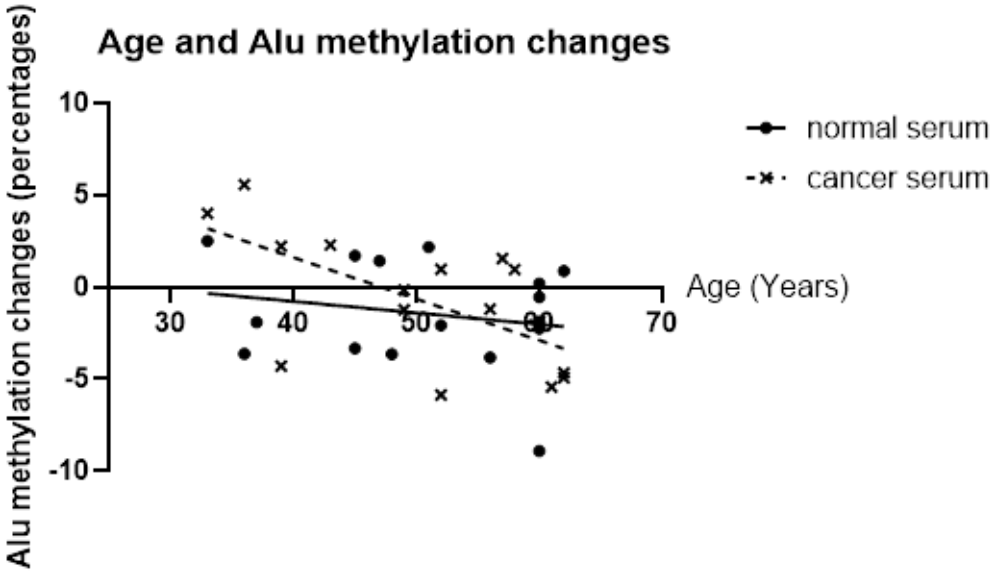

Figure 3.3 The correlation of Alu element methylation with age of participants. The line shows the trend of Alu element methylation changes with progression of age in normal serum group, and the dashed line shows the trend of Alu element methylation changes with progression of age in cancer serum group.

3.2.5 The hypomethylation of Alu elements related to cancer progression

The percentage changes of methylation of Alu elements after 48-h incubation with cancer serum were calculated as the differences from bovine serum and normal

serum groups. These differences were examined for clinical relevance. The breast cancer prognostic factors were used to examine whether the differences in Alu methylation changes could determine good or poor prognostic factors, as demonstrated in Table 3.5. Moreover, time to progression was used as a prognostic factor in this study. The time to progression was divided into 2 groups which were up to 90 days (TTP$\leq$90) and more than 90 days to progression (TTP>90). There were 7 samples in the TTP$\leq$90 group and 9 samples in the TTP>90 group. Their mean ages were 53 years old in the TTP$\leq$90 group and 48 years old in the TTP>90 group ($p = 0.31$), and the age ranges were comparable between groups which were 39-62 years in the TTP$\leq$90 group and 33-61 years in the other group. The Alu methylation changes tended to decrease in estrogen receptor negative breast cancer, but no statistical significance was observed. Interestingly, the mean of differences of Alu element methylation was significantly lower in the TTP$\leq$90 group which was -3.48%, while the mean of differences was +1.37% in the TTP>90 group ($p = 0.002$), as shown in Table 3.5 and Figure 3.4. However, the mean of differences between cancer serum and normal serum was not statistically significant. These findings seemed to suggest that the progression of breast cancer was related to hypomethylated Alu elements of circulating immune cells.

Table 3.5 The mean of differences of methylation of Alu elements changes related to prognostic factors of breast cancer.

Factors	**N**	**Cancer serum - Bovine serum**		**Cancer serum – Normal serum**	
		Mean of differences	p value	Mean of differences	p value
Grade					
1-2	6	-1.313	0.637	+0.973	0.851
3	10	-0.411		+0.525	
Estrogen receptor					
Positive	10	+0.273	0.140	+2.161	0.084
Negative	6	-2.453		-1.753	
Progesterone receptor					
Positive	6	-0.297	0.706	+2.340	0.259
Negative	10	-1.021		-0.295	
HER2					
Positive	3	-0.350	0.837	+4.460	0.100
Negative	13	-0.842		-0.176	
Treatment					
Chemotherapy	9	-1.122	0.648	+0.306	0.703
Others	7	-0.270		+1.191	
Time to progression					
≤ 90 days	7	-3.477	0.002	-1.280	0.116
> 90 days	9	+1.372		+2.228	

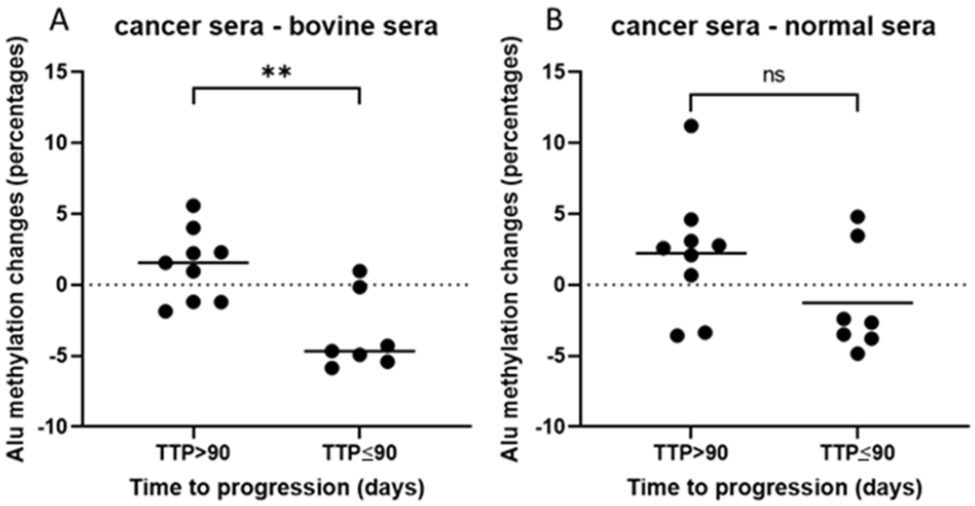

Figure 3.4 Changes in methylation of Alu elements after 48-h incubation in cancer serum of the TTP>90 group and the TTP≤90 group. These figures show the differences of methylation of Alu elements between cancer serum and bovine serum (A), and differences of Alu elements methylation between cancer serum and normal serum group (B). (N=16)

3.2.6 Changes in Alu element methylation patterns in healthy PBMCs after inoculation with cancer serum were related to early progression in metastatic breast cancer

In the quantitative combined bisulfite restriction technique, the patterns of methylation of Alu elements were characterized into 4 patterns: double methylated cytosine loci(mCmC); unmethylated cytosine followed by methylated cytosine (uCmC); methylated cytosine followed by unmethylated cytosine (mCuC); double unmethylated cytosine loci (uCuC). The percentages of Alu element methylation after inoculation with cancer serum were divided into TTP>90 and TTP≤90 groups according to the previous mention of hypomethylation in PBMCs in the early cancer progression group, hypomethylation changes of PBMCs were found as increased

mCuC loci and decreased mCmC loci. In more detail, percentages of mCuC were 17.63% and 21.34% in TTP>90 and TTP≤90 groups, respectively (p=0.008). Moreover, percentages of mCmC were 46.06 and 39.81 in TTP>90 and TTP≤90 groups, respectively (p=0.041) as shown in Figure 3.5. These findings suggested that hypomethylation pattern changes after inoculation with poor prognostic cancer serum seemed to be specific foci than globally changed.

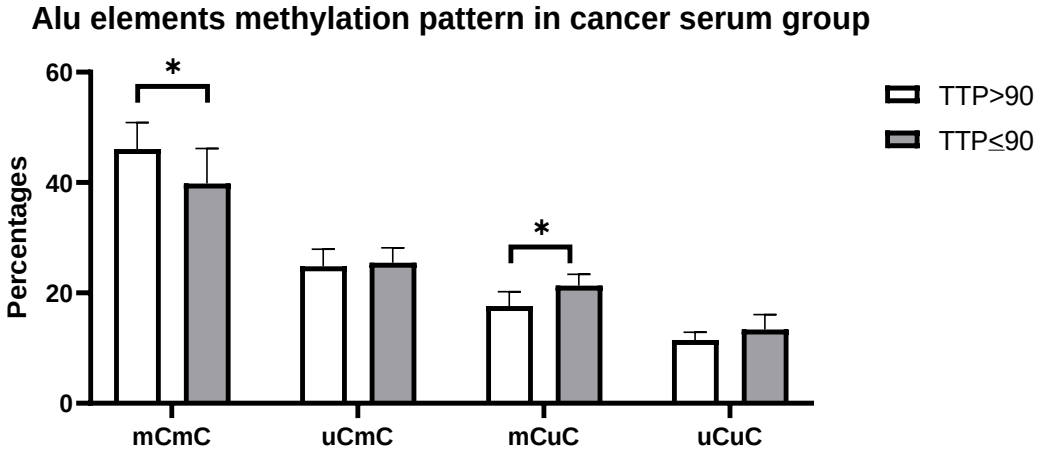

Figure 3.5 The patterns of Alu element methylation in TTP>90 group (white) and TTP≤90 group (grey).

3.3 Discussion

The plasticity of immune cells is dependent on epigenetic machinery, including DNA methylation, histone modification, and interfering RNA (17, 87). In cancer, epigenetic alterations can result from cancer-immune cell crosstalk (25, 26). These effects are well-recognized as factors responsible for the immune evasion of cancer cells (88). The methylation of Alu elements in blood has been used for cancer diagnosis and cancer prognosis for many years because of the evidence of early changes in Alu element methylation in cancer patients (71, 89, 90), and the Alu element methylation tended to be hypomethylated in breast cancer patients (72, 75,

83). In our study, the *in-vitro* cell models showed the effects of breast cancer on healthy PBMCs in non-contact fashion, and these effects resulted in global methylation changes, but there were both hypermethylated and hypomethylated Alu elements after co-culture. These features could result from the heterogeneity of breast cancer and the complexity of cancer secretion, but the Alu hypomethylation in early progression group might be explained by the early changes of T cell dysfunction as shown in recent findings in early breast cancer (54), and this needs further study.

In our study, the results showed that cancer cells were able to remotely modify the epigenetic conditions in circulating immune cells in a non-contact fashion, and likely as a consequence of cancer secretion. In a recent study, colon and breast cancer cell lines were co-cultured with healthy immune cells separated by membranes, and the global methylation was subsequently changed to LINE-1 hypermethylation (80, 81). Both cancer cells and immune cells produce several mediators and cytokines, and these substances could regulate DNA methylation in other cells. For instance, transforming growth factor-β (TGF-β) produced by cancer cells and cancer stroma was one of the key cytokines regulating the tumor microenvironment (91). In prostate cancer, TGF-β could up-regulate DNA methyltransferases in cancer cells to promote cell cycle progression (92), but TGF-β repressed DNA methyltransferases in $CD4^+$ T cells, and Forkhead box protein P3 was subsequently expressed to drive regulatory functions (93). These findings suggested that TGF-β could regulate gene expressions via both signaling pathways and epigenetic modifications. In addition, such effects were also reported in response to interleukin-6 (94).

In this chapter, hypomethylation of Alu elements was related to the early progression of metastatic breast cancer. Several previous studies have shown hypomethylation of Alu elements of immune cells in carcinogenesis (71, 72).

Moreover, other studies have shown a higher odds ratio of hypomethylated Alu elements with advanced staging and lymph node involvement (72, 95). Therefore, hypomethylated Alu elements might be more related to the presence of cancer with poor prognostic factors. As a result, hypomethylation of Alu elements might be considered as a poor prognosis cancer characteristic rather than a cancer signature. However, we did not find an association between hypomethylation of Alu elements and other tumor characteristics.

From the quantitative combined bisulfite restriction analysis technique, 2 restriction sites of methylated CpGs were evaluated, and the patterns of methylation of these two sites was determined (96). The increased mCuC loci suggested that the hypomethylation seemed to be localized rather than global in this experiment. The specific gene or region should be considered as a further study. Furthermore, the increased percentage at mCuC loci was also related to poor prognosis in head and neck cancer (95). The increase of mCuC loci in Alu elements might be represented as worse prognosis in some cancer patients.

Apart from cancer, changes in the Alu element methylation status were dynamic responses to external factors, such as viral infection, burns and tobacco (75, 97-99). Moreover, changes in Alu element methylation could be found in patients with autoimmune diseases, diabetes mellitus, dyslipidemia, and osteoporosis (40, 100, 101). Accordingly, some normal sera could hypomethylate Alu elements of normal PBMCs in our study, therefore, the use of pooled normal sera as control was difficult to exclude all confounding factors. However, the trends of Alu element hypomethylation in the early progression group were comparable from both controls.

Beside global genome-wide methylation status, the Alu element methylation was found to be associated with the ageing process and organ function impairment (102), and hypomethylation of Alu elements has been reported in the elderly (38).

The ageing process had been reported as a consequence of accumulating DNA damage and metabolic disturbances that could result in genomic instability (35). Recently, a study showed that the hypomethylation of Alu elements was associated with the increase in intracellular DNA damage markers, and use of siRNA of Alu elements could increase methylation levels of Alu elements: lower levels of DNA damage markers were subsequently reported after exposure to DNA-damaging agents in the siRNA treated group (41). These findings suggested an association between hypomethylation of Alu elements and accumulation of DNA damage, which accelerated cellular senescence (41, 100). Accordingly, Alu element hypomethylation was reported to be correlated with the progression of age (38), and these findings were also found in our study. Hence, the worse prognosis of patients with Alu element hypomethylation in their PBMCs might be related to cellular senescence of immune cells. The senescence of immune cells was increased in the elderly (103, 104), but these types of immune cells were recently recognized as immune dysfunctional in cancer patients, and resulted from cancer-immune cell crosstalk (105). The study regarding senescent immune cells in breast cancer patients was the next chapter of this thesis.

The hypomethylation of Alu elements seemed to associate with advanced staging and tumor progression. The clinical monitoring of metastatic breast cancer by radiological imaging and blood tests is recommended (54). The Alu element methylation status of PBMCs might be helpful in this circumstance in terms of tumor progression, but further study is needed. Furthermore, tumor markers and circulating tumor cells have been used previously to assess recurrence, but these measurements have low sensitivity (106, 107). Therefore, further studies on the alterations of Alu element methylation may be important in a clinical setting. In addition, DNA methylation might reprogram these Alu hypomethylated PBMCs to promote their functions, as in the previous study that used siRNA of Alu elements

(41). However, the current epigenetic treatment tended to demethylate or inhibit DNA methyltransferase function in terms of restoration of immune function (61, 108). Perhaps, global methylation patterns might not be helpful, but more specific loci methylation may be a more useful measurement.

The limitation of this study is the small sample size. This lead to inconclusive findings in terms of methylation changes, however, this *in-vitro* study could demonstrate the effects of cancer secretion on healthy PBMCs, and these effects were associated with clinical features. Moreover, normal serum that was used as control may contain confounding factors, and so pooled bovine serum was compared to the effects of cancer serum.

3.4 Conclusion

In our study, the *in-vitro* cell models showed the effects of breast cancer on Alu methylation changes in healthy PBMCs in a non-contact fashion. Although the direction of Alu element methylation changes was not in the same direction of methylation levels, the effects of serum from cancer patients on hypomethylation of normal immune cells were related to the early progression of breast cancer. Moreover, the pattern of Alu element hypomethylation in early progression group was the increased mCuC loci. In addition, because the Alu element hypomethylation is also related with progression of age, perhaps, this feature may also be related to senescence phenotypes, which were one of immune dysfunctions in cancer patients. Therefore, the presence of senescent immune cells in breast cancer patients was studied in the next chapter of this thesis.

CHAPTER 4 PREMATURE T CELL SENESCENCE IN BREAST CANCER PATIENTS

4.1 Introduction

4.1.1 T lymphocytes: development and differentiation

The development of T lymphocytes

T lymphocytes originate from progenitor cells in the bone marrow, and become prothymocytes, which circulate to the thymus gland for the maturation process and are exported to the circulation (109). These thymocytes lack expression of typical T cell markers. In this stage, Notch signaling is important to drive early thymus progenitors to develop into the T cell lineage. In contrast, NK cells and other myeloid lineage can develop in the absence of Notch signaling (110). To develop αβT lymphocytes, TCRα and TCRβ gene rearrangements occur after the activation of recombination activating gene regulation, which generates $>10^{15}$ distinct TCRs (111). TCRγ and TCRδ occasionally develop into γδT lymphocytes by similar mechanism (112). After the rearrangement of the TCR genes, double-positive thymocytes, which express both CD4 and CD8 proteins, undergo positive selection by cortical thymic epithelial cells (cTECs) (112). The cTECs derived MHC class I and MHC class II act as antigen-presenting cells to ensure the survival of ligandome-binding thymocytes to ensure of the diversity of emerging T cells (109). After positive selection, expression of either CD4 or CD8 proteins decreases, and the remaining T cells become single-positive thymocytes. This negative selection occurs at the medulla layer of the thymus gland to eliminate high self-MHC affinity of T cells. The medullar thymic epithelial cells (mTECs) and thymic resilient DCs account for T cell immune tolerance or central tolerance, while MHC class II is commonly accountable for exogenous pathogens (109). In this case, the exogenous pathway of MHC class II is not involved, and self-autophagy explains the MHC

class II presentation (111). Eventually, the presence of TCR and the low affinity to self-MHC ensure the diversity and survival of naïve T cells prior to leaving the thymus gland (112-114).

Naïve T cells and maturation

The naïve T cells are expelled from the thymus gland at a rate proportional to the number of thymocytes (109). Firstly, recent thymic emigrants (RTEs) are used to define the new naïve T cells entering into the periphery, and RTEs have lower potency of T cell function compared to mature naïve T cells (115). The T cell receptor excision circles (TREC), a byproduct of VDJ recombination, are used to identify the RTEs subpopulation. This feature is also used to evaluate thymic function (116). Although the RTEs contain the most abundant TCR repertoire, they showed limited proliferative activity and cytokine production, including interferon-γ and IL-2 (117). Their maturation occurs in secondary lymphoid organs, and epigenetic modifications are key in naïve T cell maturation (118). Furthermore, the re-circulation of naïve T cells from secondary lymphoid organs to the bloodstream occurs to enhance the antigen exposure. The presence of homing receptors, including CCR7 and CD62L is frequently expressed and promote re-circulation. The activation occurs via TCR and MHC/peptide complexes of dendritic cells, and is generated in secondary lymphoid organs to enhance pro-survival molecules, cytokines, and cell division upregulation proteins. Eventually, activated T cells differentiate into effector T cells and other T cell lineages (119).

The Differentiation of T lymphocytes

Peripheral differentiation explains the chronological differentiation of T cells after the thymic release of naïve T cells. The conversion of effector T cells and memory T cells occurs after naïve T cell activation. After T cell activation, gene

expression changes result in cytokine production, cell cycle activation, and adhesive molecule expression (120). The cytokine gene regulation and surface receptor molecules determine the functional subsets of activated T cells (121). The up-regulation of antiapoptotic proteins determines longevity of T cell subtypes, which eventually accumulate as terminally differentiated T cells or senescent T cells (112).

The effector-memory T cell lineage

After naïve T cell activation, the majority of cells enter the effector memory lineage, while CD8+ cytotoxic T cells, CD4+T helper1 and CD4+T helper2 cells are common effector T cells (120, 122). They are capable of high levels of proliferation during the inflammatory stage followed by a contraction in the resting stage, and some memory cells remain in the circulation or embed as tissue resilient T cells (119). The memory T cells display further rapid responses upon re-exposure to the same antigen, and undergo wide ranges of differentiation (123), while the plasticity of T cells gradually diminishes during the advancing stages of differentiation (124). In a previous human study, the peak T cell responses were found 14-21 days after vaccination (125), which subsequently declined to baseline after 1 month. However, the vaccine-specific memory T cells were still detected after 5-10 years (126). Because of their durable lifetime, the accumulation of memory T cells is pronounced in the elderly as senescent T cells. The activation of these senescent cells is impaired compared to the young memory T cells and because they do not proportionally contract after activation, the persistence of terminal effector T cells could result in immune tolerance of transformed cells (127).

Effector T cells

The effector T cells are generated after antigenic stimulation of naïve T cells and memory T cells, and are formed after the activation of short-lived effector cells and long-lived memory cells. The short-lived effector cells are considered terminally differentiated because of their inability for self-renewal and subsequent apoptosis (128). The expression of CD127+, KLRG1-, Bcl-2+, and IL-7α receptor is used to identify long-lived memory cells. Moreover, the expression of costimulatory molecules such as CD27 and CD28 is associated with these subsets and survival (129). This feature is responsible for homeostasis in the resting state (130).

Memory T cells

Memory T cells express costimulatory receptors and adhesive molecules, which are absent in naïve T cells, to lower the threshold for T cell activation. Those T cells have increased cyclin-dependent kinase 6 (CDK6)/cyclin D3 complex and a high levels of cytotoxic protein transcripts for the early excitatory responses (131). Hence, the maintenance of memory T cells is also important for lifetime protection by self-renewal and homeostatic proliferation (130). The majority of memory T cell cells consist of TCM and TEM cells. TCM cells containing homing receptors can be found in secondary lymphoid organs and the bloodstream, while TEM lacking homing receptors can be found in the bloodstream and tissues. The TEM cells rapidly respond to excitatory antigen presentation, while the TCM cells are late responders to activation by antigen presentation and increase with time after infection (92). Eventually, TCM cells become the prominent memory T cell proportion in the later stages of memory T cell responses. Commonly, CCR7 and CD62L are used to identify TCM cells, and these receptors allow extravasation and secondary lymphoid organ migration (132). The TEM cells consist of Th1, Th2, and CTL, express high levels of perforin and granzyme-B, which elicit their rapid

cytotoxic responses (124). A subset of TEM cells exists, which have lost their costimulatory receptor but regain CD45RA or TEMRA expression. TEM cells and TEMRA cells produce high levels of proinflammatory cytokines and demonstrate senescent phenotypes (124).

The exhausted T cell lineage

Exhausted T cells have been recognized from studies of chronic viral infection that demonstrated the expression of immune checkpoint molecules in chronic infections, leading to unresponsive immune cells (133). In cancer, several studies reported the expression of the checkpoint molecules as markers of exhaustion characteristics in several cancer, for example, programmed cell death protein-1 (PD1), which counteracts with stimulatory signaling of cytotoxic T cells (20, 134). To date, there are several additional inhibitory receptors discovered, for instance, T cell immunoglobulin domain and mucin domain protein 3 (Tim-3), lymphocyte activation gene 3 (LAG-3), signaling lymphocytic activation molecule 4 (2B4), cytotoxic T-lymphocyte-associated protein 4 (CTLA-4) and T cell immunoreceptor with immunoglobulin and ITIM domains (TIGIT) (135). There are several immune checkpoint blockages that could restore functions of these exhausted T cells and act as targets for cancer treatment (136). Moreover, the transcriptomes of exhausted CD8+ cells are also distinctive, for example, T-box expression in T cells (T-bet), eomesodermin (Eomes), and T cell factor-1 (TCF-1) were increased in exhausted T cell, and the increased expression of Eomes was observed in terminally differentiated exhausted T cells, which are senescent T cells (137).

Regulatory T cell lineage

In counterbalancing immune responses, regulatory T cells, which are CD4+ T cells, carry out immuno-suppressive activities (138). The importance of regulatory T cells is to prevent autoimmune diseases by competing with effector T cells, impairing dendritic cell function, and secreting suppressive cytokines (139). CD4+CD25+ T cells demonstrate regulatory features since the surviving of self-antigen binding T cells in thymopoisis (105). The natural regulatory T cells become mature T cells immediately after expelling from the thymus glands (139). The forkhead box P3 (Foxp3) is a common transcription factor that regulates immune suppressive mediators, and Foxp3 deficient mice have impaired development of CD4+CD25+ T cells, leading to autoimmune diseases (140). Interestingly, regulatory T cells can be generated peripherally as shown by the conversion of naïve T cells to Foxp3+ T cells after exposure to TGFβ and IL-2 (141). However, natural regulatory T cells had higher Foxp3+ and CD45RA+ expression (142). Once the regulatory T cells are activated, memory like regulatory T cells (CD25hiCD45RO+) develop, and after reaching Hayflick limits, telomere shortening, and the absence of CD28 determine the terminal differentiation (143).

4.1.2 T cell homeostasis

T cell development in humans begins in utero after 9 weeks, and regulatory T cells develop later in the fetus with the full component of T cells present after birth. As a result, the T cell repertoire is most abundant during the childhood period, and subsequently, thymic outputs decrease progressively with age, especially after puberty (144). Nevertheless, thymopoiesis remains until approximately 50 years of age (144). The maintenance of peripheral naïve T cells is dependent on thymic

output in mice, but the maintenance of human naïve T cells mainly depends on peripheral proliferation especially after puberty (145). The interaction of the TCR and self-MHC molecules maintain the levels of anti-apoptotic proteins such as Bcl2, but the decrease in IL-7 is related to the death of naïve T cells (145), therefore, the survival of naïve T cells is dependent on restricted cytokines and TCR signals (144, 146). Eventually, naïve T cells contract in the elderly, who then have T cell proliferation and homeostasis impairment, and the naïve CD4/CD8 T cells ratio was increased in those over 60 years of age (123).

In the steady state, memory T cells without antigenic stimulation are slowly turned over. Antigen exposure and hemostatic cytokines, including IL-2, IL-4, and IL-7 are responsible for sustaining memory T cells (147). As in naïve T cells, the interaction of TCR and self-MHC molecules remain important for the survival of memory T cells (148, 149). Moreover, homeostatic cytokines could stimulate the non-specific proliferation of circulating memory T cells to maintain peripheral homeostasis, and the production of TEMRA or senescent T cells are also driven through this process (124, 129).

Regulatory T cells expand during infancy, and high levels of regulatory T cells is found in cord blood. These cells are rapidly decreased in later childhood and remain unchanged afterward. After the thymic involution, these cells are maintained by homeostatic proliferation and TCR activation as other lineages. Therefore, the TCR repertoire contracts in the elderly. However, the proportion of regulatory T cells is significantly increased in the elderly, and seemed to explain the increase of carcinogenesis and infection in the elderly (150).

4.1.3 T cell senescence

Cellular senescence

The cellular senescence feature was firstly described as Hayflick phenomenon in aging fibroblasts, which is the absence of proliferation capacity in later passage of cell culture (151). The accumulation of somatic mutations during the lifespan is linked to aging of human tissues (152). By the mechanism, DNA damage sensors inhibit the cell cycle progression and activate DNA damage repair processes, and the success of these process could allow for cell cycle progression, however, during repeated incidences of DNA damage repairs, The genetic and epigenetic aberrations are increased, including the demethylation of cytosine bases, replication errors of DNA polymerase enzymes, aberrant homologous end joining repair causing frameshift mutations and chromosomal rearrangement, that perturb cellular functions, and eventually result in cellular senescence, which limits cell growth and proliferation (151, 153). Cellular senescence is associated with increased expression of cell cycle inhibitors, such as P15, P16 and P21 (154). Some researchers have hypothesized that these consequences are natural mechanisms to protect against development of carcinogenesis (155). However, the genomic instability and accumulation of DNA lesions can result in biological changes in senescent cells. In a previous study, gene expression microarrays were performed, and found common age-associated gene expression features including regulating inflammatory, mitochondrial, and lysosomal degradation pathways (156), but the pattern of expression is dependent on specific tissue subtypes (157). The inflammatory changes have been recognized as senescence-associated secretory phenotype of ageing fibroblast, which found extremely enriched proinflammatory cytokines and matrix metalloproteinases (158).

Immunosenescence

Immunosenescence describes the diverse changes in the immune system that is observed in the elderly, and it affects both the innate and adaptive immune responses (103). This presentation is occasionally found in the young but is increased in the elderly (159). T cell senescence occurs following the involution of thymus gland and the subsequent limited output causing decrease in the naïve T cell repertoire, and the earliest change is found in CD8+ T cells (160). A cross-sectional study found an increase of CD28-CD8+ T cells and contraction of naïve T cells after 65 years of age (123). Therefore, contraction of CD8+ cells or the expansion of the CD4+ compartment is one of the hallmark features. The contraction of naïve T cells and the increase in regulatory T cells, effector-memory T cells, and exhausted T cells are the alteration of T cell distribution and homeostasis in advanced aging (161). Moreover, the impairment of cell division and the accumulation of DNA damage are found in this senescent phenotype together with the defects of cytokine exocytosis and the increased production of proinflammatory cytokines (162). In both types of primary T cells, cytokine production tends to be skewed towards proinflammatory cytokines such as IL-27, interferon-β, and IL-6 which are deviated from healthy T cells, and this aberration is comparable to senescence associated secretory phenotypes(SASP) in senescent fibroblasts (103).

These immune cell features were found to be associated with disease severity in human degenerative diseases (163, 164). Other defects are also observed in the elderly, for example, defects in metabolism, cytokine production, and cell cycle progression (103). These accumulated defects result in the deterioration of the immune system in the elderly. Although age is a main factor responsible for this phenotype, chronic viral infection, such as CMV and HIV can also enhance the senescent T cell populations (165). Moreover, the effects of age overwhelm the

effects of CMV infection (166, 167), and so, the effects of CMV in causing immune senescence is not as strong as the age-related effects (168).

Characteristics of senescent T lymphocytes

Senescent T cells comprise terminally differentiated T cells in all lineages. TEMRA cells are commonly known as highly differentiated T cells which exhibit as senescent T cells (166). Surprisingly, naïve T cells can also develop a senescent phenotypes (160, 169), and the virtual memory T cells (VM), which develops under TCR responds to bystander activation or cytokine without antigen specificity, are expanded in elderly and turned to be senescent (159).

In highly differentiated phenotypes of both CD4+ and CD8+ T cells show defective proliferation and down-regulation of costimulatory molecules (170). For example, several surface markers used to identify senescent T cells, such as CD27-, CD28-, CD45RA+, KLRG1+, and CD57+ (170). The expression of these molecules not only help identify the highly differentiated T cells, but their expression levels also explain the functional defects, for instance, CD28 and CD27 are costimulatory molecules, and those without these receptors expressing are associated with short telomere length and pronounced proinflammatory cytokine production, therefore, this absence determines the defect of T cell activation (159). CD28- T cells consist of a wide range of highly differentiated T cells and may have proliferative functions (171). CD27-, and CD57+ could help classified levels of these highly differentiated cells. CD27-CD28- T cells have more proliferative defects and impaired telomerase activity, a feature of higher differentiated T cells (170), while CD57 expression may be the second step of T cell senescence after the decreased expression of CD28 (46). Both KLRG-1+ and CD57+ T cells have similar proliferative deficiencies, and expression of proinflammatory cytokines is more pronounced in CD28-CD57+ T cells. Surprisingly, CD45RA, which is abundant in naïve T cells, is re-expressed in

this terminally differentiated T cell and is known as terminal effector memory T cell with CD45RA+ (TEMRA) (103).

In CD4+ T cells, although the loss of CD28 is scarcely demonstrated, but the recently found diminished TCR signaling in old mice was convincing. The signal transduction was found to be delayed, especially in the mTOR pathway, which controlled cellular differentiation and metabolism. The epigenetic control of stem-like properties is found to be hypermethylated (172). Moreover, the trafficking function was suspected to be defective because of the decreased homing molecules such as CCR7 and CXCR4. Apparently, the CD8+ T cells display the changes of costimulatory molecules, while the CD4+ T cells illustrate the changes in signal transduction in the ageing process (161).

The cell cycle defect is also a common feature of cellular senescence. The accumulation of DNA damage and the deficiency of telomerase enzyme enhance the cell cycle inhibitory molecules. The increase of p16 and p21, which inhibit cyclin-dependent kinase-4 and cyclin-dependent kinase-6 enzymes, is the hallmark of the cell division defect in cellular senescence. These findings also found the association with CD27-CD28- T cells. Unsurprisingly, the telomere length, which figures both DNA damage and telomerase activity, is ubiquitously used as a senescent marker (127).

The cellular metabolisms control T cell functions and phenotypes. For effector T cells, aerobic glycolysis is the essential pathway in the resting state, while other metabolic pathways are required during the activation. CD4+ and CD8+ T cells require the oxidative glycolysis pathway and glutaminolysis during their activation (173). In senescence, glycolysis pathway is massively invigorated. However, impairment of mitochondria function in senescent cells results in preferentially use of non-oxidative glycolysis to generate the energy. Therefore, the

oxidative metabolism, which is generally used in effector T cells is avoided. A large amount of glucose is required for adequacy. Both non-oxidative metabolism and loss of autophagy exceed oxidative stress in senescent T cells. A study showed the activation of mTORC1 was associated with enhancing T cell proliferation by reactivation of cellular autophagy (155, 174).

4.1.4 T cell senescence in cancer immunology

T cell dysfunction in cancer immunology

T cell dysfunction is a known factor causing immune evasion in cancer and those t cells are including T cell anergy, T cell exhaustion and T cell senescence (175). T cell anergy is a hyporesponsive state of T lymphocyte, whose the activation signals lack of sufficient signals or lack of costimulatory signals, and these T cells were found in the tumor microenvironment with the absence of B7 molecules or with inhibitors of co-stimulatory molecules, and the re-expression of these molecules could restore the activation function of these T cells in animal models (46, 176, 177). T cell exhaustion and T cell senescence were overlain in previous studies, but recently, these entities has been classified differently in terms of markers, gene expressions, and etiologies (46). The presence of exhausted T cells was found in tumor microenvironment and showed the identical characteristics with those in chronic viral infection, in which the chronic stimulation or repeated activation has been proposed as the underlying mechanism, leading to progressive loss of effector functions of these T cells (134, 178). As we know, exhausted T cells express checkpoint molecules such as PD-1, TIM-3, and LAG-3, and these cells are possibly reversed by the immune-checkpoint inhibitors (178, 179), but such effects are not found in senescent T cells (180). Senescent T cells are different from exhausted T

cells in which they contain aging phenotypes like general cellular markers such as limitation of telomerase activity and upregulation of p16 and p21 (20, 181). The mechanism causing senescent T cells is also different from exhausted T cells due to the accumulation of DNA damage markers, and these phenotypes tend to be comparable with those in elder or replicative senescence (46, 180). Moreover, the presence of CD28-, CD27- and CD57+ T cells were also determined senescent phenotypes, and the distinctive features of senescent T cells are enriched of intracellular proinflammatory cytokines but impaired excretory function, proliferative function, and telomerase activity (46, 127). As in replicative senescence, this entity of cells is prominent in effector memory and terminal effector T cells which are resistant to apoptosis (155, 164, 182).

Cancer and immune cell crosstalk resulting in epigenetic changes and DNA damage to trigger senescent T cells

The senescent T cells are interesting phenotypes that can be introduced by cancer-immune cell crosstalk (105, 183). As we know, cellular senescence is associated with the accumulation of DNA damage and genomic instability (153), and these senescent T cells are also prematurely generated, leading to be pronounced in several conditions apart from replicative senescence in elderly (127, 184, 185). As mentioned in chapter 1 and chapter 3, breast cancer cells could hypomethylate human PBMCs, and these hypomethylated PBMCs were found as signature in breast cancer patients (75), therefore, these might be related to cellular senescence, in which DNA hypomethylation is one of the hallmarks (186). Apart from DNA hypomethylation, the accumulation of DNA damage is also one of the key mechanisms of cellular senescence (186). Liu et al. described the role of regulatory T cells and γ/δ-regulatory T cells in inducing T cell senescence by performing the co-culture of regulatory T cells and naïve CD4+T cells, and found the expression of

senescent phenotypes in naïve CD4+T cells (42). These findings were CD28 down-regulation without inhibitory receptors expression, and the senescence-related gene expressions were also found after 24-hour co-culture (42). Intriguingly, they showed the increase of DNA damage markers as the cause of these senescent phenotypic changes including the expression of ATM, γH2AX, CHK2 and p53 (187). Moreover, a previous study showed that the co-culture of cancer cell lines and T cells resulted in the senescent phenotypes at the lower ratio of tumor:T cells., whereas the loss of CD27 and CD28 after a 7-day co-culture was demonstrated (183). Furthermore, the researcher grew breast cancer and melanoma cell-lines in mice and found the new coming tumor infiltrating T lymphocyte and circulating T cells displayed elevated SA-β-gal signal and the increase in p53 and γH2AX (42). The findings could be implied that cancer cells could generate DNA damage events to T cells and resulted in T cell senescence (183). To date, many clinical studies could determine the presence of senescent CD8+ T cells in tumor microenvironment of those with colorectal cancer, pancreatic cancer, and breast cancer (175, 188, 189).

4.1.5 The presence of T cell senescence in breast cancer patients

As mentioned above, premature senescent T cells are found in autoimmune diseases and cancer (43, 44), and a higher proportion of senescent T cells is associated with high severity of autoimmune diseases and cancer (190, 191). Previous studies supported the evidence of cancer-induced senescent T cells from lung, head and neck, multiple myeloma, and breast cancer (45, 46). In breast cancer, the increased proportion of senescent T cells was found in the circulating immune cells including the proportion of CD28-, TEM (CD45RA-CCR7-) and TEMRA (CD45RA+CCR7-) cells, KLRG-1+CD57+ and CD28-CD57+ T cells compared to normal participants (189, 192-195), and CD8+ T cells were found to be a dominant

proportion of those T cells, where the percentages of those cells were dependent on markers, for example, 45% in CD8+TEMRA and 67.5% in CD8+CD28- T cells (192, 194). Apart from the presence of senescent T cells, a higher proportion of CD28-CD8+ T cells were found to be associated with poorer prognostic breast cancer including the lymph node spreading disease, and shorter overall survival metastatic disease (190, 196).

Currently, there are several immune checkpoint inhibitors, which could restore immune functions in exhausted T cells, but not senescent T cells. The presence of senescent T cells has been found in breast cancer patients, but the presence of non-exhausted senescent T cells in breast cancer patients is not well understood. Moreover, the impact of natural senescence on premature senescence in breast cancer patients is unknown. This gap in knowledge would be helpful regarding treatment by targeting senescent immune cells and adoptive T cell transfer in breast cancer patients. Therefore, the aim of this study was to examine the presence of non-exhausted T cell senescence in breast cancer patients.

4.2 Results

4.2.1 T cell senescence panels

To create the T cell senescence panels, a range of markers were used to identify senescence, viability, and T cell differentiation. The SPiDER- βgal kit enabled the fluorescence emission of the SA-β-gal assay as presented in Table 4.1. Zombie aqua dye was used for the detection of apoptotic cells, which emitted at a maximum wavelength of 516 nm. Other markers were the fluorophore-conjugated monoclonal antibodies used for cell surface staining, as shown in Table 4.1. Before combined staining experiment was performed, compensation and single staining were conducted. The compensation matrix was created and calibrated following the instrument protocols. Subsequently, the fluorescence minus one staining was applied to all markers as shown in Figure 4.1, then, representative flow cytometry plots were sequentially gated as shown in Figure 4.2.

Table 4.1 Markers in T cell senescence panels and their fluorophores, excitation lasers, and emission filters.

Excitation Laser	Emission filter (nm)	Fluorophore	Markers
Violet (405nm)	450/50	BV 421	CD4
	516	Zombie Aqua	Viability
	660/20	BV-650	CD8
Blue (488nm)	530-570	SPiDER- βgal	SA-β-gal
	670/14	PE-Cy5	CD3
	780/60	PE-Cy7	CD57
Red (638nm)	660/20	Alexa 647	CD45
	730/45	Alexa 700	PD1
	780/60	APC-Cy7	CD28

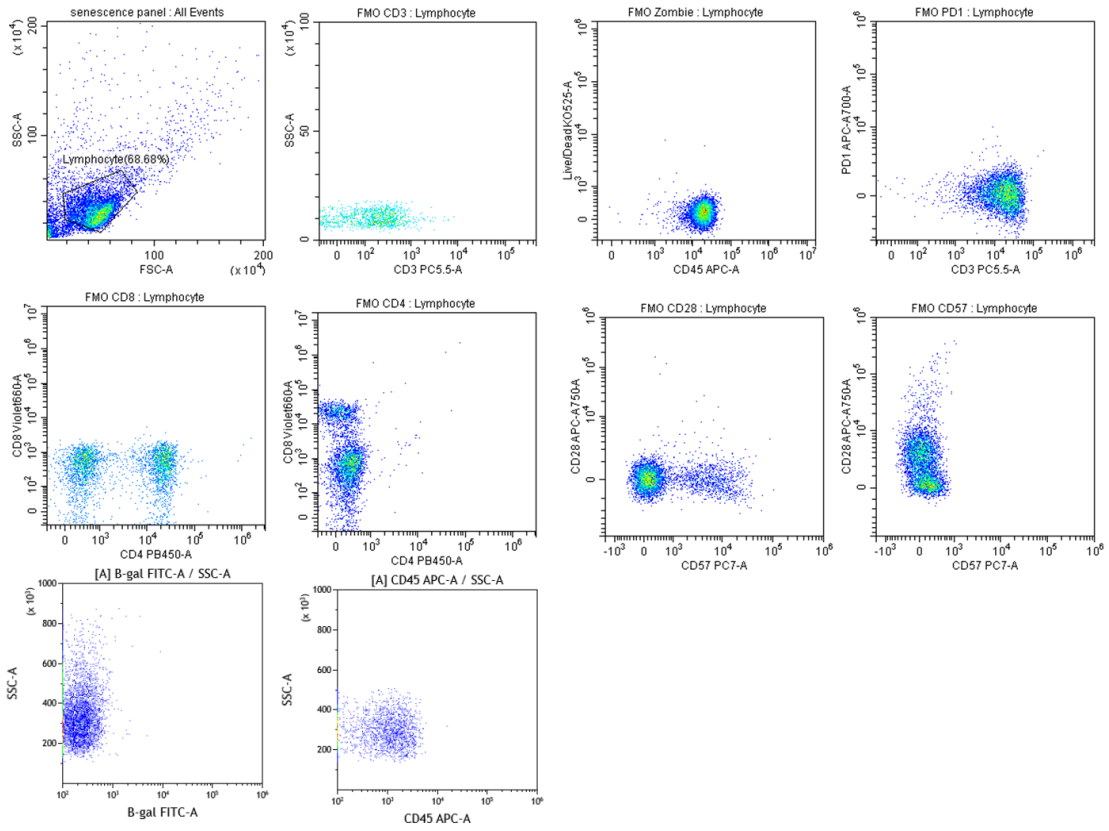

Figure 4.1 The representative flow cytometry plots of fluorescent minus one (FMO) control for each fluorescence channel are displayed.

4.2.2 The gating procedure

The representative flow cytometry plots were analyzed as follows. Firstly, the viable T cells were gated as proportions of CD4+, CD8+ and PD1+ subpopulations. In this study, PD1 negative expression was used to distinguish and exclude exhausted T cells to determine non-exhausted senescent T cells. Therefore, the CD3+PD1- cells were subsequently classified into CD4+PD1- and CD8+PD1- groups. These CD3+, CD4+, CD8+ and the PD1- subpopulations were differentiated according to their senescent markers including SA-β-gal hi+, CD28 expression, and CD57 expression as shown in Figure 4.2.

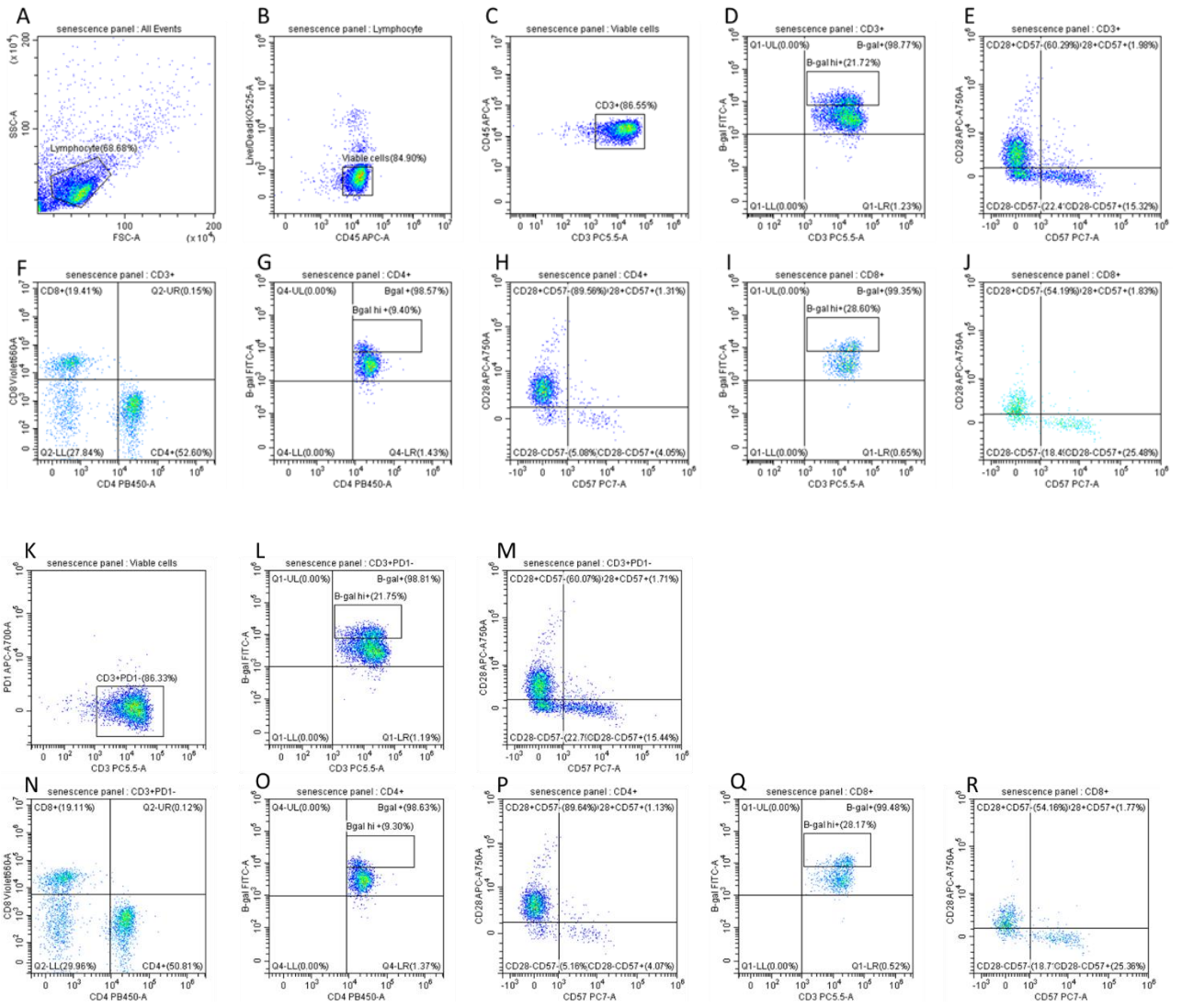

Figure 4.2 The sequence of representative flow cytometry plot selection. Lymphocytes were selected from FSC and SSC flow cytometric plot (A), and Zombies aqua negative cells were gated as viable cells (B), then, were demonstrated as CD3+ population (C) and CD3+PD1- (K). These plots were differentiated into the proportion of CD4+ and CD8+ T cells (F, N). Moreover, The CD3+, CD4+, CD8+ and their PD1- subpopulations were delineated according to the senescent phenotypes, including SA-β-gal hi+ (D, G, I, L, O, Q), CD28 expression, and CD57 expression (E,H,J,M,P,R).

4.2.3 The concordance of T cell senescence phenotypes

In this study, SA-β-gal hi+, CD28 and CD57 expression were used to differentiate the senescent T cells. The SA-β-gal assay separated the PBMCs into SA-β-gal hi+ and SA-β-gal lo+ from flow cytometry as shown in Figures 4.3. In addition, the flow cytometry plots of CD3+ T cells were differentiated by the SA-β-gal assay and the proportion of combined CD28 and CD57 expression were presented as in Figure 4.3, and nearly all SA-β-gal hi+ T cells were CD28- and either CD57- or CD57+ expression (Figure 4.3C), while SA-β-gal lo+ cells were CD28+ (Figure 4.3E). These features were used to determine the senescent cell markers.

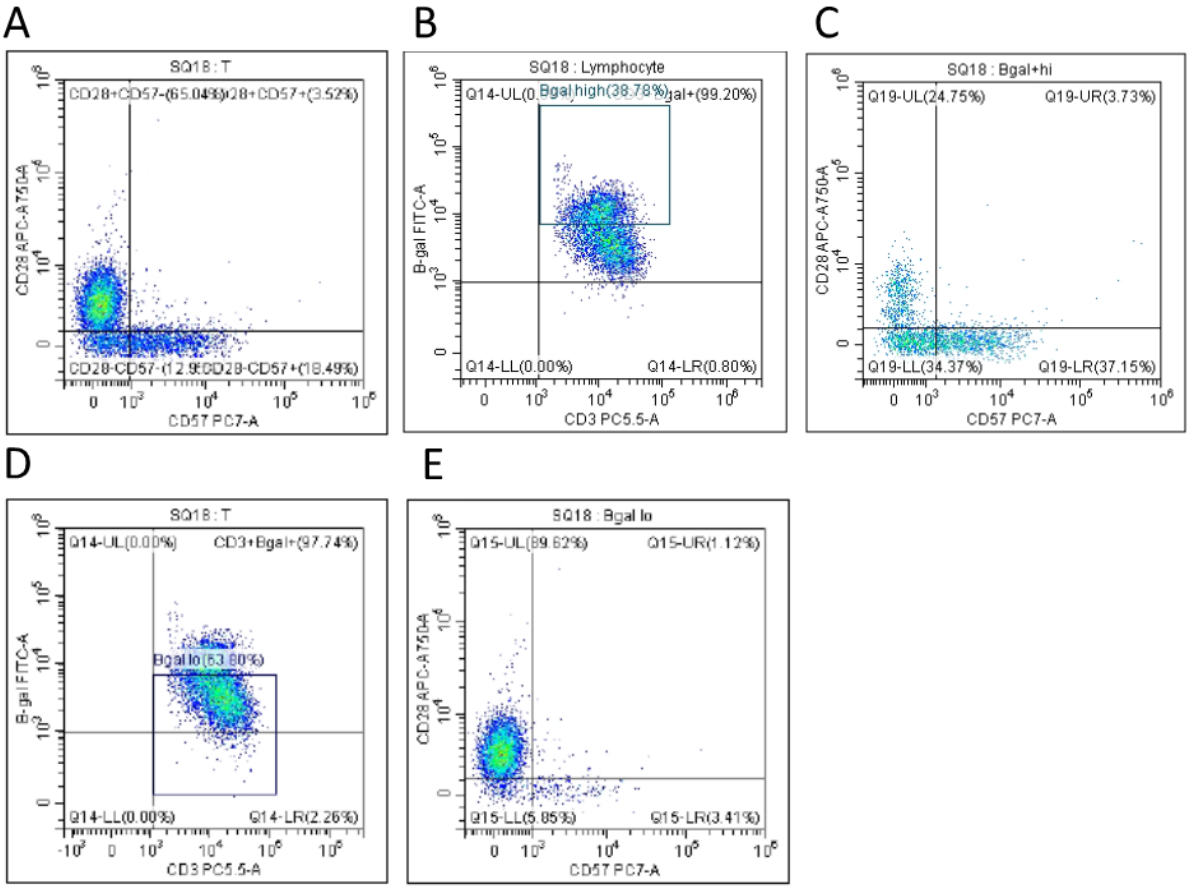

Figure 4.3 Representative plots of SA-β-gal and CD28/CD57 expression in PBMCs. The plot A shows CD28 and CD57 expression in CD3+ T lymphocytes. The plot B and D show SA-β-gal stained PBMCs divided into 2 groups: SA-β-gal hi+ (B) and SA-β-gal lo+ (D). In addition, the plot C and E show CD28/CD57 expression in the SA-β-gal hi+ which was CD28- cells (C), while SA-β-gal lo+ cells show CD28+ cells (E).

4.2.4 Patient characteristics

In this study, there were 47 breast cancer patients and 41 healthy volunteers, with a mean age of 50.74 years in the breast cancer group and 49.34 years in the control group. The body mass index and menopausal status, as well as the

clinicopathological characteristics of the breast cancer patients, were displayed in Table 4.2.

Table 4.2 Demographic data and clinicopathological characteristics in cancer group.

	Cancer (47)	**Control (41)**
Age	50.74 (30-68)	49.34 (30-69)
BMI	23.64 (16.77-37.97)	22.39 (14.81 – 29.32)
Menopausal status		
Pre-menopause	24 (51%)	19 (46%)
Post-menopause	23 (49%)	22 (54%)
Stage		
I	18 (38%)	
II	18 (38%)	
III	6 (13%)	
IV	5 (11%)	
Grade		
1	9 (19%)	
2	18 (38%)	
3	20 (43%)	
ER		
Positive	35 (74%)	
Negative	12 (26%)	
PR		
Positive	26 (55%)	
Negative	21 (45%)	
HER2		
Positive	12 (26%)	
Negative	35 (74%)	

4.2.5 The PD1 negative cells could enrich proportions of senescent T cells in both cancer patients and healthy participants

The samples from both cancer patients and healthy controls were examined for the senescent T cell proportions in CD3+, CD4+ and CD8+ T cells. PD1 was used as a marker for the exhaustion phenotype, and PD1- subpopulation was examined for the senescence phenotypes to determine proportions of non-exhausted senescent T cells. Because PD1+ T cell population was a minority of circulating T cells and the further investigation of PD1+ cells was not possible, proportions of T cells were compared with PD1- T cells to evaluate whether non-exhausted senescent T cells were different entities from exhausted T cell lineage, and whether non-exhausted senescent T cells were the majority of senescence phenotypes in circulating T cells. The comparisons were performed by paired t-test. Proportions of senescent T cells was significant higher in PD1-CD8+ T cells in all markers including SA-β-gal hi+ cells (25.80% vs 30.25%, $p = 0.0005$), CD28- cells (36.48% vs 45.68%, $p < 0.0001$), CD28-CD57- cells (18.01% vs 22.38%, $p < 0.0001$) and CD28-CD57+ cells (18.47% vs 23.40%, $p < 0.0001$) as shown in Figure 4.4. Moreover, in CD4+ T cells, these significantly higher senescent T cell proportions were also found in CD28- cells (8.97% vs 10.46%, $p = 0.008$) and CD28-CD57+ cells (18.47% vs 23.40%, $p < 0.0001$), and the higher senescent proportions were also found in in SA-β-gal hi+ cells (11.14% vs 12.91%, $p = 0.072$) and CD28-CD57- cells (5.03% vs 5.66%, $p = 0.087$), but no statistically significant differences were observed. These findings support the presence of non-exhausted senescent T cells which are different from exhausted T cell lineage, and PD1- marker could be enriched in senescent T lymphocytes especially in CD8+ T cells. These cells could be considered as non-exhausted senescent T lymphocytes.

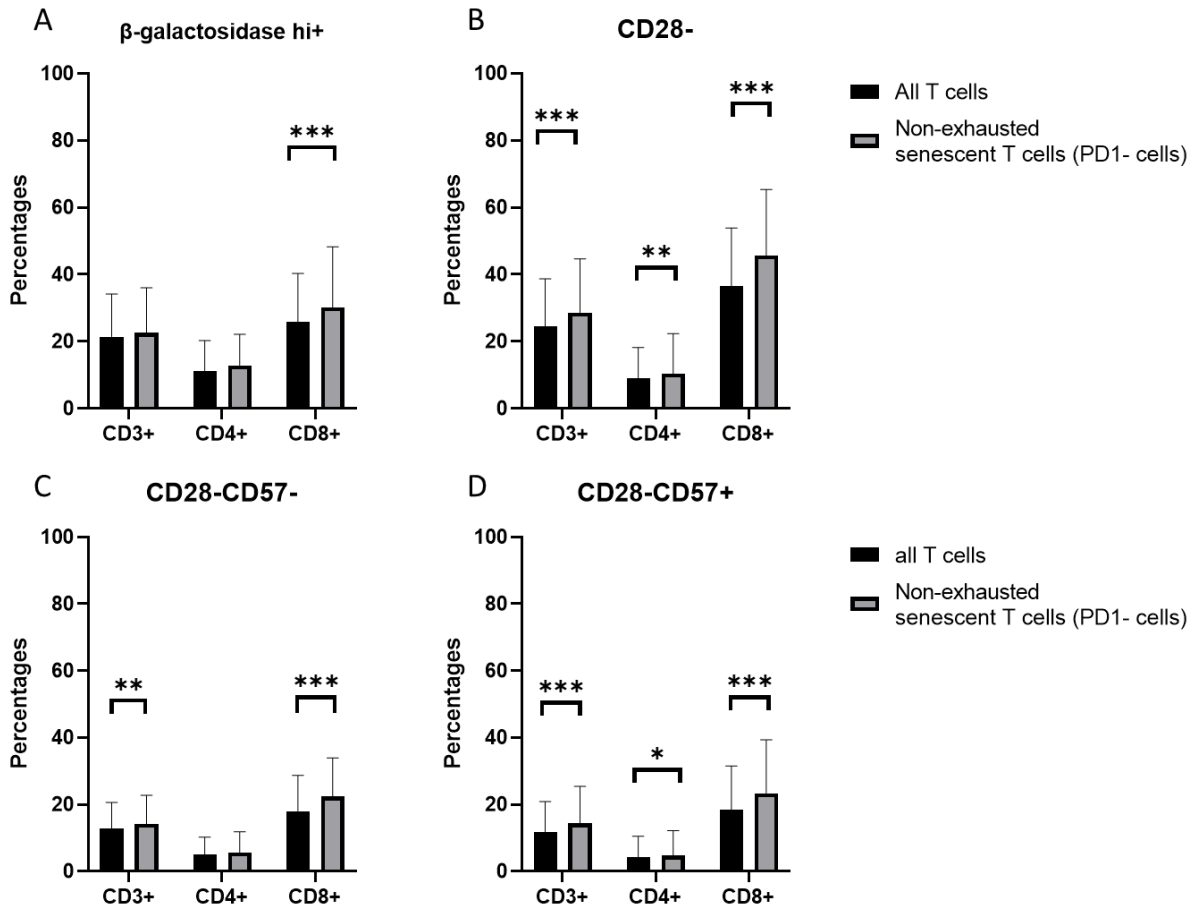

Figure 4.4 Proportions of senescent T cells in all CD3+, CD4+, and CD8+ T cells compared with non-exhausted senescent T cells (PD1-). These figures show proportions of SA-β-gal hi+ cells (A), CD28- cells (B), CD28-CD57- (C), and CD28-CD57+ (D) in all CD3+, CD4+, and CD8+ T cells (13) and non-exhausted senescent T cells (grey). (N=88 and asterisks indicate p values, *= $p < 0.05$, **= $p < 0.01$ and ***=$p < 0.001$)

4.2.6 CD28-CD57+ T cells were correlated with age in both healthy participants and cancer patients

To determine the effects of natural T cell senescence, we performed the Pearson correlation of T cell senescent phenotypes and function of age in healthy volunteers and breast cancer patients. The correlation tended to be more consistent in CD8+ T cells and non-exhausted CD8+ T cells which were significantly correlated with age in both healthy volunteers and breast cancer patients as shown in Table 4.3. For instance, in SA-β-gal hi+ cells, the CD8+ T cells showed a significant correlation in healthy group ($p = 0.014$) and cancer group ($p = 0.021$), and non-exhausted CD8+ also showed significant correlation in cancer group ($p = 0.013$), and seemed to be correlated with age in healthy group ($p = 0.098$), but no statistical significance was observed. For CD28- cells, both CD8+ T cells and non-exhausted CD8+ T cells displayed a significant correlation with age in healthy volunteers ($p = 0.044$ and 0.049, respectively), while these correlations were not observed in breast cancer group (Table 4.3). In the meantime, CD28-CD57+CD8+ T cells were significantly correlated with age in both healthy group ($p = 0.008$ in CD8+ T cells, and $p=0.019$ in non-exhausted CD8+ T cells) and cancer group ($p = 0.044$ in CD8+ T cells, and $p=0.022$ in non-exhausted CD8+ T cells), however, CD28-CD57- T cells did not show a significant correlation.

Table 4.3 The Pearson correlation coefficient of senescent markers and the progression of age in cancer group (N=47) and healthy control (N=41). (Asterisks indicate p value, *= $p < 0.05$, **= $p < 0.01$)

Phenotypes	**Healthy control**		**Cancer group**	
	Correlation coefficient (R)	p value	Correlation coefficient (R)	p value
SA-β-gal hi+				
CD3+	0.107	0.507	0.227	0.125
CD4+	0.177	0.268	0.029	0.845
CD8+	0.380	0.014*	0.336	0.021*
CD3+PD1-	0.170	0.288	0.187	0.207
CD4+PD1-	-0.046	0.776	0.011	0.939
CD8+PD1-	0.262	0.098	0.360	0.013*
CD28-				
CD3+	-0.226	0.155	-0.078	0.603
CD4+	0.151	0.347	-0.239	0.105
CD8+	0.317	0.044*	0.149	0.316
CD3+PD1-	0.225	0.158	-0.046	0.756
CD4+PD1-	0.061	0.705	-0.190	0.200
CD8+PD1-	0.310	0.049*	0.191	0.199
CD28-CD57+				
CD3+	0.370	0.017*	0.073	0.624
CD4+	0.193	0.227	-0.177	0.233
CD8+	0.409	0.008**	0.295	0.044*
CD3+PD1-	0.338	0.031*	0.092	0.538
CD4+PD1-	0.117	0.468	-0.220	0.138
CD8+PD1-	0.364	0.019*	0.334	0.022*

4.2.7 The non-exhausted senescent T cells were significantly increased in breast cancer patients

To determine the effects of breast cancer on the senescence phenotypes of T lymphocytes, the mean proportion of each senescent phenotype was compared between healthy volunteers and breast cancer patients by unpaired t-test. Firstly, the proportions of CD4+ cells and CD8+ cells were not significantly different between the cancer group and the control group. Although the CD8+PD1+ cells and CD4+PD1+ cells showed higher mean percentages in the cancer group, no statistical significance was observed (Table 4.4). In the SA-β-gal hi+ population, the CD3+ cells were significantly increased in the cancer group ($p = 0.013$), while the CD4+ and CD8+ were not significant ($p = 0.082$ and 0.085 respectively), but CD3+PD1-, CD4+PD1- and CD8+PD1- cells were significantly higher in the cancer group ($p = 0.011$, 0.026, and 0.032 respectively) as shown in Table 4.4. In the CD28- cells, the CD3+ and CD8+ T cells were increased in the cancer group, and similarly, the increased proportions were significantly increased in cancer group in non-exhausted T cells ($p = 0.001$ in CD3+PD1- and $p < 0.001$ in CD8+PD1-). CD57 expression status was further determined in CD28- T cells to examine the effects of breast cancer on CD28-CD57- and CD28-CD57+ T cells. In CD28-CD57- T cells, CD3+ T cells were significantly increased in cancer group ($p = 0.027$), but no statistical significance was observed in CD4+ and CD8+ T cells ($p = 0.115$ and 0.106 respectively), while these cells were significantly increased in non-exhausted senescent T cells in both CD3+PD1- and CD8+PD1- T cells ($p = 0.016$ and 0.003 respectively) as shown in Table 4.4. In CD28-CD57+ T cells, CD3+ T cells were significantly increased in cancer group ($p = 0.024$), but no statistical significance was observed in CD4+ and CD8+ T cells ($p = 0.065$ and 0.127, respectively), while these cells were significantly increased in non-exhausted senescent T cells in

CD3+PD1-, CD4+PD1- and CD8+PD1- T cells ($p = 0.004$, 0.044 and 0.015 respectively) as shown in Table 4.4. These findings support the presence of increased senescent T cells in breast cancer especially in non-exhausted T cells (PD1-), and these effects were significant in SA-β-gal hi+, CD28-, CD28-CD57-, and CD28-CD57+. Representative flow cytometry plots of a 45-year-old stage-2 breast cancer female, a 49-year-old healthy female, and a 62-year-old healthy female are shown in Figure 4.5, Figure 4.6, and Figure 4.7, respectively.

Table 4.4 Mean proportions of T cell phenotypes in breast cancer group and healthy control group. (Asterisk indicates p value, *= $p < 0.05$, **= $p < 0.01$ of differences between the cancer (n=47) and healthy (n=41) groups)

Phenotypes	**Percentages of cells Mean ± SEM.**		**p-value**
	cancer	control	
CD3+CD4+	49.84 ± 2.29	55.59 ± 1.88	0.059
CD3+CD8+	37.31 ± 1.99	33.33 ± 1.58	0.128
CD4+/CD8+ ratio	1.62 ± 0.13	1.94 ± 0.16	0.123
CD3+PD1+	19.88 ± 2.39	14.25 ± 1.74	0.059
CD8+PD1+	20.15 ± 2.48	14.08 ± 1.87	0.066
CD4+PD1+	19.29 ± 2.39	13.36 ± 1.64	0.050
SA-β-gal hi+			
CD3+*	24.53 ± 2.08	17.88 ± 1.51	0.013
CD4+	12.72 ± 1.39	9.33 ± 1.32	0.082
CD8+	28.28 ± 2.04	22.95 ± 2.29	0.085
CD3+PD1-*	25.97 ± 1.97	18.73 ± 1.93	0.011
CD4+PD1-*	14.94 ± 1.45	10.57 ± 1.24	0.026
CD8+PD1- *	34.07 ± 2.56	25.88 ± 2.77	0.032
CD28-			
CD3+*	28.29 ± 2.35	20.18 ± 1.58	0.001
CD4+	10.30 ± 1.52	7.45 ±1.18	0.149
CD8+*	40.19 ± 2.60	32.23 ± 2.52	0.032
CD3+PD1-*	33.76 ± 2.59	22.72 ± 1.76	0.001
CD4+PD1-	12.79 ± 2.02	7.79 ± 1.37	0.050
CD8+PD1-*	53.03 ± 2.79	37.25 ± 2.65	<0.001
CD28-CD57-			
CD3+*	14.52 ± 1.35	10.85 ± 0.80	0.027
CD4+	5.65 ± 0.85	4.32 ± 0.68	0.115
CD8+	19.74 ± 1.70	16.03 ± 1.44	0.106
CD3+PD1-*	16.27 ± 1.44	11.92 ± 0.94	0.016
CD4+PD1-	6.64 ± 1.02	4.54 ± 0.78	0.128
CD8+PD1-*	25.81 ± 1.83	18.44 ± 1.41	0.003
CD28-CD57+			
CD3+*	13.73 ± 1.49	9.33 ± 1.15	0.024
CD4+	5.20 ± 1.02	3.13 ± 0.81	0.065
CD8+	20.45 ± 1.91	16.21 ± 1.99	0.127
CD3+PD1-*	17.49 ± 1.76	10.80 ± 1.34	0.004
CD4+PD1-*	6.15 ± 1.21	3.25 ± 0.92	0.044
CD8+PD1-*	27.23 ± 2.38	19.01 ± 2.28	0.015

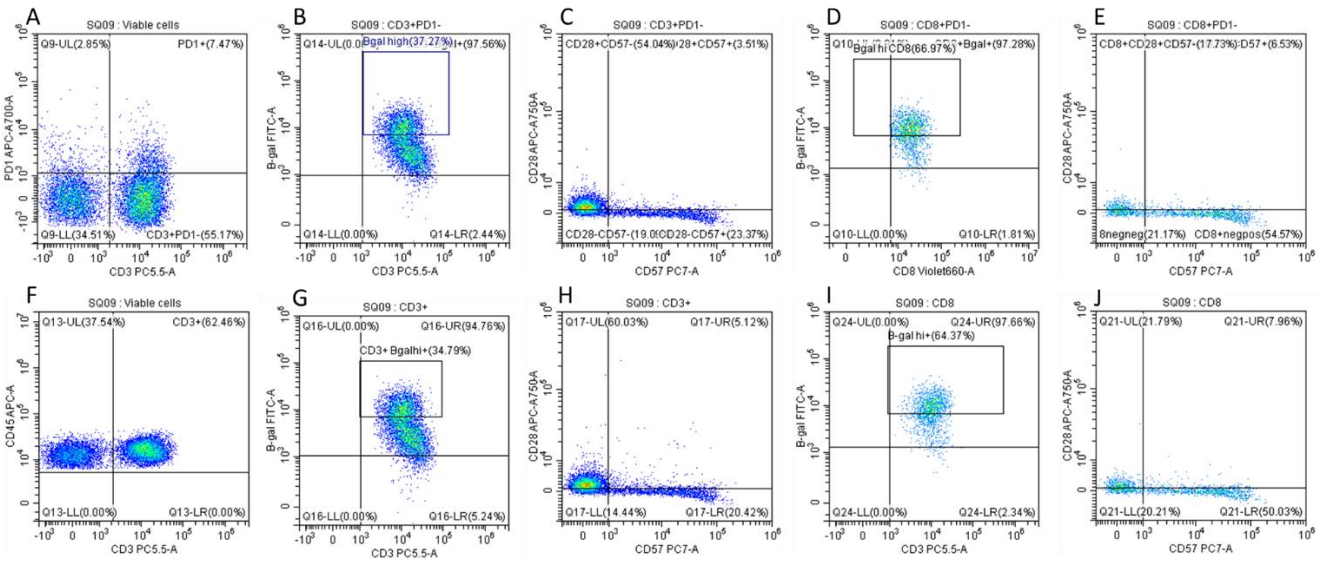

Figure 4.5 Representative flow cytometry plots are demonstrated for a 45-year-old stage-2 breast cancer female. Plots A-E are the CD3+PD1- and CD8+PD1- population, and plots F-J are the CD3+ and CD8+ population.

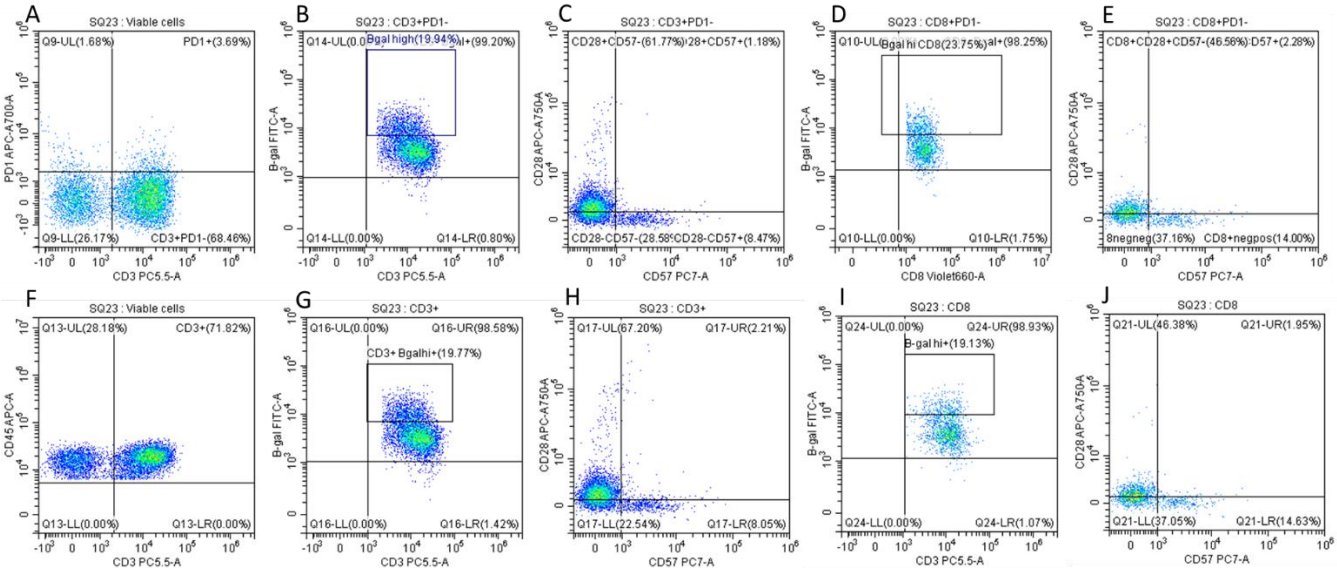

Figure 4.6 Representative flow cytometry plots are demonstrated for a 49-year-old healthy female. Plots A-E are the CD3+PD1- and CD8+PD1- population, and plots F-J are the CD3+ and CD8+ population.

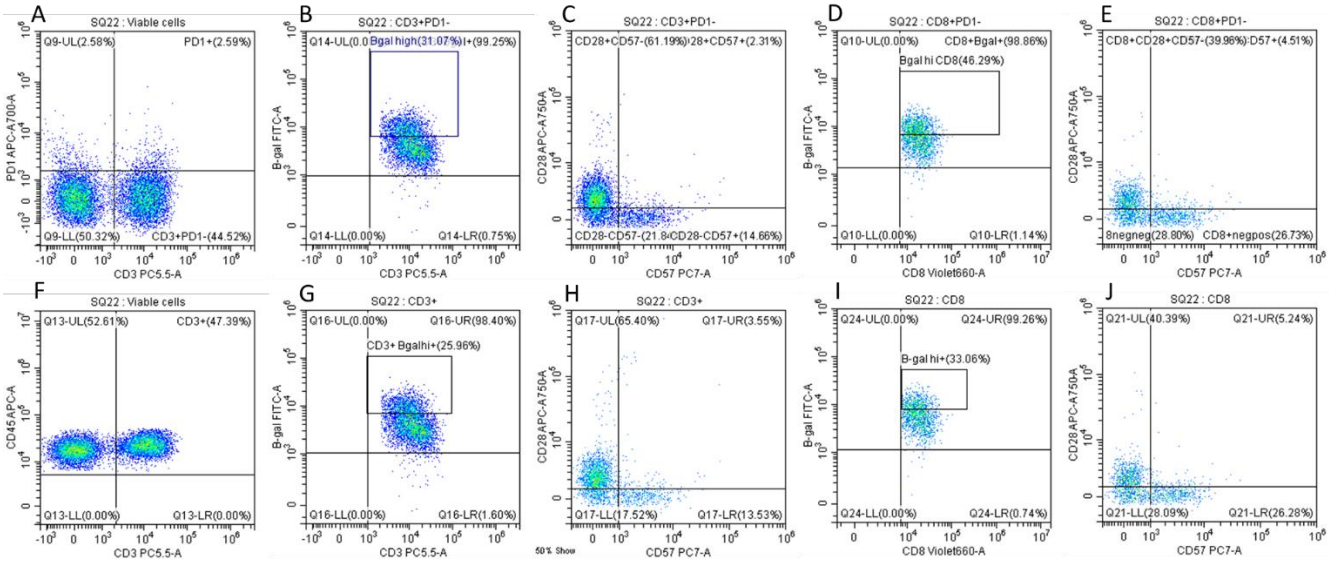

Figure 4.7 Representative flow cytometry plots are shown for a 62-year-old healthy female who was the oldest age group in this study. Plots A-E are the CD3+PD1- and CD8+PD1- population, and plots F-J are the CD3+ and CD8+ population.

4.2.8 The cancer associated T cell senescence phenotypes differently increase in young age and old age groups

The cancer patients were classified into 4 age groups which were 30-39, 40-49, 50-59, and 60-69 years old, with at least 10 participants in each group, and these stratified age groups were divided into 2 age groups : young age group (30-49 years old) and old age group (50-69 years old) to compare proportions of non-exhausted senescent T cells between healthy participants and cancer patients by unpaired t-test. Cancer-associated changes of SA-β-gal hi+ cells tended to be affected with the progression of age in CD8+PD1- group, but no statistical differences were observed between healthy participants and cancer patients in both age groups ($p = 0.233$ in young age group and $p=0.093$ in old age group) as shown in Figure 4.8. The increase of CD28- cells in cancer patients was associated with increased proportions of both

CD28-CD57- and CD28-CD57+ T cells as mentioned above. In young age group, both CD28-CD57- T cells and CD28-CD57+ T cells were significantly increased in breast cancer patients (28.37% vs 19.32%, p = 0.018 and 22.39% vs 13.66%, p = 0.033 respectively), while CD28-CD57- T cells were significantly increased in old age group (23.74% vs 17.52%, p = 0.047) and CD28-CD57+ T cells were slightly increased without statistical significance. Therefore, the senescent T cells were prematurely increased in young breast cancer patients in both phenotypes, and the increase in CD28-CD57- T cells was cancer effects irrespective of age.

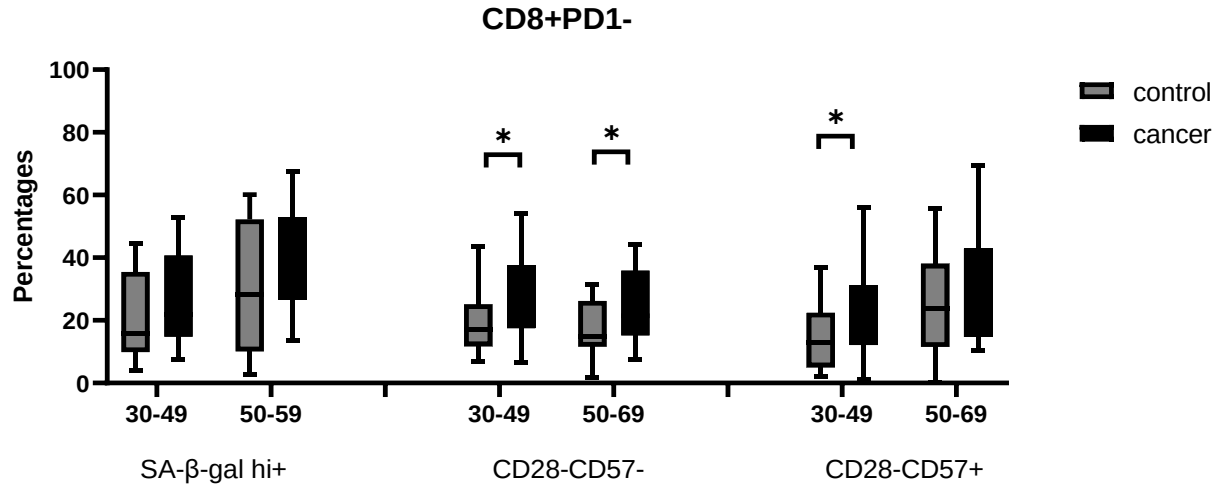

Figure 4.8 Proportions of non-exhausted senescent CD8+ T cells in healthy participants and breast cancer patients in young age group (30-49 years old, N=21 in both cancer and control groups) and old age group (50-69 years old, N=20 in control group and N=22 in cancer group). These figures show the percentages of SA-β-gal hi+ cells, CD28-CD57-, and CD28-CD57+ in breast cancer patients (13), and healthy participants (grey), whereas stratified into young-age group and old-age group. (asterisk indicates p values, *= $p < 0.05$)

4.2.9 The prominently increased CD28-CD57- senescent T cells were attenuated after 52 years of age

The increase of senescent T cells was altered by the progression of age such that the increase of CD28-CD57- was found irrespective of age in cancer patients, while the expansion of CD28-CD57+ subpopulation was also the effects of replicative senescence. The proportion of these progressive changes could determine major senescence phenotypic changes in particular age group, and could imply for further intervention. To determine this cut point, a linear regression model was calculated as the CD28-CD57+/CD28- ratios with age in cancer and control groups and these models seemed fit with linear regression models as shown in Figure 4.9 (R^2=0.124, p=0.015 and R^2 = 0.10 p = 0.047, respectively). The equation was used to determine the specific age at which the CD28-CD57+ population became dominant or gained a ratio of 0.5. As a result, this inversion effect occurred at 57.1 years old in control group and 52.6 years old in cancer group. Therefore, the cancer-associated T cell senescence would be dominantly affected by the CD28-CD57+ subgroup after 52.6 years of age.

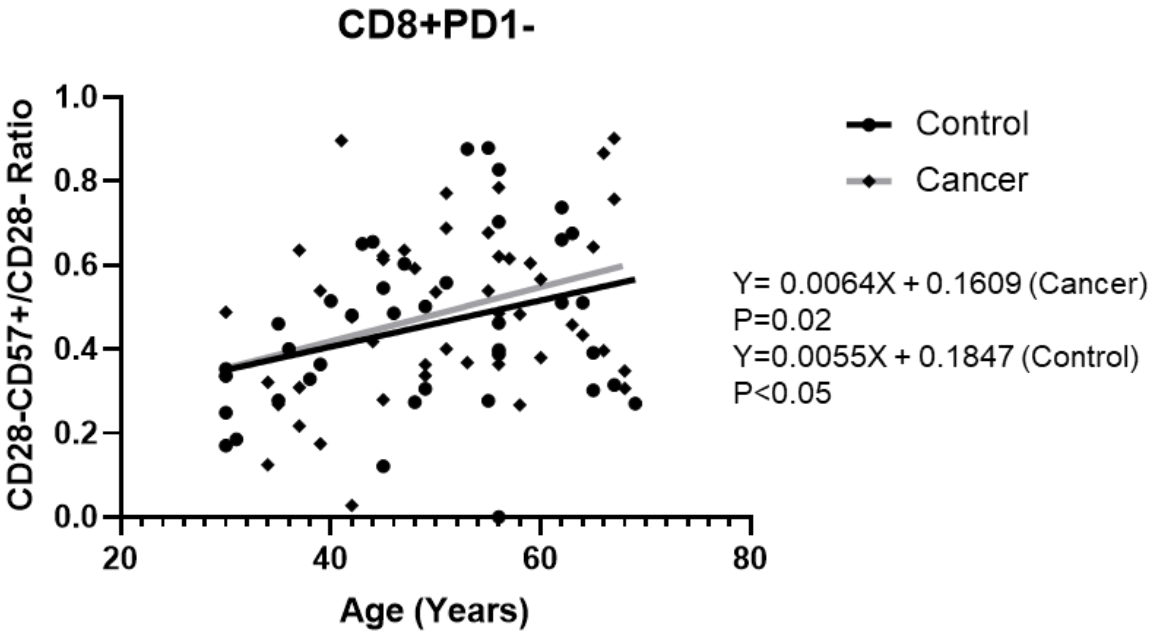

Figure 4.9 The linear regression of CD28-CD57+/CD28- ratios with age in cancer and control groups. (N=47 in cancer group, and N=41 in control group)

4.2.10 Breast cancer associated T cells and impairment of activation functions

To evaluate the function of circulating T cells, 15 PBMC samples (from 6 breast cancer patients and 9 healthy volunteers) were analyzed. Mean age of healthy volunteers was 51.78 years old, ranging from 36-69 years old, while the mean age of cancer participants was 49.33 years old, ranging from 30-66 years old. AntihumanCD3, antihumanCD28 and IL-2 were used to activate T cells. CD69 was used to identify activated T cells in CD3+, CD4+, and CD8+ subgroups. The proportion of CD69+ cells was examined by flow cytometry as shown in Figure 4.10. In CD3+ T cells, the mean proportions of CD69+ were 23.67% in the cancer group and 30.35% in the control groups. Subsequently, the percentages of CD69+ were further examined in CD4+ and CD8+ subgroups. The proportions of

CD4+CD69+ were 26.00% and 31.26% in cancer and control groups, respectively. Moreover, the proportions of CD8+CD69+ were 18.27% and 27.05% in cancer and control groups, respectively. However, no statistically significant differences were observed (Figure 4.11).

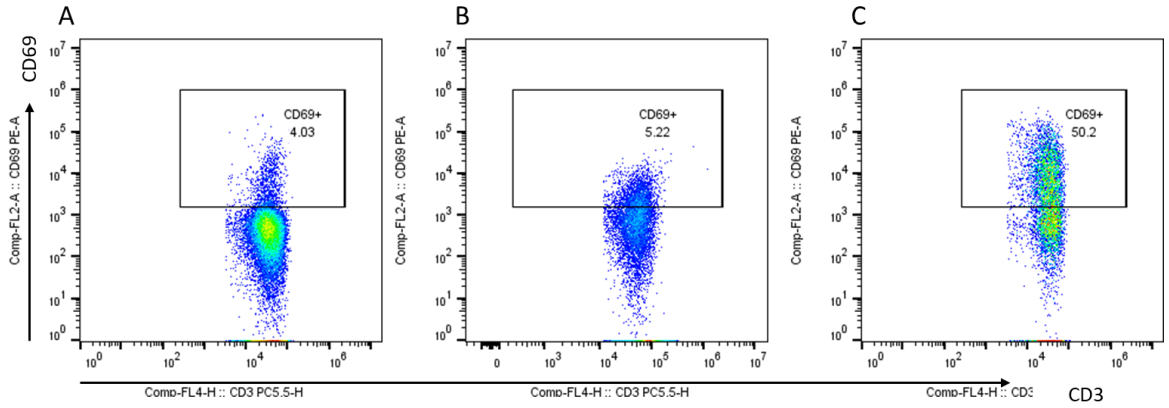

Figure 4.10 Representative flow cytometry plots show the CD69+ after antihuman CD3, antihuman CD28 and IL2 activated T cells in cancer patients (B), and healthy participants (C). Plot A shows CD69+ expression in non-activated PBMCs.

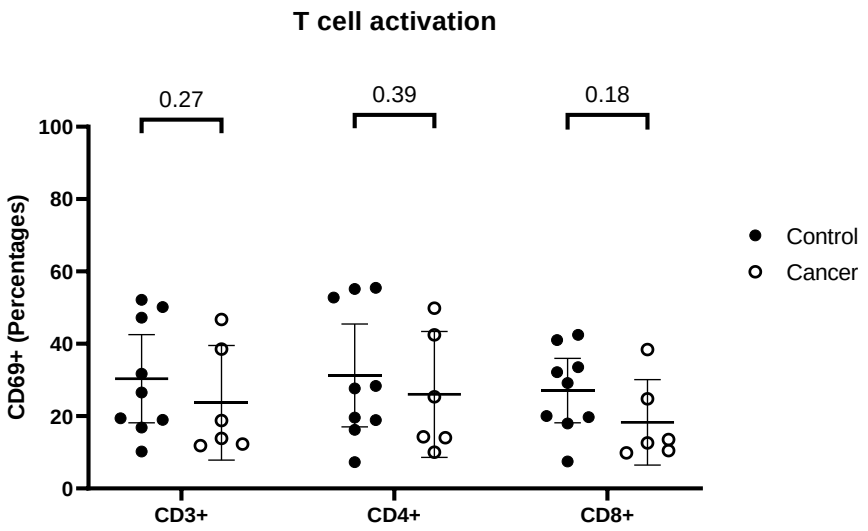

Figure 4.11 Proportions of CD69+ T cells after antihuman CD3, antihuman CD28 and IL2 activated T cells. The figures show scatter plots of percentages of CD69+ cells in CD3+, CD4+, and CD8+ T lymphocytes. The p-values were determined by t-test comparison. (N=6 in cancer group and N=9 in control group)

4.2.11 Non-exhausted senescent CD8+ T cells in breast cancer patients

Our cohort of 47 breast cancer patients was examined for the proportion of T cell senescence phenotypes and the association with cancer characteristics. From the previous data, the CD8+ T cells were affected by cancer-associated senescent phenotypes, and the non-exhausted senescent T cells demonstrated a significant increase in cancer patients, therefore, the senescent CD8+PD1- subpopulation was used to examine for differences of these proportions according to breast cancer prognostic factors, including anatomical staging, histologic grade, surrogate subtypes, estrogen receptor status, progesterone receptor status, and human epidermal growth factor receptor-2 status. The senescent phenotypes included SA-β-gal hi+, CD28-, CD28-CD57-, and CD28-CD57+. The mean proportions of T cell

senescence phenotypes are shown in Table 4.5. The mean proportion of CD28-CD57- T cells showed significantly increased in metastatic disease compared to non-metastatic disease (38.53% vs 24.05%, p = 0.015) as shown in Figure 4.12, however, the surrogate subtypes were not different among groups as shown in Figure 4.13.

Table 4.5 Proportions of senescent T cells as a function of breast cancer prognostic factors. (N=47)

Factors (N)	Mean age (Y)	β-gal(%)	P-value	$CD28^-$ (%)	P-value	$CD28^-CD57^-$(%)	P-value	$CD28^-CD57^+$(%)	P-value
Stage			0.123		0.240		0.015		0.700
Non-metastasis (5)	50.67	33.91		52.35		24.05		28.30	
Metastasis (42)	51.40	46.94		63.67		38.53		25.13	
Subtype			0.407		0.576		0.423		0.719
Luminal A(10)	52.00	39.68		59.01		27.63		31.37	
Luminal B(25)	50.92	32.15		49.58		23.11		26.46	
HER2+(197)	59.00	54.89		60.90		24.06		36.84	
TNBC(11)	48.45	31.46		54.75		30.43		24.31	
Grade			0.283		0.766		0.866		0.717
1 (9)	51.89	28.58		51.33		23.75		27.59	
2 (18)	52.67	39.01		55.67		26.22		29.45	
3 (20)	48.50	32.10		51.43		26.36		25.07	
ER			0.882		0.645		0.194		0.651
Positive (35)	51.23	34.30		52.27		24.40		27.87	
Negative(12)	49.33	33.41		55.26		29.90		25.36	
PR			0.795		0.960		0.494		0.558
Positive(26)	49.88	34.68		53.16		24.67		28.50	
Negative(21)	51.81	33.32		52.88		27.22		25.65	
HER2			0.557		0.707		0.720		0.472
Positive(12)	48.92	31.46		51.21		26.95		24.27	
Negative(35)	51.37	34.97		53.66		25.42		28.24	

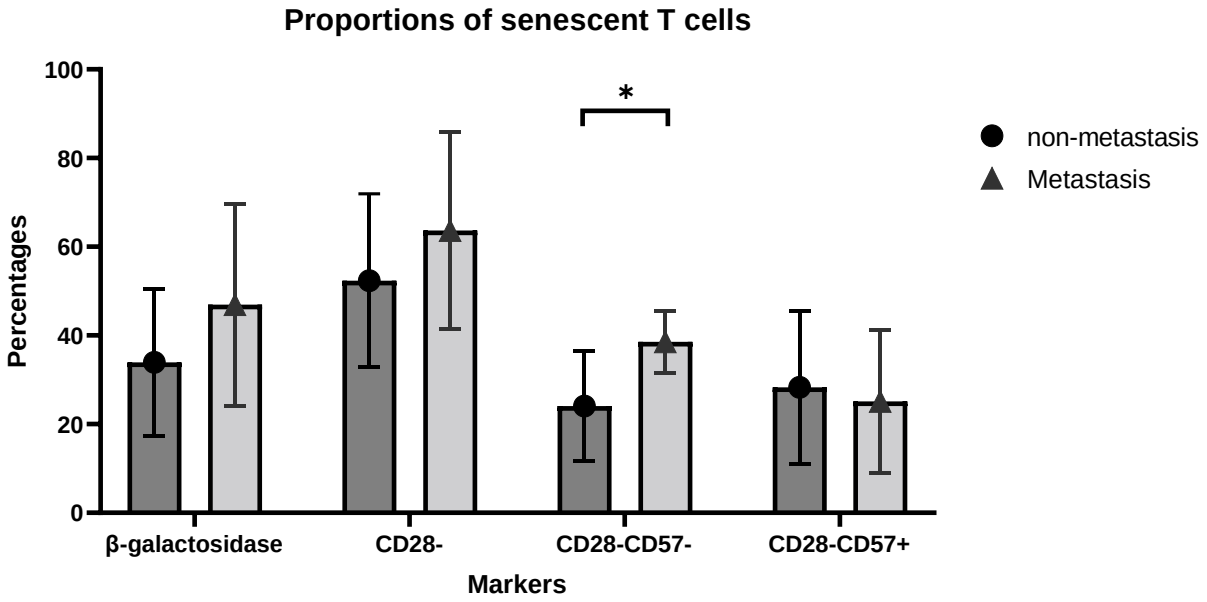

Figure 4.12 Proportions of senescent T cells according to anatomical staging. The bars show mean and standard deviation of proportions of non-exhausted senescent T cells according to metastatic conditions. The proportion of CD28-CD57- T cells shows significant differences according to staging ($p = 0.015$). (N=47)

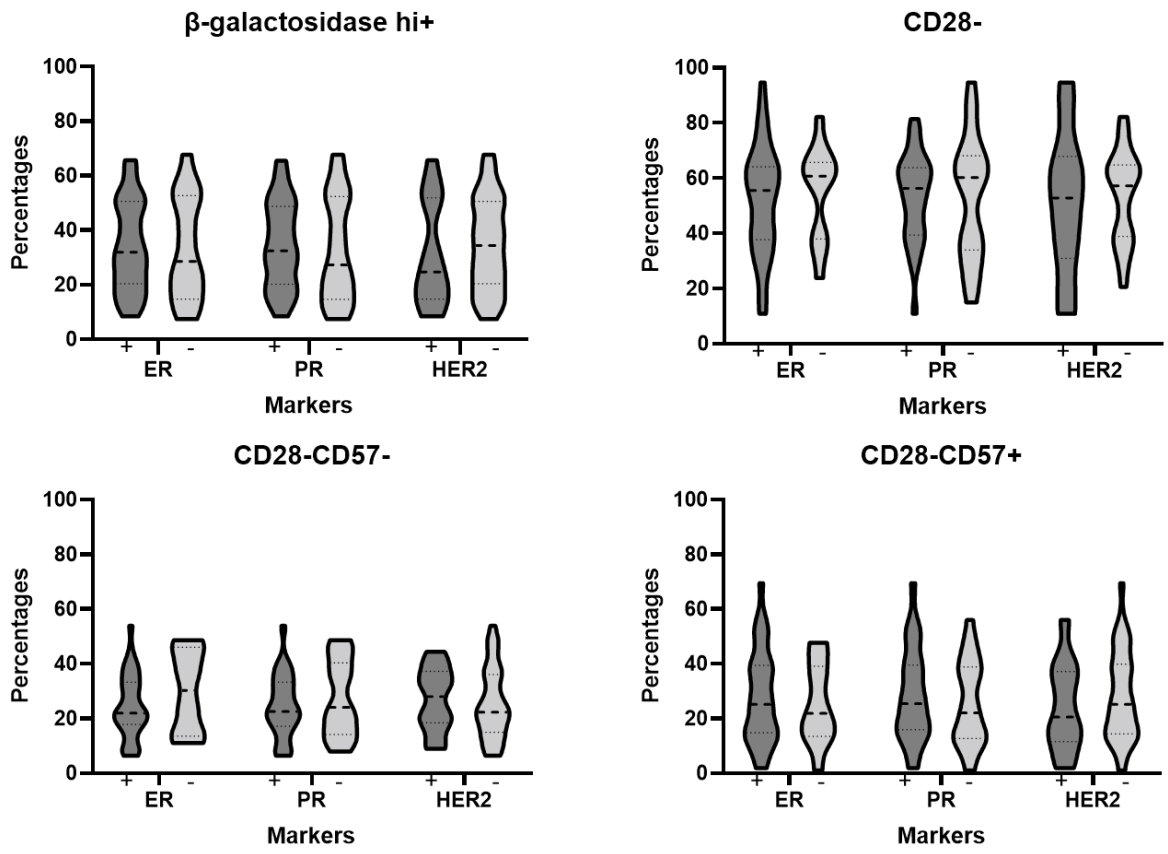

Figure 4.13 Proportions of non-exhausted senescent T cells according to breast cancer markers. The violin plots show the distribution and mean proportion of T cell senescent phenotypes according to breast cancer markers including estrogen receptor status (ER), progesterone receptor status (PR), and human epidermal growth factor receptor-2 (HER2). (N = 47)

4.3 Discussion

Senescent T cells are differentiated from exhausted T cells by expressing immune checkpoint molecules (46, 134). Many articles have suggested that the T cell senescence is one type of cancer-associated dysfunctional T lymphocytes because of the distinctive pathological features (180, 183, 198). Moreover, some reports have shown the predictive roles of the senescent T cells for myeloid leukemia patients who were poor responders to checkpoint inhibitors, whereas their dysfunctions were not merely exhausted phenotypes (184, 199). Several biological mechanisms, that resulted in the accumulation of DNA damage events, have been described (183, 187), and these events accelerated the appearance of senescent phenotypes (187). Previous *in-vitro* studies demonstrate T cell senescence phenotypes after co-culturing with various types of cancer cell-lines or tumor-derived suppressive immune cells, and these senescent T cells had increased DNA damage markers (183, 198, 200). Moreover, Martinez-Zamudio et al. reported that PD1 expressing CD8+ T cells expressed a very low proportion of key senescent features, and gene expression of those cells did not share the profiles with the terminally differentiated T lymphocytes (201). These findings suggested the different etiology and physiology of these entities of T cells. However, PD1+ T cells might be associated with senescence phenotypes, but additional co-expressing markers such as TIM-3 and LAG3 determined the terminal T cell dysfunction of this lineage, and these populations were inevitably intertwined (188, 202). In this thesis, PD1- was used to characterize non-exhausted senescent T cells which could exclude the exhausted phenotypes from the analysis, and PD1+ T cells were increased in breast cancer patients. However, statistically significant differences were not observed. Perhaps, the breast cancer related immune dysfunction was more related to T cell senescence compared to exhausted T cells. As in clinical studies,

checkpoint inhibitors seemed not to have convincingly positive results in majority of breast cancer patients especially in those with low levels of PDL-1 expression (197, 203).

In this study, we identified two types of SA-β-gal signals in T lymphocytes, the SA-β-gal hi+ and SA-β-gal lo+, and we demonstrated the prominence of CD28- T cells in the SA-β-gal hi+ population. In a previous study, Martinez-Zamudio et al. found the abundance of hi β-galactosidase activity of CD8+ T cells in ageing healthy blood donors and showed that this type of T cell impaired proliferation function and loss of telomere length (201). Therefore, SA-β-gal hi+ is the relevant marker of senescent T cells, while the CD28- T cells represent both senescent phenotype and co-stimulation functional impairment. Several studies have shown an increased proportion of CD28- T cells in the advanced age population (123, 171). However, CD28- T cells showed a wide range of chronology and dysfunctional phenotypes of senescence-associated T cells (180). In addition, several studies reported additional markers to determine the terminally differentiated T cells: for example Onyema et al. studied the CD28 and CD57 expression in aging and found CD8+CD28-CD57+ T cells were significantly increased in old participants and other studies used CD45RA+ or CD27- to classify late senescent T cells (104, 127). In addition, the CD57+ T cells demonstrated increased expression of aging markers such as p16, p21, and CD95 compared to CD57- T cells (104, 180). In our study, the SA-β-gal hi+ population seemed to determine a wide range of senescence phenotypes, but we did not identify the specific chronology of these senescence phenotypes in the SA-β-gal hi+ population, and further studies are needed to determine this point.

Ageing is a major factor related to senescent T cell expansion and impaired T cell homeostasis (144), while CD28- and SA-β-gal hi+ cells have been found to associate with advanced age (180). As in our study, SA-β-gal hi+, CD28-, and

CD28-CD57+ T cells were found to be correlated with age, but CD28-CD57- T cells were not, perhaps, because the increase in CD28-CD57- T cells was not common in the replicative senescence or these T cells did not increase in the elderly.

Several conditions have reported to accelerate immune cell senescence, for instance, autoimmune diseases, obesity, and chronic medical diseases (43, 204). Moreover, many cancer patients have reported an association with increased senescent immune cells (43, 45, 180). Recently, immune senescence was shown in patients with cancers of the lung, head and neck, multiple myeloma, and breast cancer (45, 46). Moreover, the cancer-associated senescent T cells were more abundant in circulating T cells than infiltrating T cells, and this abundance impaired cancer prognosis (180), and CD28- T cells were increased in several cancer patients (43, 192, 193). These phenotypes were commonly found in CD8+ T cells in cancer-associated T cell senescence and also in breast cancer patients (164). In our study, both CD28- and SA-β-gal hi+ T cell proportions were increased in breast cancer patients. Cancer-associated SA-β-gal hi+ T cells were increased in both CD4+ and CD8+ T cells, whereas cancer-associated CD28- T cells were increased in CD8+ T cells rather than CD4+ T cells. CD4+ T cells had impaired downstream signaling pathways such as T cell receptor signaling and in the mTOR pathway (161, 205). Therefore, additional markers are necessary to detect senescence-related signaling pathway defects. Furthermore, CD28-CD57- T cells were increased in breast cancer patients, and this was not correlated with age, and the increased in these phenotypes were irrespective of age. Perhaps, this marker was the preferential breast cancer-related senescent T cell phenotype. Interestingly, this phenotype was early senescent T cells, which were able to restore their proliferative function (206). The treatment strategies targeting rejuvenation might be helpful in this circumstance, and became the aim of the following chapter in this thesis.

CD28-CD57- T cells increased in the early age group and tended to decrease after 52 years old. The CD28-CD57+ cells also increased at a younger age and became the main proportion of senescent T cells in advanced age. These findings demonstrated an inversed proportion of cancer-associated T cell senescence with progressive age. Furthermore, the senescent effects were more abundant in breast cancer patients and worsened after 52 years of age. In cancer, both the aging process and carcinogenesis could reciprocally accelerate the appearance of senescence phenotypes of T cells (180). A previous study found that the abundance of a naïve CD8+ T cell repertoire and potent thymic epithelial cell activity remained in young adults till 50 years of age, leading to a strongly decreased naïve CD8+ T cell proportion in the elderly (123, 207). Apart from the lowing of T cell output, cancer-associated T cell senescence was worse in the elderly because of the decreased telomere length and senescence-associated epigenetic changes in replicative senescence (208). These effects lead to the increase in proportions of the terminally differentiated senescent T cells or CD28-CD57+ T cells after 50 years of age, and these cells demonstrated some apoptotic features (45).

CD28- and CD57+ T cells are terminally differentiated T cells with shortened telomere, and CD57 expression was found to impair proliferative function in peripheral T cells and increased its proportion in many cancer patients (192, 209, 210). The CD28-CD57- T cells were pre-terminally differentiated cells, which could express CD57 after additional stimuli (164). The CD28-CD57- T cells seemed to restore their function even after immune checkpoint inhibitor treatment, but CD28-CD57+ T cells did not and were found to attenuate their impairment by interleukin-15 in lung cancer (210). Although recent evidence could demonstrate proliferative functions of CD28-CD57+ T cells, CD28-CD57- T cells were more predictable in terms of function restoration (164). Recently, CD28-CD57- T cells

were found increased in lung cancer patients (210), however, the clinical significance of CD28-CD57- T cells in cancer patients was not well understood as CD28-CD57+ T cells. Moreover, the CD28-CD57- T cells seemed to be abundant in tumor-infiltrating T cells compared to PBMCs (210). A further study regarding CD28-CD57- T cells in tumor-infiltrating T cells in breast cancer patients would be more informative. In addition, CD28-CD57- T cells were also increased in those with chemotherapy and chronic HIV infection (211).

Immune evasion is an important mechanism of cancer cell survival in humans. The impairment of T cells regarding their activation, signaling pathways, and metabolic pathways can support carcinogenesis (20). CD69 was not only the T cell activation marker but CD69+ circulating T lymphocytes are effective in cancer elimination in several circumstances (212-214). A previous study evaluated the function of T lymphocytes by phytohemagglutinin activation, and showed that CD3+ T cells contained a significantly lower proportion of CD69+ T cells and lower concentration of interferon-γ in breast cancer group compared with both the metastatic lung cancer group and the control group (215). Interestingly, the melanoma study showed that this deficiency was specific to MART-specific T cell responses, which were cancer specific. Perhaps. there is a cancer specific mechanism to senescence phenotypic changes (216).

The breast cancer-associated senescent T cells were found to be one of the most important dysfunctional T cells which could impair cancer prognosis (181). In our study, we could demonstrate the increased proportions of T cell senescence in breast cancer patients, and these were more increased in metastatic disease, while tumor factors did not affect these T cell senescence. Perhaps breast cancer associated T cells senescence might be related to the burden of disease rather than tumor factors. Moreover, in metastatic disease, both ancillary gene expression in

tumor cells and immune-evasion capability reciprocally accelerate cancer spreading (217-219). Immune cell expression profiling showed decreased expression levels in immune function cluster, T cell activation cluster, and antigen presentation cluster in metastatic breast cancer group compared to primary breast cancer which may be crucial genes of metastatic diseases (217). These might be related to the expansion of senescent immune cells in metastatic disease. However, further studies are needed to clarify this due to the limited sample size in this study.

The increase in non-exhausted senescent T cells in breast cancer has implications in terms of treatment targeting rejuvenation and use of senolytic drugs. In this chapter, the presence of increased pre-senescent cells was more significant in the patients below 50 years old, and these might provide better success of therapeutic rejuvenation or senescence attenuation in young patients with breast cancer. In support of this idea, a previous study in animal models showed the synergistic efficacy of combining checkpoint inhibitors and targeting senescent T cells (220). Moreover, the combination of rejuvenation treatment in adoptive T cells transfer might be helpful in terms of T cell function improvement and the capability of *in-vitro* T cell expansion.

Although we excluded immunosuppressed and immunocompromised patients, a limitation of our study was a lack of socioeconomic information including childhood maltreatment which has been associated with senescent T cells in a previous study (193). Another limitation is the limited range of age groups which were from 30 to 69 years old in this thesis, but this was the common age group with a high incidence of breast cancer (221).

4.4 Conclusion

Immune senescence is one of the important immune dysfunctions in cancer immunology. In this study, non-exhausted senescent T cells were determined to be a different entity from exhausted T cells, and resulted from a combination of age and the presence of breast cancer. SA-β-gal hi+ T cells were a consequence of natural ageing and carcinogenesis. Notably, CD28- T cells were significantly increased in cancer patients, and CD28-CD57- T cells were increased in all age groups. In contrast, CD28-CD57+ T cells were increased in the younger age group, but slightly increased in the older age group. Interestingly, the presence of CD28-CD57- cells in breast cancer patients was decreased after 52 years of age, and CD28-CD57+ cells became predominant thereafter. The increase in non-exhausted senescent T cells seemed to be related with cancer burden. These findings could underpin future applications of immunotherapy by targeting immune senescence in breast cancer especially in the young age group, and those with a high burden of disease.

CHAPTER 5 THE EFFECTS OF 17β-ESTRADIOL ON CELLULAR SENESCENCE MODELS

5.1 Introduction

5.1.1 Anti-senescence strategies

There are common pathways to alleviate senescence phenotypes and genetic instability including insulin-like signaling pathway, target of rapamycin (mTOR), sirtruin, and antioxidant (49). Insulin-like signaling pathway is the down-stream pathway of insulin growth factor receptor, leading to cell growth and proliferation, however, long-term exposure to insulin growth factor-1 resulted in p53 activation by sirtuin-dependent p53 acetylation and premature cellular senescence (222). The inhibition of this pathway could prolong lifespan in animal models (223). However, insulin growth factor could polarize and promote suppressive immune cells, as a previous study showed the polarization of macrophage type 2 and proliferation of regulatory T cells (224). Rapamycin is commonly used for its antifungal effects, but a target of rapamycin has been identified in humans (49). This target connects down-stream molecules from growth factor receptors to cell proliferation and cellular metabolic controls (49). The inhibition of target of rapamycin (mTOR) could extend lifespan and rejuvenate organs in animal models and even in old-age mice (48). The main mechanisms are caloric restriction to prevent metabolic stress and cellular autophagy, however, the inhibition of mTOR resulted in the suppression of T cell proliferative function (48). The sirtuin family has been recognized as histone deacetylases and is regulated by nicotinamide adenine dinucleotide (NAD) (225). Sirtuin has been studied regarding regulating lifespan in yeasts, and was found to be associated with genomic stabilization (226). Apart from genomic effects, previous studies equivocally determined that sirtuin could attenuate cellular oxidative stress and caloric restriction (226, 227). The production of oxygen free radicals may

accelerate the ageing process by the accumulation of DNA damage, and these free radical molecules also accumulated in mitochondria, resulting in metabolic dysfunction(49). Increases in oxygen concentration result in increased DNA damage markers and impaired proliferative function *in-vitro* (228), but scavengers of oxygen radicals could attenuate mitochondrial impairment and improve cellular survival (229). In animal models, a few compounds have been shown to increase lifespan including rapamycin, estradiol, metformin, and sirtuin activators (50).

Rapamycin analogues have been preclinically used to target the mTOR pathway and were found positive effects on heart function, cognitive function, and lifespan (230). A recent clinical trial found that supplements of rapamycin analogues might improve immune responses and reduce infection rates (231), but they failed to determine these efficacies in phase I and phase II clinical trials in the elderly, where the increased in suppressive immune cells has been reported (232). Rapamycin suppresses proliferative function of immune cells, and is an immune suppressive agent to prevent graft rejection in organ transplanted patients, where the improvement of cognitive function in these population was also reported (230, 233).

Resveratrol, a polyphenol commonly found in fruit, is a potent sirtuin activating compound, which has been found to exert anti-inflammatory effects *in-vitro* and following supplementation in animal models, and this compound is also useful to prolong lifespan in animal studies (225). However, the levels of resveratrol seem not to relate with age-related disease mortality in old human participants (234). Recently, a randomized controlled trial showed the positive effects on cognitive function and bone health in post-menopausal women (235, 236). However, the supplement of resveratrol might impair cytotoxic function of human lymphocytes in dose-dependent effects (237).

NAD, the sirtuin co-reactor, plays several roles in cell biology, and its interesting anti-senescence functions are a reduction-oxidation coenzyme and co-reaction with sirtuins, where the acyl group is removed from histone proteins (238). In senescent cells, NAD is decreased in both the cytoplasm and subcellular organelles, and so many studies have determined the effects of NAD on restoring degenerative organ functions in the elderly including brain, heart, and kidney in animal models (239, 240). In clinical trials, nicotinamide ribonucleoside was used to promote NAD synthesis, and this compound seemed to have positive effects on neurodegenerative disease and heart disease, but further larger clinical trials are needed to confirm these findings, and elucidate the mechanisms responsible for lifespan extension (241, 242). In immune systems, decreased levels of NAD and telomere length were found in the elderly that might impair immune responses (243), and NAD supplement or replenishment is proposed to have immunomodulatory effects (243, 244).

Metformin is an insulin sensitizing anti-hyperglycemic drug, which had been studied for the capability to extend lifespan (47). Its mechanisms are to activate AMPK, which is an up-stream inhibitor of mTOR, involve in anti-oxidation function, and inhibit insulin growth factor-1 signaling (47, 245). In animal models, metformin could increase lifespan in mice (47). Recently, a study found increased lifespan in metformin-taking diabetic patients compared to non-diabetic population (246), and among diabetic patients, metformin was reported to decrease all-cause mortality in systematic reviews (246), and there are several convincing findings related to improve ageing related chronic diseases including cardiovascular risk, neurodegenerative disease and the incidence of cancer (47, 246). Such findings leaded to the conduct of a large clinical trial, targeting aging with metformin (TAME) study, where 3,000 elderly subjects were enrolled, and the aim was specific

to the effects on ageing (47). In the immune system, metformin seems to improve both cell mediated and humoral immune responses in mouse models, but the clinical trial showed that the supplement of metformin could increase circulating helper T cells and alleviated senescent phenotypes of CD4+ T cells, while CD8+ T cells seemed unchanged after vaccination (247).

Estradiol (E2) and estriol have been wildly used as anti-senescence effects for many years because the effects of upregulation of telomerase activity and p53, antioxidant enzymes E2, and inhibitory upstream mediators of mTOR were reported (229, 248). In previous studies, estrogens could demonstrate their functions as neuroprotective, cardiovascular risk minimizing, preventing of osteoporosis, and extending longevity (249). In immune systems, estrogens could promote adaptive immune responses, accordingly, these responses were deteriorated after menopause (250). As a result, estradiol seems to have anti-senescence effects without impairment of immune responses.

To our knowledge, these 4 strategies are related to lifespan extension, but there are 2 strategies that seem to have positive effects on immune responses including metformin and estradiol. However, metformin seems to have effects on CD4+ T cells more than CD8+ T cells, while CD8+ T cells are the main breast cancer associated senescent T cells from the previous chapter. Hence, the anti-senescence effect of estradiol on senescent T cells is the aim of this chapter.

5.1.2 Estrogen hormone

The estrogens are produced from theca cells and granulosa cells of ovaries (251). The synthesis of sex hormones is the cleavage of carbon atoms in cholesterol by cytochrome P450 enzymes in mitochondria to produce androgens, which are firstly produced and aromatized to estrogens in theca cells (251). This aromatase activity is also found in muscle, fat, and neural systems. The natural estrogens include estrone (E1), 17β-estradiol(E2) and estriol(E3) (252). E2 is the most abundant and potent estrogen in the circulation, and binds to globulin and excretes into bile and urine, while a part of conjugated E2 is reabsorbed in enterohepatic circulation (251). In females, the dynamic changes of estrogens level are remarkable during a menstrual cycle, pregnancy, and menopause period (253). During puberty, the gonadotropin pulse of the pituitary gland generates 55-122 pM of E2 (15-35 pg/ml). Thereafter, the preovulatory phase exhibits the highest concentration of serum E2, which is 1-2 nM (250-500 pg/ml), and the serum E2 level is decreased below 73 pM (20 pg/ml) after the menopausal period. As a result, estrone (E1) becomes predominant in this phase (252).

The biology of estrogens and estrogen receptors

The estrogenic effects are determined by the formation of estrogen-estrogen receptor complex, becoming DNA binding domains and driving transcription factor formation to activate estrogen-response elements of DNA (252, 253). Occasionally, the complex is formed at cellular surfaces and modulates downstream signals, known as non-nuclear action of estrogens (251). There are two subtypes of estrogen receptors : estrogen receptor-α and estrogen receptor-β. The distribution of these receptors is tissue specific, for example, estrogen receptor-α is predominant in breast and endometrial tissue, while bone, brain, and intestinal mucosa harbour estrogen receptor-β (252). These receptors recognize similar genomic regions of estrogen-

response elements, but the results are often antipathetic. Alternatively, estrogen receptors are phosphorylated by nuclear protein kinases and exhibit as estrogen independent activation (254). Their effects involve cellular proliferation and growth, for instance, breast tissue proliferation, bone anti-resorption, and vaso-protection (252).

Estrogens and adaptive immune responses

In the immune system, the estrogen receptors are found in the thymus gland. In the innate immune system, estrogens support the differentiation and regulate functions of dendritic cells and macrophages (255). Moreover, estrogens are related to proinflammatory cytokine production (255). In the meantime, the production of antibodies is dependent on estrogen levels (256). However, there is equivocal evidence to support the effects of estrogen on T cell function (253). The estrogen receptor-α ubiquitously express in CD4+ and CD8+ T lymphocytes (257). In comparison, CD4+ T cells harbour higher estrogen receptor-α, which is almost 100 fold of estrogen receptor-β (254). In contrast, the proportion of estrogen receptor-β is remarkable in B lymphocytes and persists after menopause (258). Although estrogen inhibits the thymopoiesis, the oophorectomized mice show peripheral proliferation of T cells (259). Moreover, E2 affects the polarization of CD4+ T cells, which predominate Th1 over Th2 in the low dose E2 supplement group (260). These effects amplify the regulation of interferon-γ and T-bet in Th1 population, while a high dose of E3 contrarily affects the CD4+ T cell responses (260). In human, several autoimmune diseases are aggravated in pregnancy, early menarche, and hormone supplement menopausal women (261). Furthermore, the rise of CD3-zeta protein and calcium influx are found in estradiol-treated lymphocytes (262, 263), and these could resulted in promoting T cell activation and cytokine production (264). Moreover, the estradiol supplemented mice can increase the memory function

in tissue resilient CD4+ T cells (265). These findings seem to support that high estrogen levels aggravate T cell immune responses.

5.1.3 The effects of estradiol on DNA damage and cellular senescence

Estradiol and DNA damage

In human, the increase of serum E2 is determined as a breast cancer risk (253). In the metabolism of E2, cytochrome P450 enzymes or peroxidase enzyme converts E2 to semiquinones and quinones, which cause single strand break and DNA adducts (266). Moreover, these cytochrome P450 enzymes, such as CYP1A1 and CYP1B1, are abundant in breast tissue (266). As a result, E2 is associated with the prosperity of reactive oxygen species, which eventually become deleterious to DNA strands (267, 268), and the elevated E2 level magnifies the by-products and becomes a mutagen especially in breast tissue (269). Moreover, a study demonstrated genomic instability models of E2 dependent replication stress, whereas estrogen-estrogen receptor complex surges transcription factors and DNA synthesis, resulting in genomic instability and replication errors in estrogen receptor positive cells (270). The *in-vitro* observations show increased DNA damage in estradiol supplemented conditions (268, 271), for instance, 100-1000 nM E2 treated MCF7 cell line showed an increased DNA damage markers, while the lower doses of E2 supplement did not induce DNA damage (268). Moreover, a previous study showed that the increase of γH2AX foci was found in estrogen receptor-α positive breast cancer (MCF-7) after exposure to E2, but DNA damage foci did not change in estrogen receptor-α negative breast cancer cells (MDA-MB-231) (268). Hence, the strength of E2 effects is dependent on the abundance and the subtypes of estrogen receptors and dose-dependent manner (272). Furthermore, E2-induced DNA response foci are abundant

in S/G2 phase of the cell cycle (272). Interestingly, these foci were enriched at estrogen receptor-α mediated promoters, suggesting that E2 targeted site and cell cycle phase-specific DNA damage events (272). In contrast, estrogen-estrogen receptor complex was found to activate cyclin D1, which was recruited by γH2AX foci to enhance the expression of Rad51, which is the major mediator of homologous recombination repair (273). These findings might extrapolate as the maintenance of replication fork integrity by E2. Recently, the blockage of topoisomerase IIβ was found to decrease γH2AX foci in estradiol supplemented cells (272). From this, E2 appears to control the replication stress and DNA stability during proliferation rather than produce the DNA damage events.

Estrogen hormone and cellular senescence

Although the effects of estrogens on DNA damage were both deterioration and prevention, their effects on cellular senescence were attenuation (274, 275). In a previous study, estrogen-supplemented vascular endothelial cells were decreased the senescent phenotypes in H_2O_2 treated cells, and these findings were related to sirtuin protein family production (276). Moreover, the estrogen-related up-regulation of p53 could attenuate the effects of H_2O_2 in isolated hepatic mitochondria, which was found to contain estrogen receptors (229). These warrant the anti-oxidant properties and p53 up-regulation of estradiol. Furthermore, the previous study found that E2 inhibited upstream mediators of mTOR, which could attenuate senescent phenotypes of endothelial cells (277).

Estradiol (E2) and estriol have been wildly used as anti-senescence effects for many years. The effects of estrogens are neuroprotective, cardiovascular risk minimizing, and preventing of osteoporosis in both animal models and clincal studies (249, 275). In animal models, the incidence of cardiovascular disease and chronic medical disease was lower in the reproductive age of females compared to

males (278, 279). Moreover, the E2 supplement mice were found to have a longer life span in the animal models (280). In human, the deprivation of estrogen is remarkable in post-menopausal period, whereas physical well-being, cognitive functions, and age-related disease are worsen (275), and the senescent immune systems are also accelerated (257, 281). The supplement of estradiol after menopause showed increased antioxidant effects and increased longevity related genes in human (274). Moreover, the hormone replacement therapy could reverse the worsen T cell homeostasis and serum cytokines after menopause (282), but the study of immune responses to influenza virus vaccine failed to demonstrated this benefit in hormonal supplemented group (257).

17β-estradiol showed anti-ageing effects on longevity and organ functions in clinical studies, however, the E2 supplement in animal models and clinical studies were limited in terms of dose and the direct effects on senescent cells. Moreover, adoptive T cell transfer treatment allowed *ex-vivo* culture of T cell before becoming autologous cell transfer. To our knowledge, the effects of E2 on senescent T cells was poorly understood, and *ex-vivo* culture of T lymphocytes allowed higher dose of E2 exposure. In this chapter, we aimed to examine for the effects of various dose of E2 on senescent T cells in terms of DNA damage markers and senescence phenotypes, and those effects on the estrogen receptor positive breast cancer cell-line as a strongly estrogen receptor positive cell control.

5.2 Results

5.2.1 Jurkat cell senescence model

For T cell senescence models, treatment induced changes in primary T cells is a very challenging experimental model, therefore, Jurkat cells, T-cell leukemic cell-line, were used to replace T cells in this study. However, the low expression of estrogen receptor-α was taken into account regarding result interpretation and analogies to effects on primary T cells. Moreover, use of T-47D cell-lines, an estrogen receptor-α expressing breast cancer cell-line, was used as control in this study. Etoposide was used to induce senescent Jurkat cells in this study. The dose of etoposide was optimized to induce optimal phospho-γH2AX positivity. In this optimization experiment, 1-h incubation with 30 μM etoposide and 50 μM etoposide induced a comparable proportion of highly positive phospho-γH2AX cells as shown in Figure 5.1. After exposure to etoposide, the Jurkat cells were washed twice and placed in a fresh RPMI 1640 medium, and percentages of CD28+ cells were examined immediately after exposure to etoposide and 24 h thereafter. The percentages of CD28+ cells were decreased from 73.4% at 1 h to 19.9% at 24 h as shown in Figure 5.2. The senescent Jurkat cells were then activated by addition of 10 μg/ml antihuman CD3 and 10 μg/ml antihuman CD28 for 24 h. The percentage of CD69+ cells and phospho-γH2AX positive cells were measured (Figure 5.3). Phospho-γH2AX positive cells increased from 9.64% to 67.70% and CD69+ cells decreased from 25.29% to 10.49% after 30 μM etoposide exposure. Therefore, a 1-h exposure to 30 μM etoposide was used to generate senescent Jurkat cells in this study.

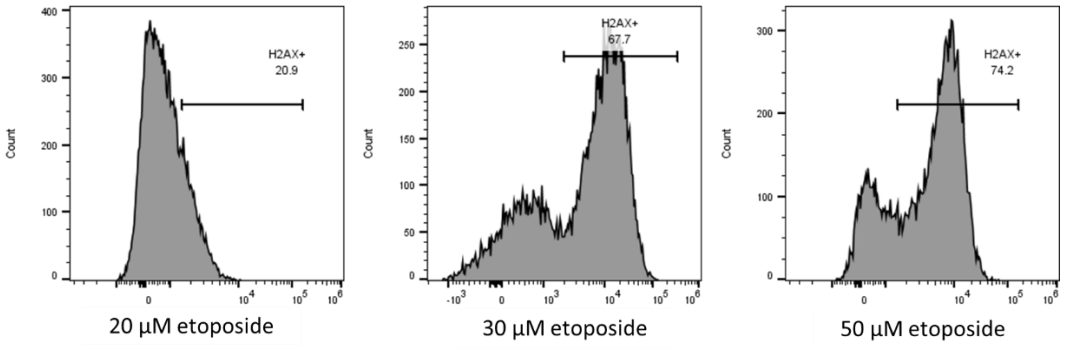

Figure 5.1 Representative histogram of phospho-γH2AX expression in Jurkat cells. The percentage of highly positive phospho-γH2AX was comparably increased after 30 or 50 μM of etoposide treatment for 1 h.

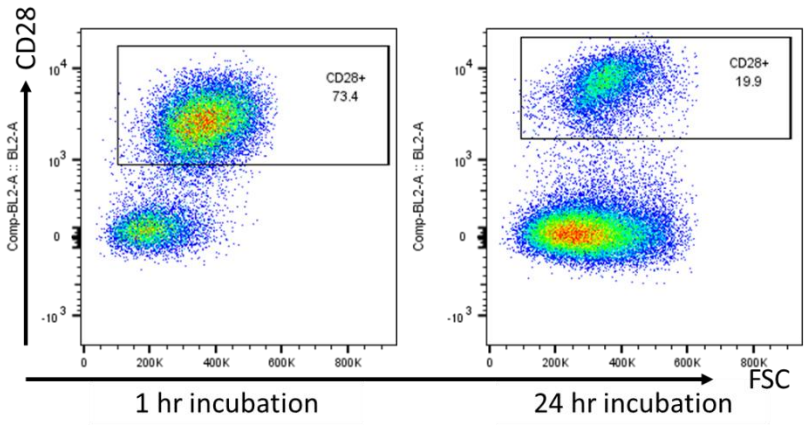

Figure 5.2 Proportions of CD28+ Jurkat cells at 1 hour after 30 μM etoposide treatment and then incubated for 24 h

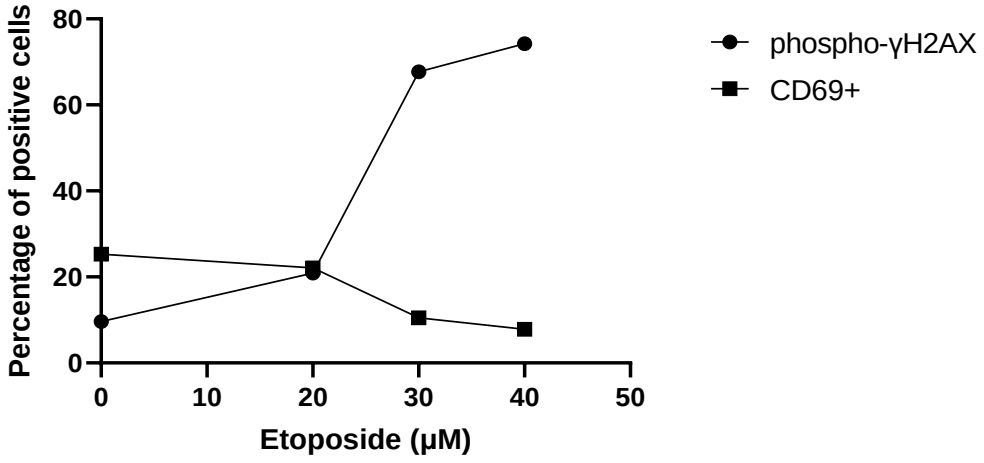

Figure 5.3 Percentage of phospho-γH2AX positive cells after 1-h exposure to etoposide and the percentage of CD69 positive cells after1-h exposure to etoposide and then 24-h activation with anti-CD3 and anti-CD28. In 30 μM Etoposide, the percentage of phospho-γH2AX positive cells was 73.4%, and the percentage of CD69 positive cells was 10.49%.

5.2.2 The effects of 17β-estradiol on DNA damage in senescent Jurkat cells

DNA damage markers (phospho-γH2AX, p21, and p53) were examined in various concentrations of E2 treated senescent Jurkat cells, which those E2 additions were performed following etoposide treatment as previously mentioned, whereas vehicle treated cells following etoposide treatment were used as control in this study. Firstly, a gating strategy for phospho-γH2AX positive cells was mentioned in Figure 5.1.

Median fluorescence intensity and percentages of phospho-γH2AX high positive cells were examined at 24 h, 48 h, and 72 h. Histograms were compared E2 treated senescent cells with the vehicle treated cells as shown in Figure 5.4. The percentages of phospho-γH2AX were 32.97%, 33.7%, 28.07%, and 33.17% in

vehicle, 1 nM E2, 10 nM E2, and 100 nM E2 treated cells respectively, after 24 h exposure to E2 or vehicle. The median fluorescence intensities were 2941, 3035, 2888, 3412 in vehicle, 1 nM E2, 10 nM E2, and 100 nM E2 treated cells respectively, after 24 h exposure to E2 or vehicle. In comparison, the percentage of phospho-γH2AX high positive cells and the median fluorescence intensity were not different among cells treated for 24-h, 48-h and 72-h incubation with E2 and vehicle (Figure 5.5).

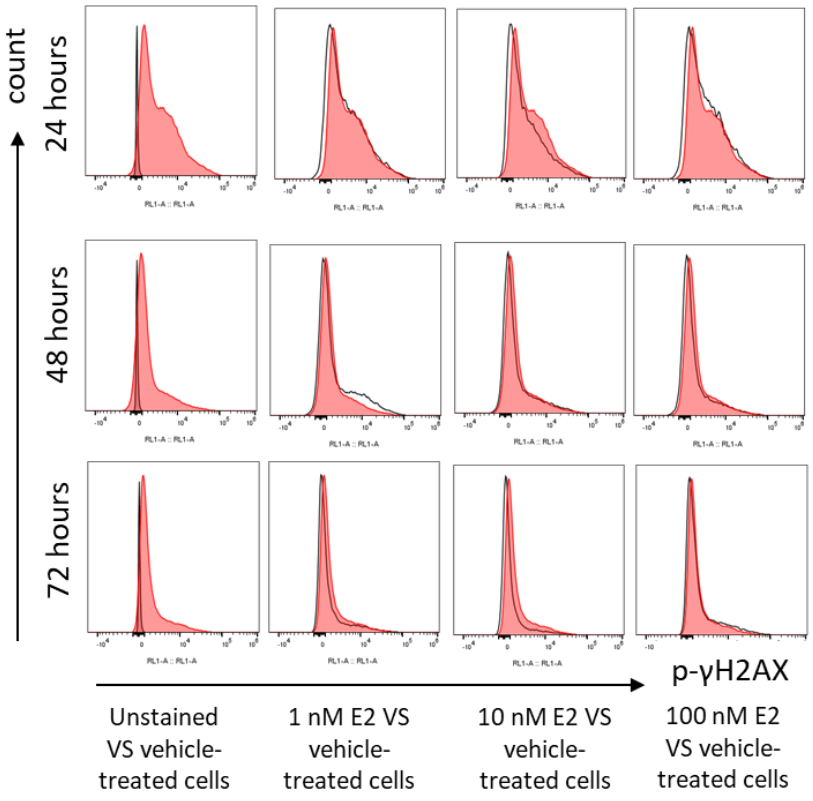

Figure 5.4 Comparative histograms of phospho-γH2AX expression after 24-h, 48-h and, 72-h Jurkat cells incubated with various concentrations of E2 or vehicle. The red histogram is vehicle treated cells, the grey histogram is unstained cells, the white histograms are E2 treated cells.

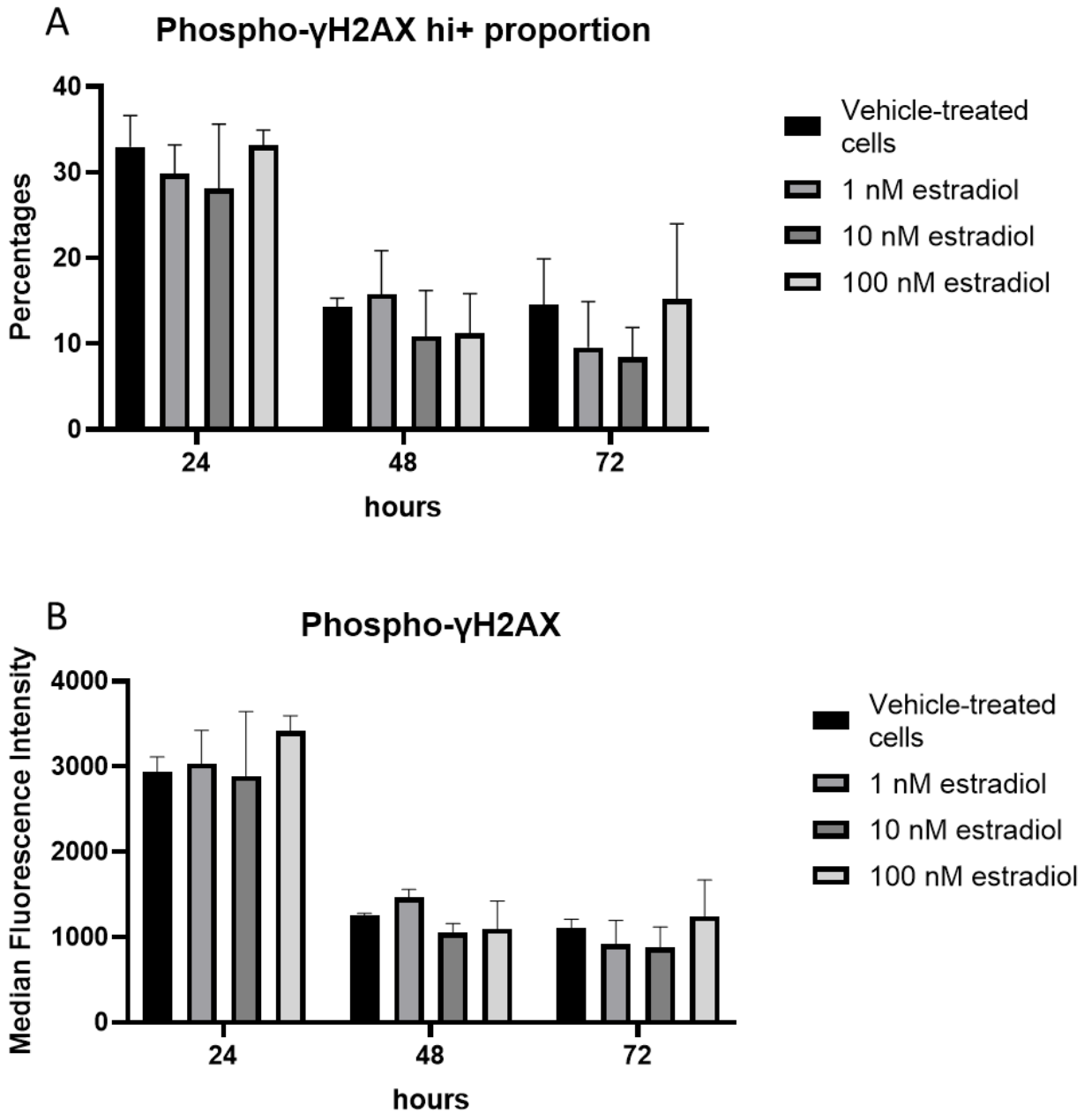

Figure 5.5 Expression levels of phospho-γH2AX in 24-h, 48-h, and 72-h Jurkat cells incubated with 30 μM etoposide followed by various concentrations of E2 or vehicle. The figures include percentages of high positive phospho-γH2AX (A) and median fluorescence intensity of phospho-γH2AX (B). (N=3)

The percentages of p53, and p21 expressing cells were calculated from the Overton percentages from the unstained cell histogram (Figure 5.6).

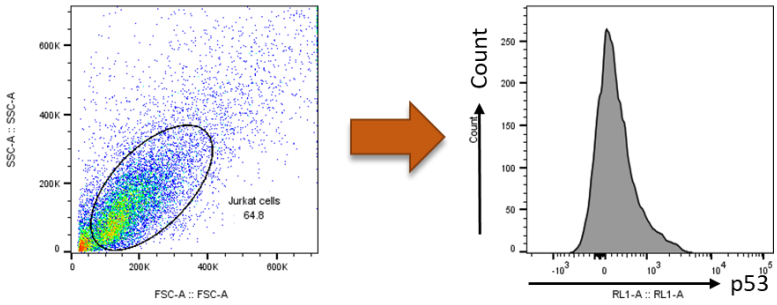

Figure 5.6 Gating strategy of p53 and p21 expression level in Jurkat cells and T47D cells. The selected population from FSC and SSC representative plots was used to determine the expression of p53.

The median fluorescence intensity of p53 expression was examined, and the effects of E2 incubation at different concentration at 24 h, 48 h and 72 h are shown in Figure 5.7. The percentage of p53 positive cells and the median fluorescence intensity were not different among groups at 24-h, 48-h, and 72-h incubation (Figure 5.8), but the histogram seemed to increase the proportion of highly positive cells in E2 supplemented cells, therefore, median fluorescence intensity of the first interquartile range was used to compare between groups. The intensity of highly positive cells tended to increase in 10 nM and 100 nM E2 group at 24 h, and 1 nM E2 seemed to have such effect at 48 h, and this increased intensity seemed to decreased at 24 h thereafter as shown in Figure 5.9. In the comparison, 10 nM E2 group showed significantly increased intensity compared to vehicle treated cells at 48 h ($p=0.008$).

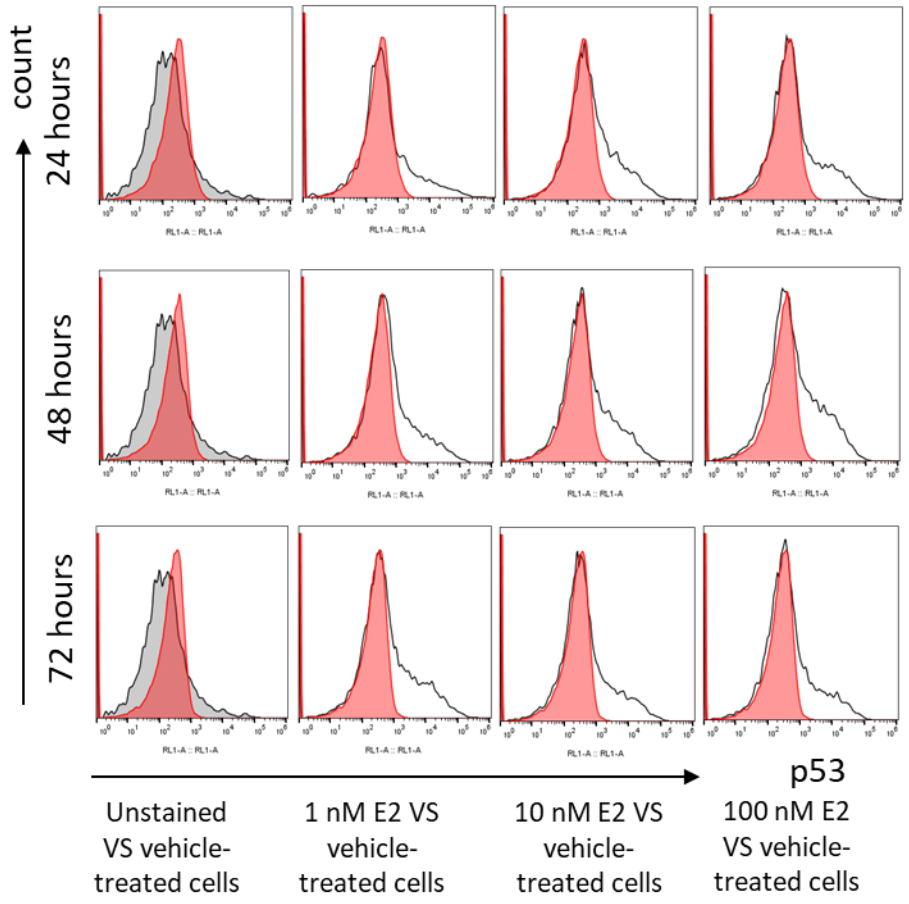

Figure 5.7 Comparative histograms of p53 expression in 24-h, 48-h, and 72-h Jurkat cells incubated with various concentrations of E2 or vehicle. The red histogram is vehicle treated cells, the grey histogram is unstained cells, the white histograms are E2 treated cells.

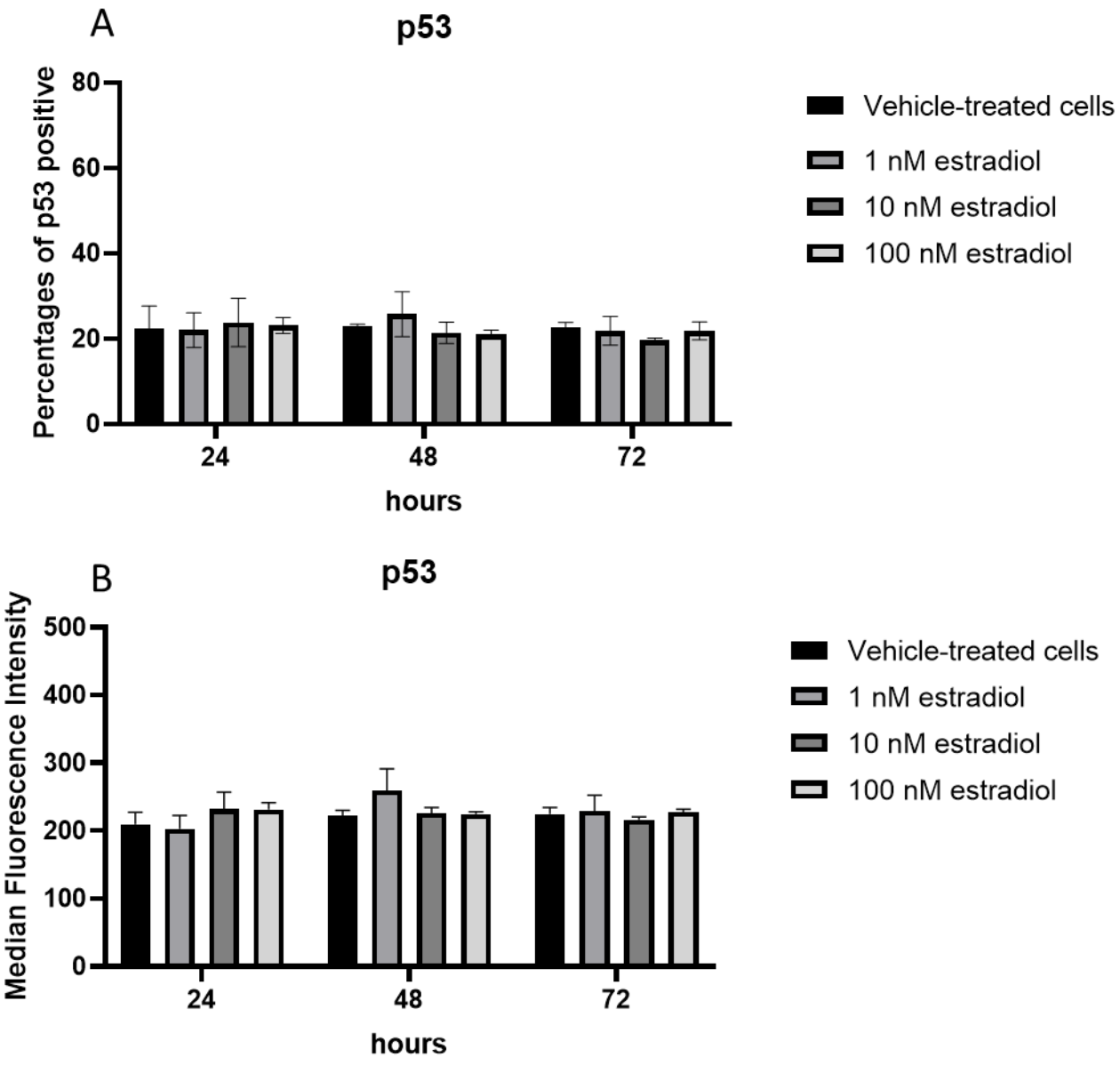

Figure 5.8 Expression level of p53 in 24-hour, 48-hour, and 72-hour Jurkat cells incubated with 30 μM etoposide followed by various concentrations of E2. The figures show percentages of p53 positive cells (A) and median fluorescence intensity of p53 (B). (N=3)

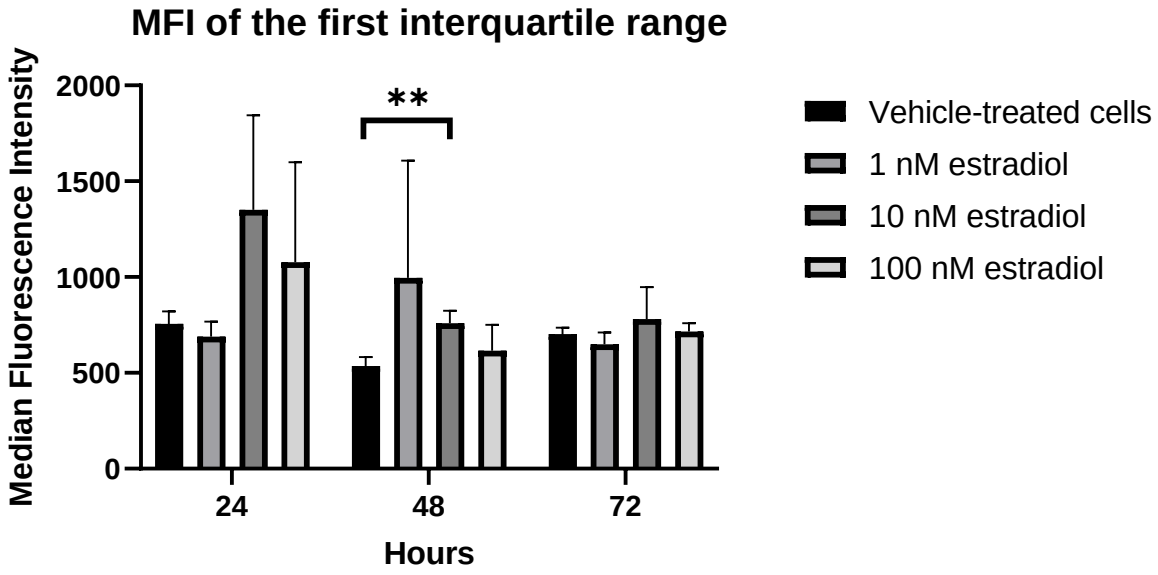

Figure 5.9 Median expression level of the first interquartile range of p53 at 24-hour, 48-hour, and 72-hour Jurkat cells incubated with 30 µM etoposide followed by various concentrations of E2. The figures show median fluorescence intensity of p53 of the first interquartile range. (N=3)

The expression of p21, a downstream mediator of p53-DNA damage responses, was investigated to assess the effects of p53 on DNA damage events. Level of p21 expression was examined, and the comparative histograms were shown in Figure 5.10. The proportion of p21 positive cells and median fluorescence intensity were not different among groups incubated in the presence or absence of E2 (Figure 5.11), but the histogram seemed to slightly increase the proportion of highly positive cells in E2 supplemented cells, therefore, median fluorescence intensity of the first interquartile range was used to compare between groups. The intensity of highly positive cells were marginally increased in 10 nM and 100 nM

E2 group at 24 h, and 1nM, 10 nM and 100 nM E2 groups seemed to have such effect at 48 h as shown in Figure 5.12. In the comparison, 10 nM and 100 nM E2 group showed significantly increased intensity compared to vehicle treated cells at 48 h (p=0.046, and 0.036 respectively).

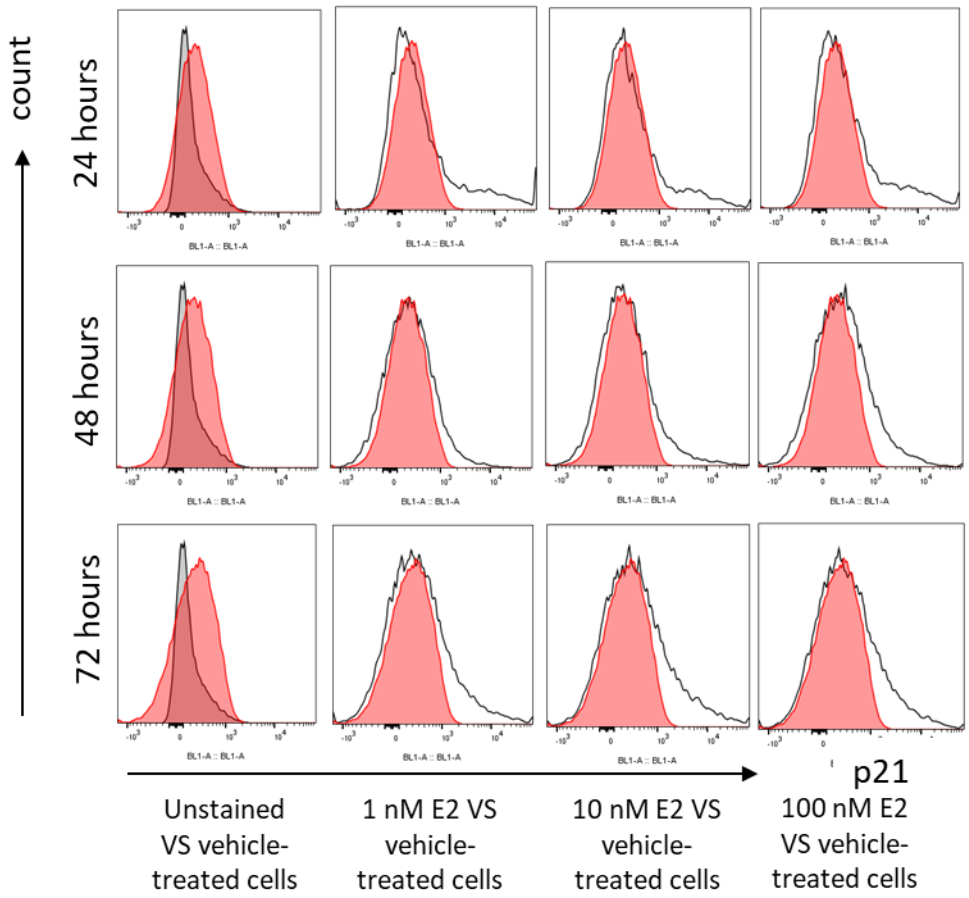

Figure 5.10 Comparative histograms of p21 expression in 24-h, 48-h, and 72-h senescent Jurkat cells incubated with various concentrations of E2 or vehicle. The red histogram is vehicle treated cells, the grey histogram is unstained cells, the white histograms are E2 treated cells.

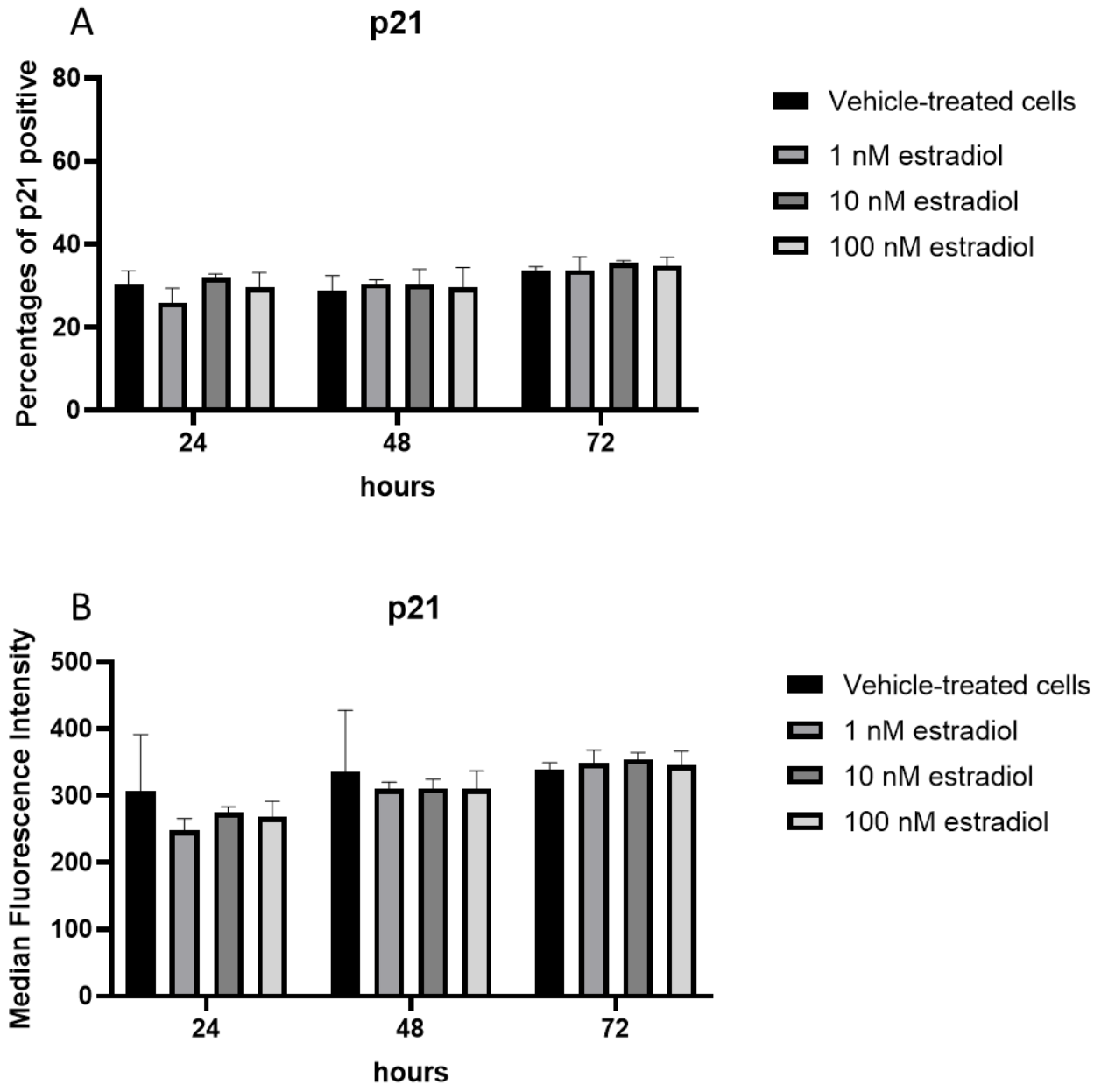

Figure 5.11 Expression levels of p21 in 24-h, 48-h, and 72-h Jurkat cells incubated with various concentrations of E2 or vehicle. The figures show percentages of p21 positive cells (A) and median fluorescence intensity of p21 (B). (N=3)

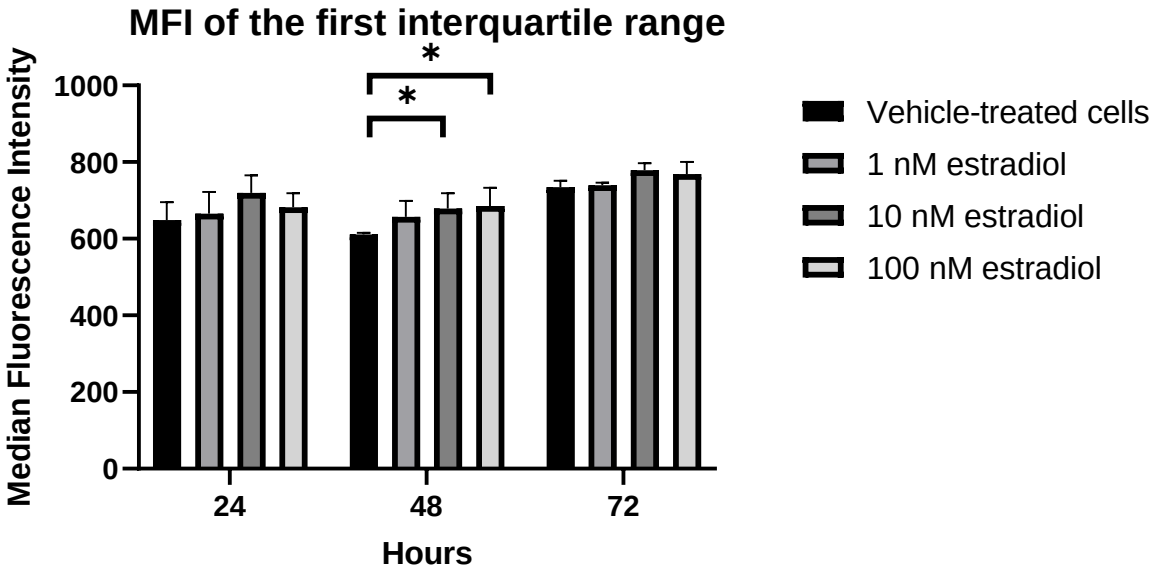

Figure 5.12 Median expression level of the first interquartile range of p21 at 24-hour, 48-hour, and 72-hour Jurkat cells incubated with 30 µM etoposide followed by various concentrations of E2. The figures show median fluorescence intensity of the first interquartile range of p21. (N=3)

5.2.3 17β-estradiol attenuated senescent phenotypes in Jurkat cells

The gating strategy analyzing CD28 expressing cells is shown in Figure 5.13, and the percentages of CD28+ cells were examined with CD45+ counterstaining.

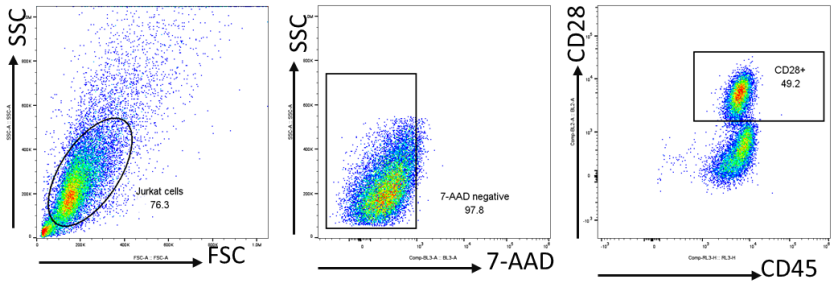

Figure 5.13 Gating strategy of CD28 expression level in Jurkat cells. The selected population from FSC and SSC representative plots was used to determine cell viability by 7-AAD. The viable cells were further stained forCD28 expression with CD45 expression counterstaining.

The 72-h E2 incubated Jurkat cells were examined for senescent phenotypes and representative flow cytometric plots are shown in Figure 5.14. The proportion of CD28+ cells increased after incubation with 10 nM E2 and 100 nM E2 (Figure 5.15). The 100 nM E2 treated group showed a statistically significant increase in CD28+ cell proportions compared to the vehicle treated group, which were 29.53% and 24.40%, respectively ($p = 0.007$). This finding suggested attenuation of senescence after E2 treatment.

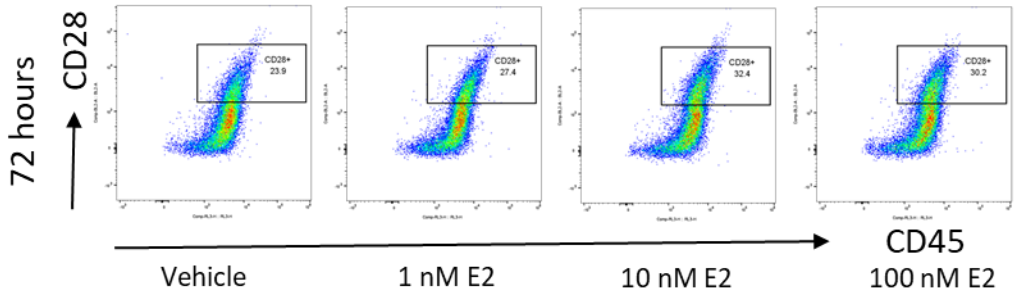

Figure 5.14 Flow cytometric plots of CD28 in 72-h E2 incubated Jurkat cells in the presence of E2.

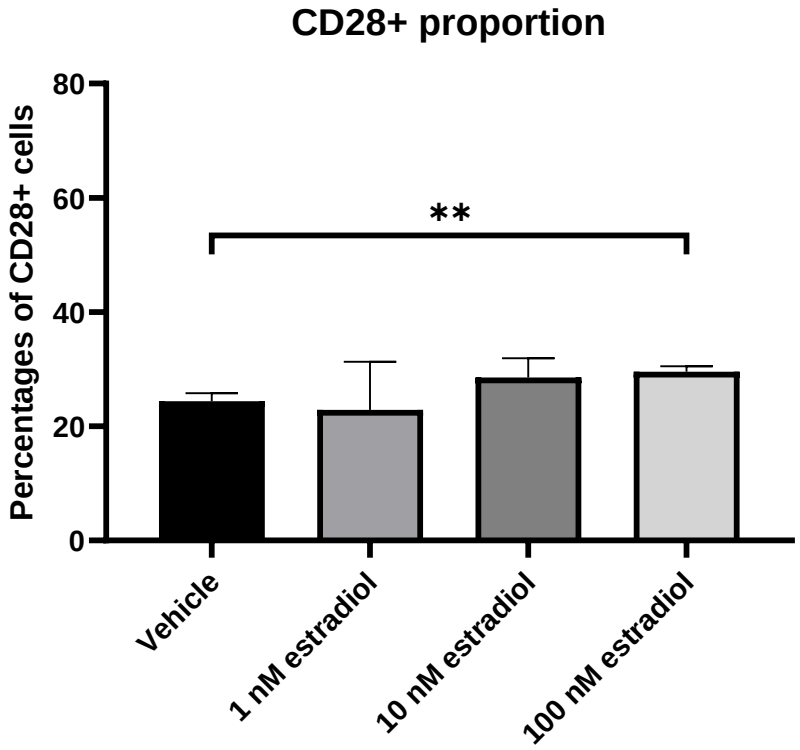

Figure 5.15 Percentages of CD28+ Jurkat cells at 72-hour E2 incubation. Two asterisk marked p-value < 0.01.

In addition to CD28 expression, arginase-2 expression was also examined. The 72-h incubated samples were examined for the senescent phenotype regarding mitochondrial dysfunction as measured by arginase-2 expression. Arginase-2 expression in Jurkat cells was measured by immunofluorescence (Figure 5.16) and by flow cytometry (Figure 5.17), the percentage of positive cells and median fluorescence intensity of arginase-2 were increased in the vehicle treated group, and the increase was diminished in E2 supplemented cells compared to vehicle treated cells ($p = 0.16$ in 1nM E2, $p=0.16$ in 10nM E2, and $p=0.12$ in 100 nM E2) (Figure 5.18).

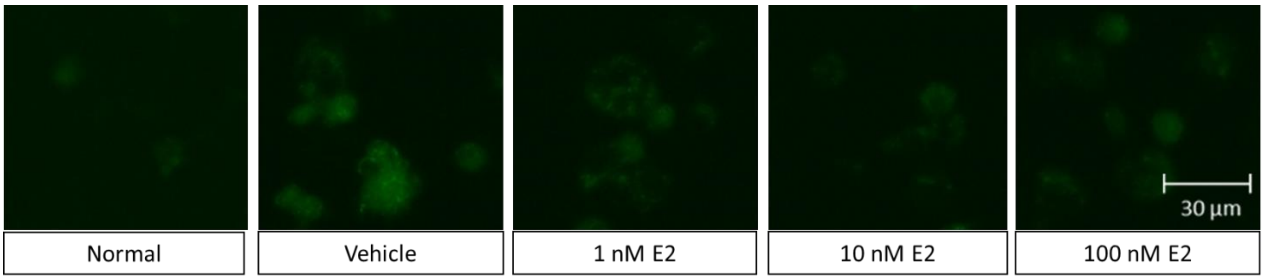

Figure 5.16 Immunofluorescence staining of arginase-2 in 72-h E2 incubated Jurkat cells and normal Jurkat cells.

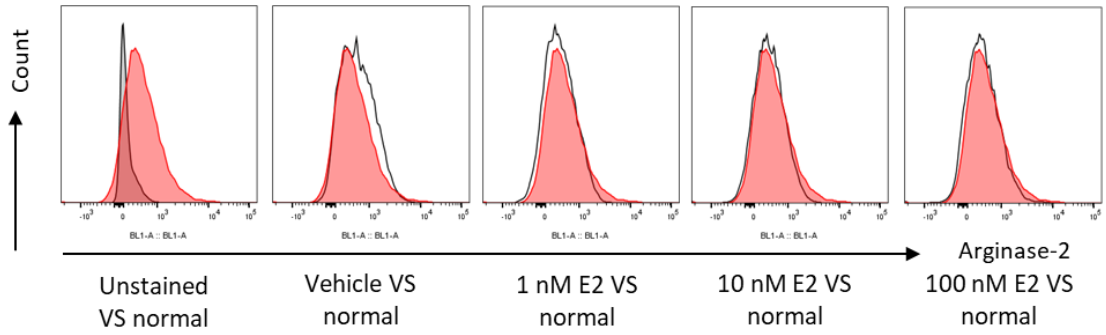

Figure 5.17 Comparative histograms of arginase-2 expression in 72-h E2 incubated Jurkat cells and normal Jurkat cells (red).

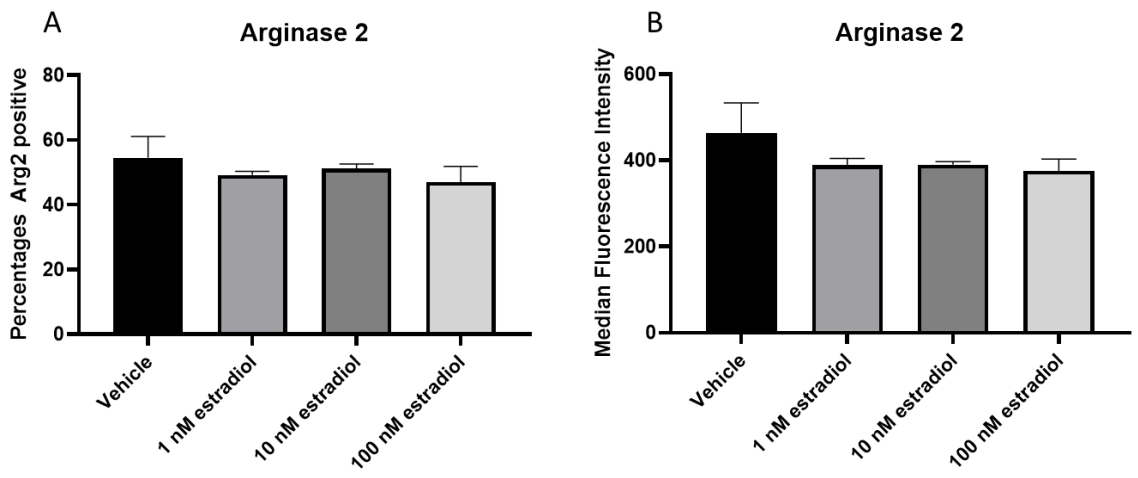

Figure 5.18 Proportions of positive cells and median fluorescent intensity of arginase-2 expression in 72-h incubated senescent Jurkat cells in the presence and absence of E2. (N=3)

5.2.4 Effects of 17β-estradiolon Jurkat cell activation

After 72-h E2 incubation of senescent Jurkat cells, the samples were washed, and the medium was replaced with new E2 supplemented medium. Antihuman-CD3 and antihuman-CD28 antibodies were used to activate the cells for 24 h. Subsequently, activated Jurkat cells were examined for CD69 expression. The gating strategy was performed as presented in Figure 5.19. The percentages of CD69+ cells were determined with CD45+ counterstaining.

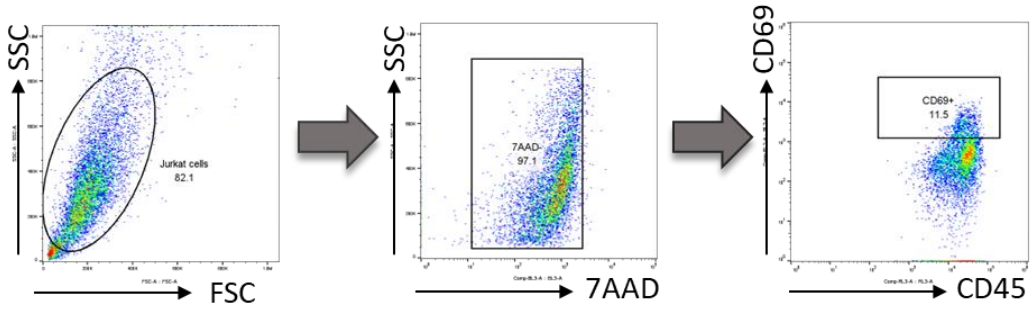

Figure 5.19 Gating strategy of CD69 expression level in Jurkat cells. The selected population from FSC and SSC representative plots was used to determine the viability by 7-AAD. The viable cells were subsequently stained for CD69 expression plus CD45 counterstaining.

The proportion of CD69+ cells was measured in control and treated Jurkat cells, as shown in Figure 5.20. In the activated Jurkat cells, the proportion of CD69+ cells were 12.17% and 9.65% in the vehicle treated group and 1 nM E2 group, respectively which were statistically significant differences ($p = 0.03$) (Figure 5.21), while the 10 nM E2 and 100 nM E2 were comparable to vehicle treated group (Figure 5.21). In addition to measurements of surface markers, IL-2 concentrations were examined in supernatants. The IL-2 concentration was not different among groups (Figure 5.22).

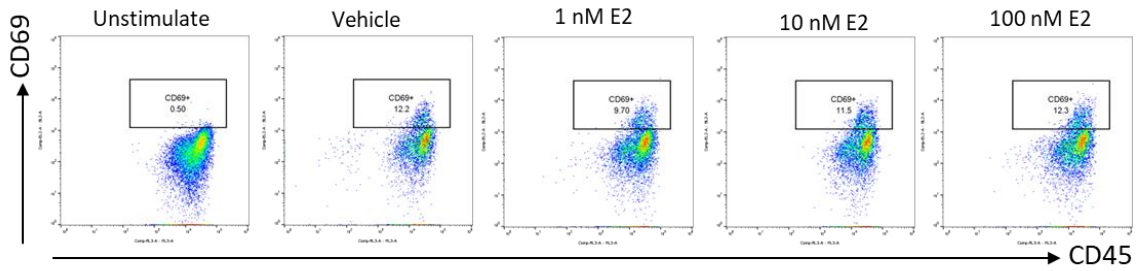

Figure 5.20 Flow cytometric plots of CD69 in activated Jurkat cells in the absence and presence of E2.

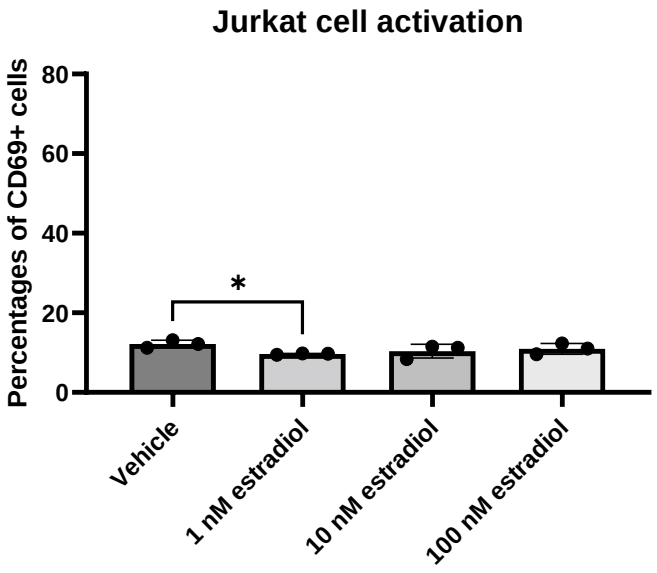

Figure 5.21 Percentages of CD69+ cells after activation in the presence and absence of E2. One asterisk marked p-value < 0.05. (N=3)

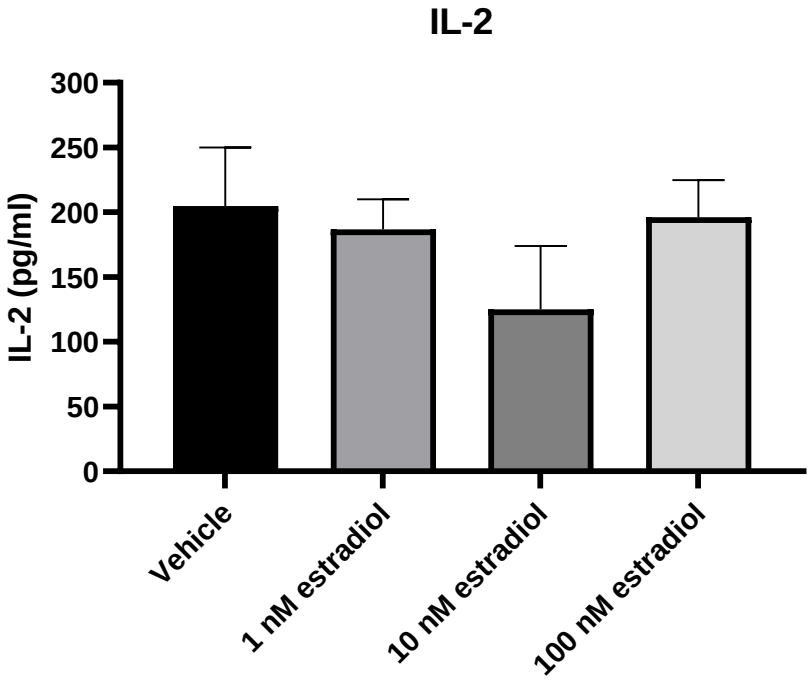

Figure 5.22 IL-2 concentration in supernatants after Jurkat cell activation. No statistical difference was observed. (N=3)

5.2.5 T47D cell senescence model

In addition to Jurkat cells, breast cancer cell-line containing estrogen receptor was further examine for the effects of E2 in the senescent condition which might be different from Jurkat cells. Etoposide was also used to induce senescent T47D cells in this study. The doses of etoposide were from 2.5 μM to 10 μM, and the duration was 24 h. In this optimization, 7.5 μM etoposide resulted in the highest proportion of phospho-γH2AX positive cells which was 67.7%, and this proportion was decreased at 10 μM etoposide treatment which was 9.83% (Figure 5.23).

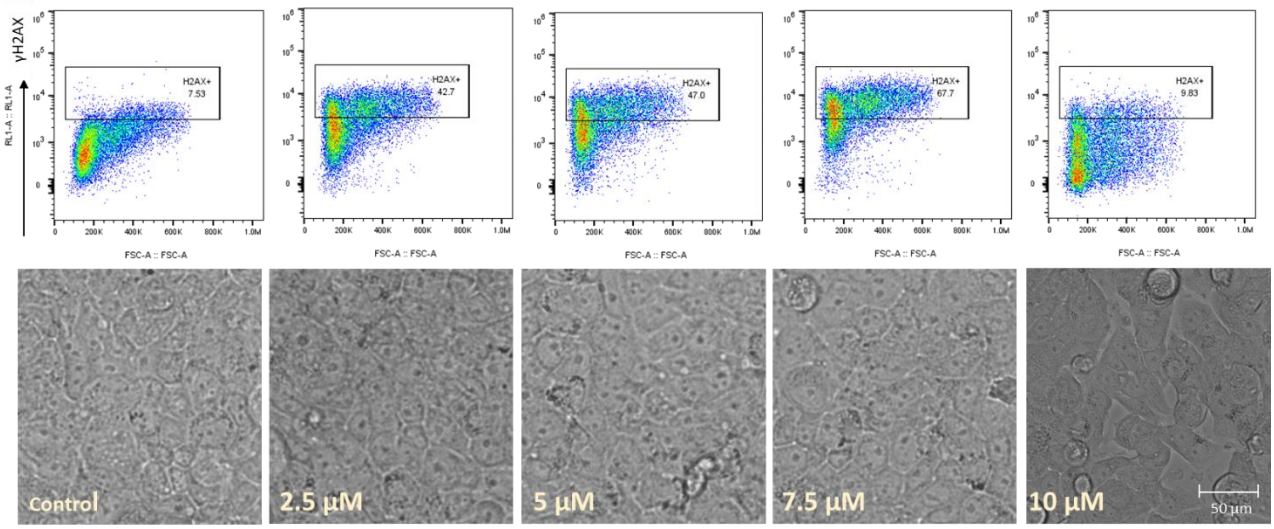

Figure 5.23 The morphology and the expression level of phospho-γH2AX in T47D after 24-h exposure to various concentrations of etoposide. Light microscopy shows enlarged cells after exposure to etoposide and loss of adhesive property after exposure to 10 μM etoposide.

5.2.6 17β-estradiol and DNA damage in senescence T47D cells

To examine the effects of E2 on breast cancer cells, the hormonal positive breast cancer cell line, T47D, was used to determine E2 effects on DNA damage

events. The presence of estrogen receptor expression on these cells might result in different levels of E2-related responses compared to Jurkat cells. As in the previous experiment, 1 nM E2, 10 nM E2, 100 nM E2, and vehicle treated cells were examined for the DNA damage markers including phospho-γH2AX, p21, and p53 measured by flow cytometry. Gating strategy analyzing phospho-γH2AX utilized the selected population as presented in Figure 5.24. Median fluorescence intensity was examined from the whole histogram. Moreover, the phospho-γH2AX positive cell proportion was determined from the cut point of untreated T47D histogram and 7.5 μM etoposide treated T47D cells as shown in Figure 5.24.

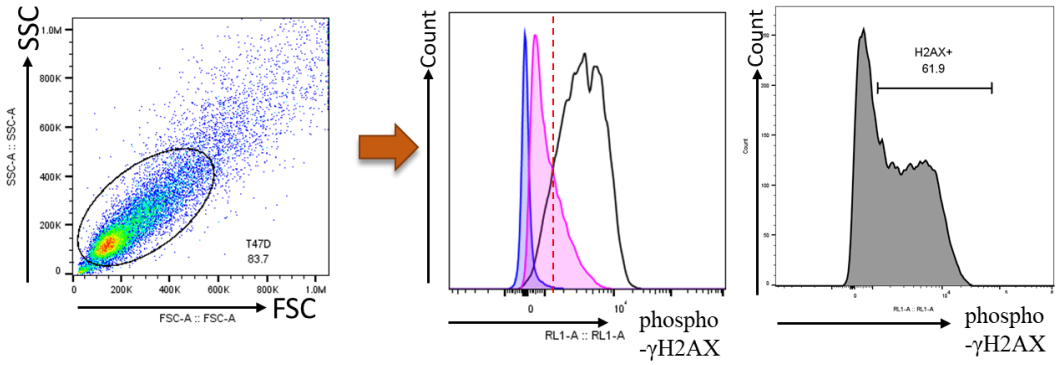

Figure 5.24 Gating strategy of phospho-γH2AX expression level in T47D cells. The selected population from FSC and SSC plots was used to determine the expression of phospho-γH2AX in T47D cells. The percentage of phospho-γH2AX expression was determined at the cut point of normal T47D (purple) and 7.5 μM etoposide treated T47D (white) which showed the higher peak of phospho-γH2AX expression, and the blue histogram was represented the unstained T47D cells.

The median fluorescence intensity and percentages of phospho-γH2AX positive cells were examined at 24 h and 48 h after E2 treatment. The histograms are shown in Figure 5.25. In this experiment, the percentage of phospho-γH2AX

positive cells and median fluorescence intensity were not different among groups (Figure 5.26).

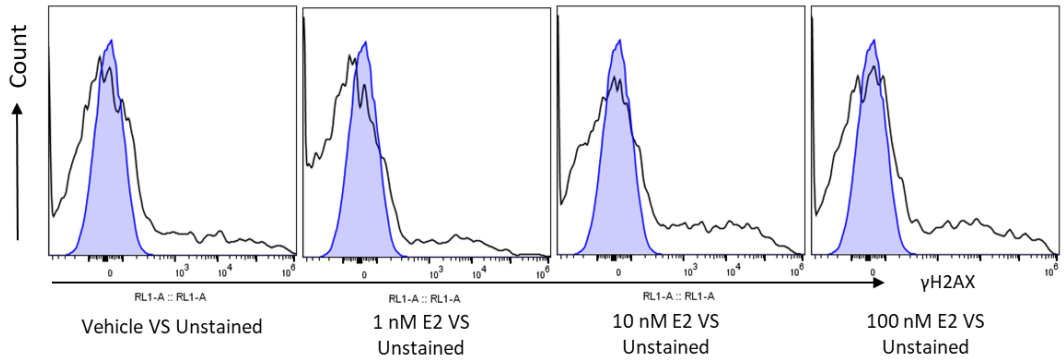

Figure 5.25 Comparative histograms of phospho-γH2AX expression in 24-h E2 or vehicle treated T47D cells (white) compared with unstained cells (blue).

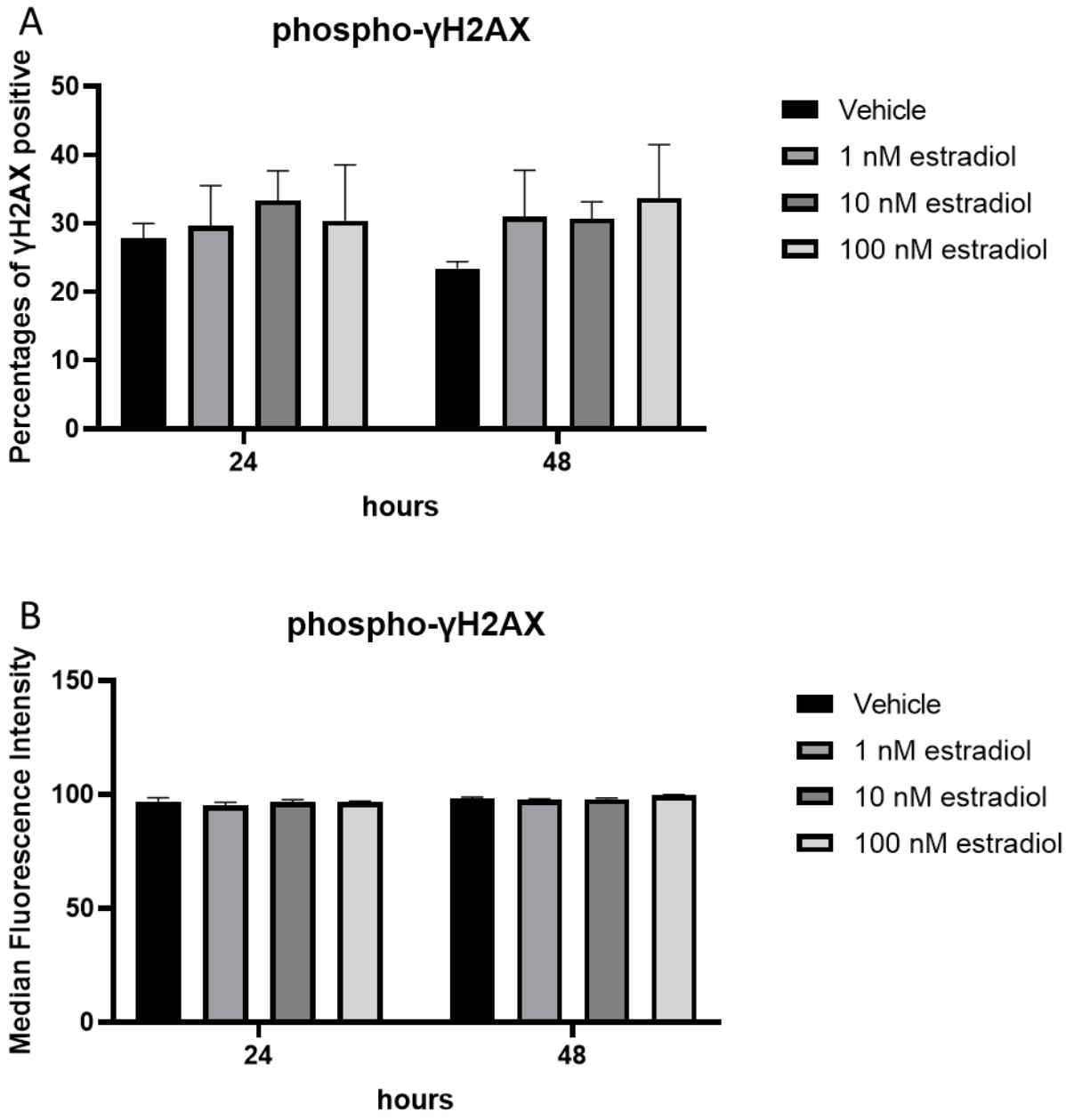

Figure 5.26 Expression levels of phospho-γH2AX in 24-h and 48-h of E2 or vehicle incubated T47D cells. The figures demonstrate percentages of phospho-γH2AX positive cells (A) and median fluorescence intensity of phospho-γH2AX (B). (N=3)

The median fluorescence intensity and percentages of p53 positive cells were examined at 24 h and 48 h (Figure 5.27). The proportion of p53 positive cells was significantly increased in the 100 μM E2 supplemented group after 48-h incubation ($p = 0.004$) (Figure 5.28), and the median of the first interquartile range of the highly positive cells were also significantly increased in this group ($p < 0.0001$) as shown in Figure 5.29.

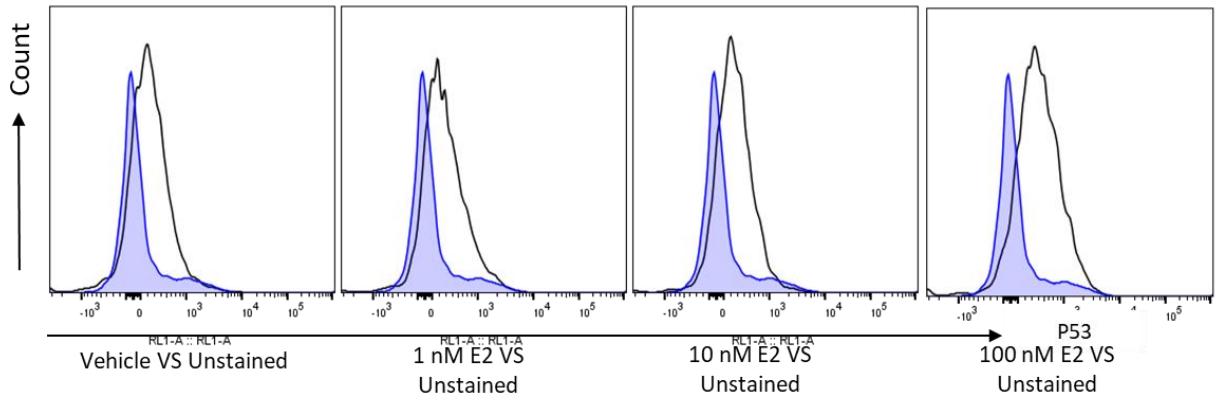

Figure 5.27 Comparative histograms of p53 expression in 24-h E2 or vehicle incubated T47D cells (white) compared with unstained cells (blue).

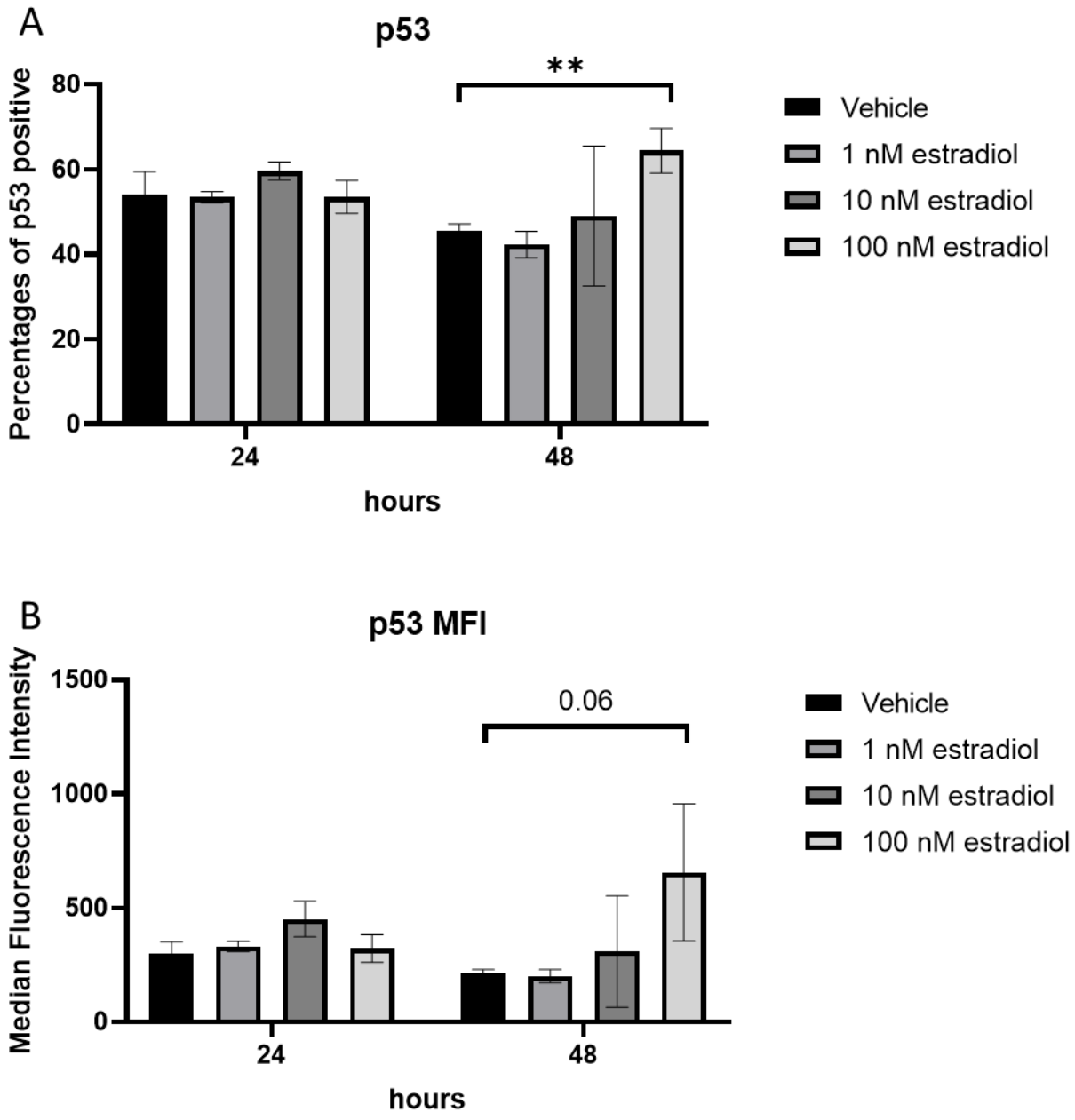

Figure 5.28 Expression levels of p53 in 24-h and 48-h E2 or vehicle incubated T47D cells. The figures show percentages of p53 positive cells (A) and median fluorescence intensity of p53 (B). Two asterisks marked p-value < 0.01. (N=3)

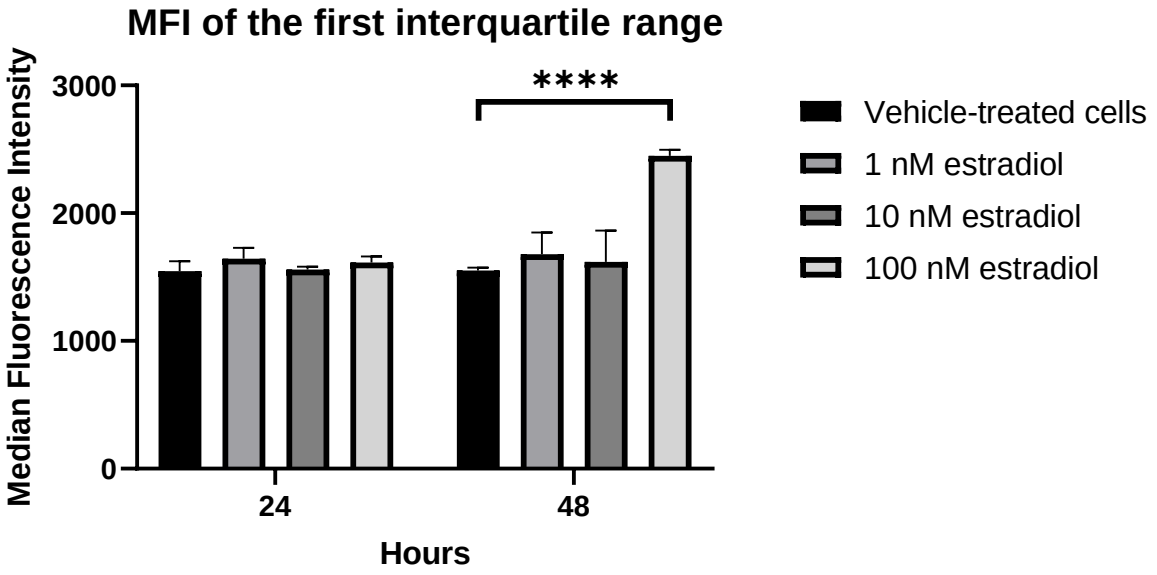

Figure 5.29 Median expression level of the first interquartile range of p53 at 24-hour, and 48-hour T47D cells incubated with 30 µM etoposide followed by various concentrations of E2. The figures show median fluorescence intensity of p53 of the first interquartile range. (N=3)

The median fluorescence intensity and percentages of p21 positive cells were examined at 24 h and 48 h (Figure 5.30). The 100 nM E2 supplemented group showed significantly decreased p21 positive cells ($p = 0.05$) and significantly decreased median fluorescence intensity compared to the vehicle treated cell at 24-h incubation ($p = 0.039$), as shown in Figure 5.31, while these were not different among groups at 48-h incubation, and the median of the first interquartile range or the highly positive cells were also significantly decreased in 100 nM E2 supplemented group ($p = 0.043$), but these seemed to increase at 48-h incubation as shown in Figure 5.32.

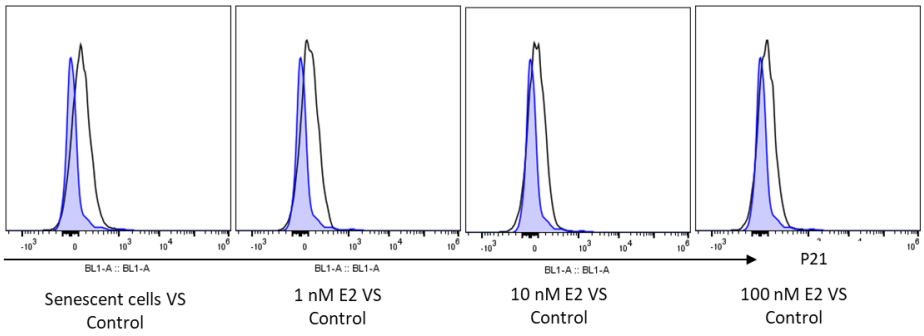

Figure 5.30 Comparative histograms of p53 expression in 24-hour E2 incubated T47D cells with negative control histogram(blue).

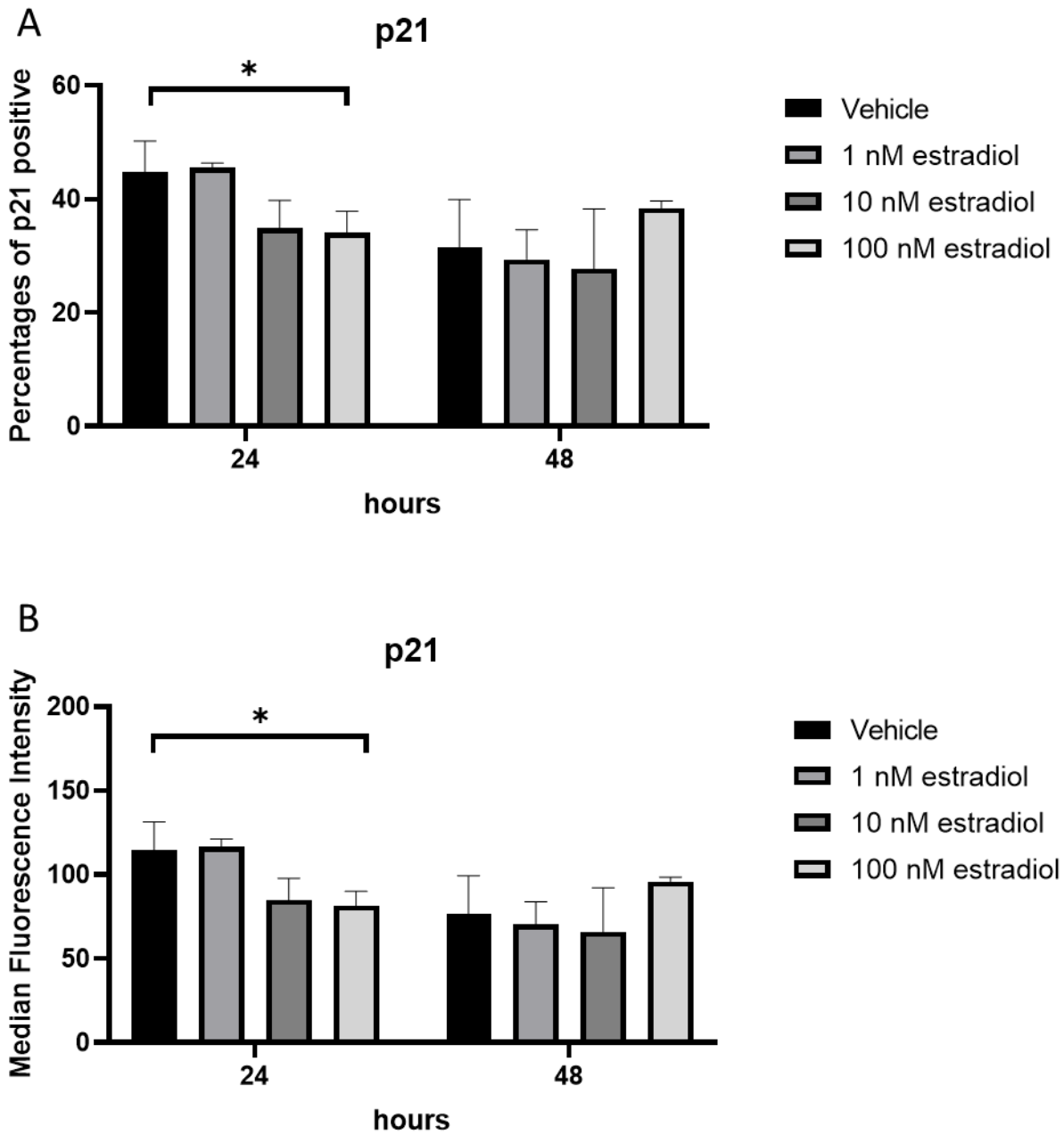

Figure 5.31 Expression levels of p21 in 24-h and 48-h E2 or vehicle incubated T47D cells. The figures show percentages of p21 positive cells (A) and median fluorescence intensity of p21 (B). One asterisk marked p-value < 0.05. (N=3)

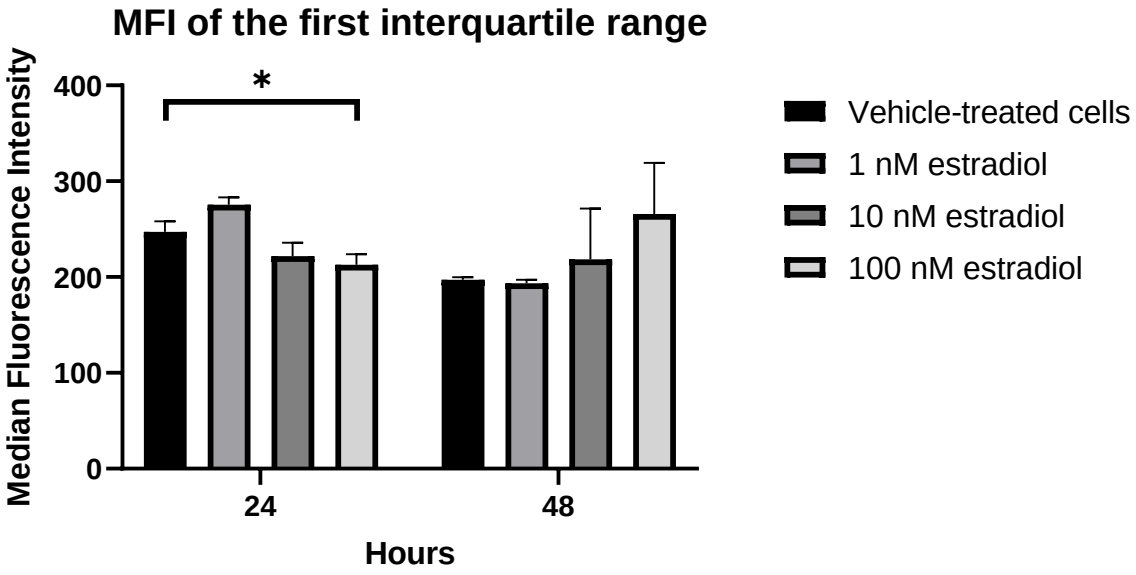

Figure 5.32 Median expression level of the first interquartile range of p21 at 24-hour, and 48-hour T47D cells incubated with 30 µM etoposide followed by various concentrations of E2. The figures show median fluorescence intensity of p21 of the first interquartile range. (N=3)

5.2.7 Effects of 17β-estradiol on senescent phenotype in T47D cells

The expression of arginase-2 was analyzed after 72-h incubation of the E2 supplement, and representative histograms are shown in Figure 5.33. In this experiment, the expression of arginase-2 tended to decrease in E2 supplemented groups (Figure 5.34), but no statistical significance was observed. The immunofluorescence staining is also shown in Figure 5.35.

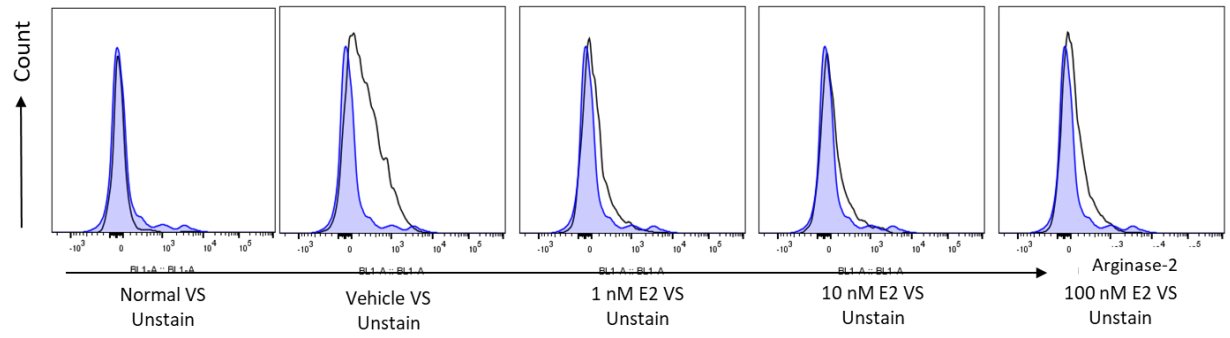

Figure 5.33 Comparative histograms of arginase-2 expression in 72-h of E2 or vehicle incubated T47D cells (white) and normal T47D cells (white) compared with unstained cells (blue).

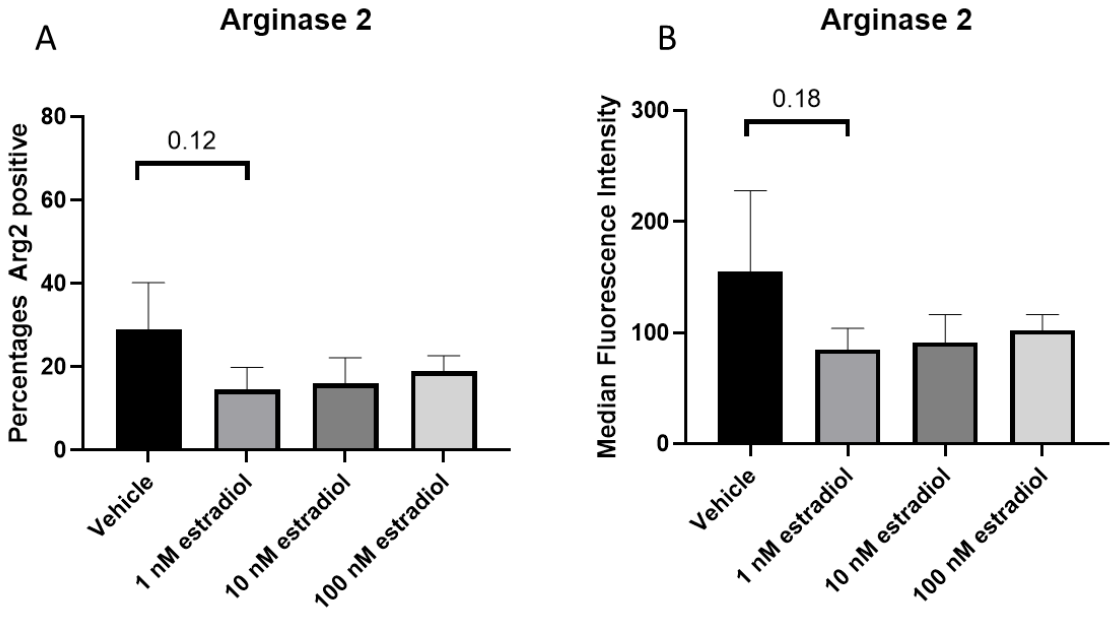

Figure 5.34 Expression of arginase-2 in 72-h E2 or vehicle incubated T47D cells. These figures show the percentages of arginase-2 positive cells (A) and median fluorescence intensity of arginase-2 expression (B). (N=3)

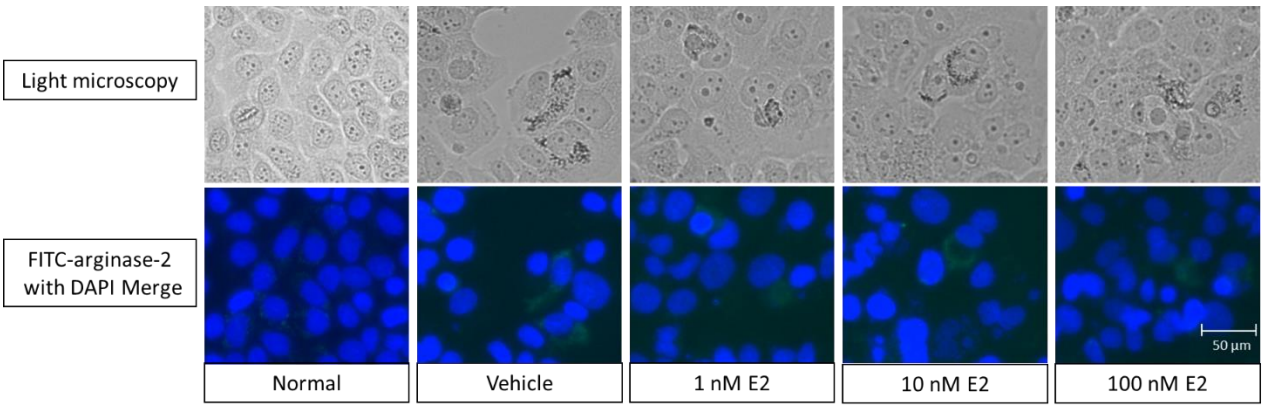

Figure 5.35 Light microscopy of 72-hour E2 incubated T47D cells and immunofluorescence staining of arginase-2(FITC) with DAPI staining.

5.3 Discussion

In this study, we used Jurkat cell senescence models instead of using primary T cells, because Jurkat cells are T cell leukemic cell lines, whose biology is very close to normal T cells (283). However, a previous study showed low expression of estrogen receptor-α in Jurkat cells, leading to attenuate estrogenic effects compared to CD8+ T cells. Therefore the effects of E2 on Jurkat cells might require higher doses compared to high estrogen receptor expressing cells (284). Moreover, the senescence induction of primary T cells is likely to be more complex (285), and so Jurkat cells were used to construct hypotheses for further studies on primary T cells. In addition, we also used T47D cells as a control in this study to demonstrate the effects of E2 on high estrogen receptor-expressing breast cancer cells. Therefore, results in this chapter have determined the effects on both estrogen receptor enriched cells and breast cancer cells, and provided models that may be more amenable to intervention than using primary mammary epithelial cells (HMEC).

In our study, E2 seemed not to increase DNA damage in senescent cells. Both senescent Jurkat cells and T47D cells demonstrated unchanged γH2AX expression in both vehicle-treated cells and E2-supplemented cells, and γH2AX expression in those cells decreased with time. This might be different from the previous studies, in which non-senescent cells were used. Recently, a study showed the importance of topoisomerase II-β that induced transient double-strand breaks in estrogen receptor-α sensitive genes during estrogen-induced replication stress, and the estrogen receptor-α complex formed γH2AX foci and RAD51 to accelerate DNA damage repair (272), supporting the genomic stabilization effects of E2. In our results, etoposide blocked topoisomerase effects in senescent Jurkat cells and senescent T47D cells, and DNA damage markers were not increased in E2 supplemented groups, while the expression of p53 was increased, and the expression

of p21 decreased. These findings determined that E2 might drive DNA damage repair mechanisms that could attenuate senescence phenotypes. To validate the direct effects of E2 on senescent cells, natural senescent cells or other treatment induced senescent cells are helpful in further studies.

The expression of p53 is related to DNA damage response events, but some studies have revealed that p53 is also the estrogen receptor-α targeted gene, which intensified the level of p53 in both p53 mutant cell-lines and p53 wild-type cells after exposure to E2 (273, 286). For instance, a study showed that the p53 level was significantly depleted after the knockdown of the estrogen receptor-α (287). Furthermore, p53 expression was more intensified in stress conditions with E2 supplemented medium compared to an estrogen-free medium (288). In our results, the increase of p53 was more pronounced in 100 nM E2 supplemented T47D cells at 48 hour and such effects were also found in some population of E2 supplemented Jurkat cells at 24 hours for higher dose and at 48 hours for lower does, while p21 was not increased. These finding supported that increased p53 expression was one of estrogen receptor-α targeted gene rather than DNA damage events, and this showed time and dose dependent manner of estrogen receptor-α targeted p53 regulation, but Jurkat cells were estrogen receptor-α deserted cells, therefore, the increase was marginal.

In our results, the reduction of p21 was found in E2 supplemented T47D cells and Jurkat cells, and a significant decrease was found in 100 nM E2 supplemented group. DNA damage seemed to decrease in E2 supplemented senescent cells, but the highly p21 expressing Jurkat cells showed different trends, where p21 expression level was increased. As previously mentioned, several DNA damage repair-related genes were estrogen-responsive elements (270), therefore, estrogen-estrogen receptor-α could drive the DNA repair machinery, and estrogen receptor-α could

restore cell cycle by targeting cyclin D1, p21, and CDK (289, 290). Perhaps, the reduction of p21 might be from DNA repair drive and as a direct target of E2 (273). However, a small proportion of Jurkat cells and T47D cells increased p21 expression, causing cell cycle arrest. This finding might represent irreversible senescent cells.

Estrogens have long been considered as anti-senescent agents, and their clinical usage is for hormonal replacement and chronic medical disease prevention (249). After the menopausal period, deterioration of organ function may be attenuated by E2 (278, 279, 291). In our study, E2 could attenuate senescence phenotypes in senescent Jurkat cells, and senescent T47D. Although the increase in non-senescent proportion of Jurkat cells was low, both CD28 and arginase-2 expression were concordant after 72-hour exposure to 10 nM and 100 nM of E2. These findings suggested that senescence phenotype attenuation was dose- and time-dependent, and these effects might be dependent on the abundance of estrogen receptors. The use of estrogen receptor-α overexpressing Jurkat cells might be helpful in this circumstance. Moreover, senescence attenuation was also demonstrated as decreased arginase-2 expression in both Jurkat cells and T47D cells. The estrogen receptor was found to regulate mitochondrial function, and estrogens also had antioxidant effects (229). In addition, this senescence attenuation might be related to up-regulation of p53. We found chronological changes in p53 expression, which increased in the upper interquartile of p53 expression levels in a dose- and time-dependent manner. In a previous study, E2 could activate p53 expression to enhance autophagy in breast cancer cells and endothelial cells (276), and this activation of p53 inhibited upstream mediators of mTOR and TSC, which decelerated senescence phenotypes (277). Moreover, the significant senescence attenuation in both cell-lines was found in the 100 nM E2 supplemented group,

which was higher than physiologic doses. The use of such a high dose of E2 may only be achieved by ex-vivo treatment of senescent T cells instead of intravenous delivery.

The deprivation of E2 as in menopausal females decreases immune responses (250). E2-exposed Jurkat cells at physiologic doses produced higher levels of IL-2 after activation, while the IL-2 levels decreased at menopausal levels of E2: therefore, post-menopausal levels of E2 deteriorated T cell activation function (263). However, the supplement of E2 to T lymphocytes resulted in complex consequences with both immune activation and immune suppression effects (264, 292). In the activation effects, E2 could intensify the calcium influx and the CD3-zeta protein complex (262, 263), where the increased CD69+ T cells were observed after 24-h of non-T cell receptor specific activation in E2 supplemented T lymphocytes (263). E2 seemed to increase CD69+ expression after anti-CD3 activation, but not after anti-CD3 with anti-CD28 or high-level activation (264). In the suppression effects, supplement of estrogen resulted in decrease cytokine production in human PBMCs such as interferon-γ (293). In our study, the supplement of E2 did not increase CD69+ expression and IL-2 production in senescent Jurkat cells, which was different from previous studies in non-senescent Jurkat cells (264) . The further study in estrogen receptor expressing immune cells is necessary to determine the estrogen receptor dependent effects.

From the results in chapter 4, the proportion of senescent CD8+ T cells was significantly increased in breast cancer patients, and so treatment that targets senescent T cells may restore immune functions. The use of E2 could attenuate senescence phenotypes in senescent Jurkat cells, and these findings supported the concept that E2 may be beneficial for senescent T cells. However, a further study to strengthen support for these effects in primary senescent T cells is needed.

Moreover, the effective dose in this study was much higher than the physiologic doses. Perhaps, the use of E2 in *ex-vivo* T cell expansion is another interesting point in a further study.

In this study, the use of Jurkat cells has limited the implication of the results because of their low expression levels of estrogen receptor. Moreover, the observation of DNA damage was indirect because we measured changes in expression of markers rather than directly measuring DNA damage events. Also, the observation of senescence phenotypes was limited to expression of cell surface and mitochondrial markers, which might be different from other senescent phenotypes including cell cycle checkpoint defectd and chromosomal defects.

5.4 Conclusion

E2 did not increase DNA damage in senescent Jurkat cells. In contrast, E2 seemed to decrease DNA damage in both senescent Jurkat and T47D cells. Moreover, E2 could alleviate senescent phenotypes in senescent Jurkat cells and T47D cells, including CD28 and mitochondrial arginase-2. However, E2 did not improve the activation function of senescent Jurkat cells.

CHAPTER 6 GENERAL DISCUSSION AND CONCLUSION

6.1 General discussion

Epigenetic changes in breast cancer-associated leukocytes are likely to result in immune dysfunction. This could be one mechanism of immune-evasion in breast cancer, and the findings in this thesis demonstrated these changes in *in-vitro* studies to identify a non-cellular contact mechanism. Moreover, this study demonstrated the presence of immune senescence in breast cancer lymphocytes that might be related to the capability of cancer serum to modify immune cell phenotypes. However, the supporting evidence regarding the relation of these two findings from this thesis had some limitations. The epigenetic changes may be due to the release of immune modifying molecules by cancer cells or even suppressive immune cells (187). Moreover, these changes showed the clinical significance to disease progression. In order to evaluate a clinical translation, the specific loci of these changes is needed, but such approaches are challenging. The use of COBRA techniques were not sufficient to fully identify these changes in specific pathways or phenotypes. The use of sequencing techniques or specific gene analysis would be helpful to develop this approach to identify biomarkers. Currently, blood-based signatures are becoming popular in terms of screening, diagnosis, and treatment monitoring, and perhaps specific gene methylation changes will be more useful than global methylation changes.

The cancer-associated immune cell senescence is one feature of dysfunctional T cells in cancer patients, and the presence of these cells in cancer patients is associated with a high burden of disease and impaired immunotherapy efficacies (190). In this study, the senescent T cells was prominent in CD8+ T cells, whose functions are normally for cancer cell elimination, and so perhaps their dysfunction could play a role in cancer prognosis. Moreover, this study implicated replicative

senescence on cancer-associated premature senescence, which resulted in the higher proportion of CD28-CD57- T cells in young age group, and the contraction of those cells in the old age group. These lead to the possibility of treatment that target rejuvenation in the young age-group, where their proliferative and cytotoxic function were able to be restored. This possibility was partially demonstrated in the previous chapter, but further study is required using of primary T cells. Moreover, the increase in these T cells was found in a metastatic setting, where the immune rejuvenation is possibly helpful. In the old-age group, an increase in CD28-CD57+ T cells was found as the combination effects of replicative senescence and cancer-associated phenotypes, which might worsen their dysfunctions. However, a study showed the possibility that these phenotypes may be attenuated (202). Perhaps, treatment targeting T cell senescence might be different regarding the impact of replicative senescence.

The cancer-associated senescent immune cells is one of the T cell entities, for which possible treatment strategies may be proposed. Many anti-ageing treatments have been proposed, and their demands in clinical settings are increased because of the ageing society.

In females, several organ functions are regulated by the cycle of estrogen changes. The withdrawal of estrogen hormone after menopause results in the deterioration of function of several organs. In this thesis, the effects of E2 on senescent cells were examined in Jurkat cells, and E2 could attenuate DNA damage events, and senescence phenotypes in senescent cells. Moreover, the ex-vivo experiments provided an opportunity to test the effects of supra-physiologic doses of E2, and this strategy could be expanded upon by the ex-vivo modification of T cells for cancer treatment.

6.2 Limitation of this study

The demonstration of effects of cancer cells on circulating immune cells is challenging in *in-vitro* studies. Although there were several confounding factors in these *in-vitro* studies, these could demonstrate the early changes of circulating immune cells and might be clinically relevant. To validate this hypothesis, the use of clinical samples and specific site methylation analysis in a further study are required. Our study mainly examined the senescence phenotypes in circulating T lymphocytes, but other immune cells such as B lymphocytes, NK cells and macrophages also contribute to cancer eradiation, and cancer associated senescence might affect to these cells. Moreover, other cellular senescence markers may be used to identify different aspects of the senescent phenotypes. The low proportion of senescent phenotypes in CD4+ T cells reported in this study may underestimate their dysfunction, therefore other additional markers may provide more information regarding senescence phenotypes. In addition, the use of Jurkat cells, which are low estrogen receptor expressing cells, might not directly mimic findings of primary T cells, and so a further study in primary T cells is needed in this aspect.

6.3 Prospects for future research

The determination of T cell senescence in breast cancer provides new line for future research. The effects of cancer-associated senescent cells may impair immune functions of infiltrating T lymphocytes with negative effects on tumor growth and survival. Correlation of the function of circulating immune cells and those of infiltrating immune cells would provide insights into the understanding of cancer-associated senescent immune cells. Moreover, future studies of the effects of E2 on primary senescent T cells and tumor infiltrating T cells could provide new direction for our findings.

6.4 Conclusion

The cancer-associated epigenetic modification of circulating immune cells were determined in *in-vitro* models as a non-contact mechanism, and these may be one of the immune evasion mechanisms in breast cancer. The presence of non-exhausted senescent T cell was found in breast cancer patients, and seemed to have an association with metastasis. The proportion of terminally differentiated T cells were increased in the old-age group as the possible effects of replicative senescence, therefore, the rejuvenation of senescent T cells might be possible in young-age patients. Interestingly, the E2 could attenuate the senescent phenotypes in cellular senescence models. These features potentially ameliorate the senescence phenotypes in cancer-associated immune cells and therapeutic promotion of this reversal in function may have clinical benefits

CHAPTER 7 APPENDIX

7.1 Material lists

0.4% Trypan blue dye (Sigma-Aldrich, USA)

1% formaldehyde (Sigma–Aldrich, USA)

10% charcoal stripped fetal bovine serum (Sigma–Aldrich, USA)

10% sodium dodecyl sulfate (Sigma-Aldrich, USA)

100% Ethanol

10M Ammonium acetate

17β-estradiol (Sigma–Aldrich, USA)

1X PBS (Thermo Scientific, USA)

7-aminoactinomycin D (7-AAd) (Biolegend, USA)

8% Polyacrylamide gel

Alexa fluor® 488 conjugated goat antirabbit antibody (Thermofisher, USA)

Alexa Fluor®647 labeled antihuman CD45 (Biolegend, USA)

Alexa Fluor®700 antihuman CD279(PD-1) (Biolegend, USA)

Allophycocyanin conjugated goat antimouse antibody (Thermofisher, USA)

Allophycocyanin conjugated goat antirabbit antibody (Thermo Scientific, USA)

Allophycocyanin-cyanine7 labeled antihuman CD28 (Biolegend, USA)

Allophycocyanin-cyanine7 labeled antihuman CD45(Biolegend, USA)

BamHI enzyme (NEB, USA)

Brilliant violet 421 labeled antihuman CD4 (Biolegend, USA)

Brilliant violet 650 labelled antihuman CD8 (Biolegend, USA)

Cell lysis buffer II (0.75 M NaCl, 0.024M EDTA at pH 8)

CutSmart® buffer (NEB, USA)

DAPI (Thermo Scientific, MA USA)

DMSO (Sigma-Aldrich, USA)

Dulbecco's Modified Eagle's Medium (DMEM) phenol red free (Invitrogen, USA)

Dulbecco's Modified Eagle's Medium (DMEM)+GlutaMAX™-I (Invitrogen, USA)

Escherichia coli (DH5α) competent cells (Invitrogen, USA)

Etoposide (Cayman Chemical, USA)

EZ DNA methylation-GoldTM kit (Zymo Research, CA USA)

Fetal bovine serum (Gibco, UK)

FITC conjugated rat anti-mouse IgG1 antibody (Thermofisher, USA)

Hanks' balanced salt solution (Gibco, UK)

HindIII enzyme (NEB, USA)

IL-2 ELISA kit (Thermo Scientific, MA, USA)

Ingenio® electroporation solution. (Mirus Bio LLC, USA)

L-glutamine (Thermofisher, USA)

Luria-Bertani (LB) agar

Lymphoprep™ (Stemcell™, UK)

MiuI enzyme (NEB, USA)

Mouse anti FLAG M2 antibody (Sigma-Aldrich, USA)

Mouse antihuman p53 monoclonal antibody clone DO-1 (Sigma–Aldrich, USA)

NE bufferIII (NEB, UK)

One shot® (Invitrogen, USA)

Opti-MEM (Thermofisher, USA)

Penicillin-Streptomycin (10,000 U/mL) (Gibco, UK)

Phenol/chloroform (Thermo Scientific, USA)

Phycoerythrin antihuman CD28 (Thermo Scientific, USA)

Phycoerythrin antihuman CD69 (Thermo Scientific, USA)

Phycoerythrin-cyanin 5.5 labelled antihuman CD3 (Biolegend, USA)

Phycoerythrin-cyanin7 labelled antihuman CD57 (Biolegend, USA)

PowerUp™ SYBR™ Green Master Mix (Invitrogen, USA)

Proteinase K (USB, OH, USA)

Pureyield™ plasmid miniprep (Promega, USA)

Purified antihuman CD28 clone cd28.2 (Thermo Scientific, USA)

Purified antihuman CD3 clone UCHT-1 (Thermo Scientific, USA)

Rabbit antihuman arginase-2 monoclonal antibody (Abcam, USA)

Rabbit antihuman p21 polyclonal antibody (Sigma–Aldrich, USA)

Rabbit monoclonal antihuman phosphorylated γH2AX (Ser139) antibody (Cell signaling, USA)

Recombinant interleukin-2 (Thermo Scientific, USA)

RevertAid H Minus First Strand cDNA Synthesis Kit (Thermo Scientific, USA)

RNeasy Mini Kit (Qiagen, Germany)

Roswell Park Memorial Institute (RPMI) 1640 medium (Sigma-Aldrich, USA)

Senescence associated β-galactosidase (SA-β-gal) kit (Cell Signaling, USA)

SuperScript™ IV First-Strand Synthesis System (Invitrogen, USA)

SYBR green (SYBR® Green JumpStart™ TaqReadyMix™, Sigma-Aldrich, USA)

SYBR™ Safe (Invitrogen, USA)

Taq1 (Thermo Scientific, USA)

TransIT-X2 reagent (Mirus Bio LLC, USA)

Triton X-100 (Sigma-Aldrich, USA)

Tween20 (Sigma-Aldrich, USA)

Zombie Aqua (Biolegend, USA)

Zymopure™II plasmid maxiprep (Zymo, USA)

7.2 Publication

CANCER DIAGNOSIS & PROGNOSIS
2: 731-738 (2022) doi: 10.21873/cdp.10168

Breast Cancer Sera Changes in Alu Element Methylation Predict Metastatic Disease Progression

SIKRIT DENARIYAKOON[1], CHAROENCHAI PUTTIPANYALEARS[2], KRIS CHATAMRA[1] and APIWAT MUTIRANGURA[2]

[1]*Queen Sirikit Centre for Breast Cancer, The Thai Red Cross Society, Bangkok, Thailand;*
[2]*Center of Excellence in Molecular Genetics of Cancer and Human Diseases, Department of Anatomy, Faculty of Medicine, Chulalongkorn University, Bangkok, Thailand*

Abstract. *Background/Aim: During metastatic disease development, the cancer-immune system crosstalk induces epigenetic modifications to immune cells, impairing their functions. Recently, Alu elements methylation changes were widely studied in terms of early cancer detection. This study aimed to demonstrate in vitro Alu element methylation changes in peripheral immune cells in a metastatic setting and examine their prognostic values in metastatic breast cancer. Materials and Methods: Sera from sixteen metastatic cancer patients and sixteen healthy participants were obtained and used to culture normal peripheral immune cells. After 48 h of incubation, the percentage and pattern of Alu element methylation were examined for clinical relevance. Results: We found that the Alu element hypomethylation was affected by age in the cancer group. Intriguingly, a decrease in Alu element methylation was found in patients with early progressive disease. Moreover, an increase in unmethylated cytosine (mCuC) loci was related to the poorer prognosis group. Accordingly, the decrease in Alu element methylation and the increase in mCuC loci pattern in peripheral immune cells correlated with poorer prognosis and early progression in metastatic breast cancer. Conclusion: Alu element hypomethylation in immune cells and their increased mCuC foci were related to the early progression of breast cancer. These warrant the use of Alu element methylation changes for diagnostic and therapeutic purposes in breast cancer.*

Correspondence to: Apiwat Mutirangura, Center of Excellence in Molecular Genetics of Cancer and Human Diseases, Department of Anatomy, Faculty of Medicine, Chulalongkorn University, Bangkok 10330, Thailand. Tel: +66 22564683, e-mail: apiwatmutirangura@gmail.com

Key Words: Alu elements methylation, breast cancer, metastasis, cancer serum.

Breast cancer is the most globally prevalent cancer and the leading cause of death in females (1). Although multimodality treatment has been proven to improve oncologic outcomes, 10%-20% of curative breast cancer patients still develop metastatic diseases (2). To date, the understanding of cancer biology provides specific treatments and precise prognoses (3, 4). However, metastatic recurrences are not prevented. Currently, immune cell surveillance is found to be necessary to control the occurrence of transformed cells, and these durable immune responses could prevent metastatic events (5).

The infiltrating immune cells and circulating immune cells are widely examined in breast cancer research (6, 7). Although the self-immune responses are the self-protective systems which recognize and eradicate cancer development, the cancer-associated epigenetic alteration of immune cells eventually causes host immune dysfunction, which promotes cancer cell survival (8, 9). This plasticity of immune cells results from global methylation changes in breast cancer-associated immune cells (10).

The blood DNA methylation level has been studied as a non-invasive biomarker because blood DNA methylation is affected by cancer-immune cell interactions. Therefore, blood DNA methylation can early detect carcinogenesis (11). Many researchers use the methylation level of transposons as global methylation surrogates. Because the intersperse elements approximate 45% of human genomes, the Alu element methylation is generally demonstrated as the global methylation status (12). Since the CpG sites of Alu elements are usually methylated in normal cells, the hypomethylation

CHAPTER 8 REFERENCES

1. DeSantis CE, Bray F, Ferlay J, Lortet-Tieulent J, Anderson BO, Jemal A. International Variation in Female Breast Cancer Incidence and Mortality Rates. Cancer Epidemiol Biomarkers Prev. 2015;24(10):1495-506.

2. Fisher B, Anderson S, Redmond CK, Wolmark N, Wickerham DL, Cronin WM. Reanalysis and results after 12 years of follow-up in a randomized clinical trial comparing total mastectomy with lumpectomy with or without irradiation in the treatment of breast cancer. N Engl J Med. 1995;333(22):1456-61.

3. Harris JR, Lippman ME, Morrow M, Osborne CK. Diseases of the breast. Fifth edition. ed. Philadelphia: Wolters kluwer Health; 2014. xxii, 1196 pages p.

4. Perou CM, Sorlie T, Eisen MB, van de Rijn M, Jeffrey SS, Rees CA, et al. Molecular portraits of human breast tumours. Nature. 2000;406(6797):747-52.

5. Masuda N, Lee SJ, Ohtani S, Im YH, Lee ES, Yokota I, et al. Adjuvant Capecitabine for Breast Cancer after Preoperative Chemotherapy. N Engl J Med. 2017;376(22):2147-59.

6. Mamounas EP, Untch M, Mano MS, Huang CS, Geyer CE, Jr., von Minckwitz G, et al. Adjuvant T-DM1 versus trastuzumab in patients with residual invasive disease after neoadjuvant therapy for HER2-positive breast cancer: subgroup analyses from KATHERINE. Ann Oncol. 2021;32(8):1005-14.

7. Xu Q, Chen S, Hu Y, Huang W. Landscape of Immune Microenvironment Under Immune Cell Infiltration Pattern in Breast Cancer. Front Immunol. 2021;12:711433.

8. Burstein MD, Tsimelzon A, Poage GM, Covington KR, Contreras A, Fuqua SA, et al. Comprehensive genomic analysis identifies novel subtypes and targets of triple-negative breast cancer. Clin Cancer Res. 2015;21(7):1688-98.

9. Lehmann BD, Jovanovic B, Chen X, Estrada MV, Johnson KN, Shyr Y, et al. Refinement of Triple-Negative Breast Cancer Molecular Subtypes: Implications for Neoadjuvant Chemotherapy Selection. PLoS One. 2016;11(6):e0157368.

10. Seo AN, Lee HJ, Kim EJ, Kim HJ, Jang MH, Lee HE, et al. Tumour-infiltrating CD8+ lymphocytes as an independent predictive factor for pathological complete response to primary systemic therapy in breast cancer. Br J Cancer. 2013;109(10):2705-13.

11. Van Berckelaer C, Rypens C, van Dam P, Pouillon L, Parizel M, Schats KA, et al. Infiltrating stromal immune cells in inflammatory breast cancer are associated with an improved outcome and increased PD-L1 expression. Breast Cancer Res. 2019;21(1):28.

12. Kurozumi S, Inoue K, Matsumoto H, Fujii T, Horiguchi J, Oyama T, et al. Prognostic utility of tumor-infiltrating lymphocytes in residual tumor after neoadjuvant chemotherapy with trastuzumab for HER2-positive breast cancer. Sci Rep. 2019;9(1):1583.

13. El Bairi K, Haynes HR, Blackley E, Fineberg S, Shear J, Turner S, et al. The tale of TILs in breast cancer: A report from The International Immuno-Oncology Biomarker Working Group. NPJ Breast Cancer. 2021;7(1):150.

14. Kresovich JK, O'Brien KM, Xu Z, Weinberg CR, Sandler DP, Taylor JA. Prediagnostic Immune Cell Profiles and Breast Cancer. JAMA Netw Open. 2020;3(1):e1919536.

15. Allen BM, Hiam KJ, Burnett CE, Venida A, DeBarge R, Tenvooren I, et al. Systemic dysfunction and plasticity of the immune macroenvironment in cancer models. Nat Med. 2020;26(7):1125-34.

16. Takeshita T, Torigoe T, Yan L, Huang JL, Yamashita H, Takabe K. The Impact of Immunofunctional Phenotyping on the Malfunction of the Cancer Immunity Cycle in Breast Cancer. Cancers (Basel). 2020;13(1).

17. Schmidl C, Delacher M, Huehn J, Feuerer M. Epigenetic mechanisms regulating T-cell responses. J Allergy Clin Immunol. 2018;142(3):728-43.

18. van Veldhoven K, Polidoro S, Baglietto L, Severi G, Sacerdote C, Panico S, et al. Epigenome-wide association study reveals decreased average methylation levels years before breast cancer diagnosis. Clin Epigenetics. 2015;7:67.

19. Tang Q, Cheng J, Cao X, Surowy H, Burwinkel B. Blood-based DNA methylation as biomarker for breast cancer: a systematic review. Clin Epigenetics. 2016;8:115.

20. Thommen DS, Schumacher TN. T Cell Dysfunction in Cancer. Cancer Cell. 2018;33(4):547-62.

21. Chen DS, Mellman I. Oncology meets immunology: the cancer-immunity cycle. Immunity. 2013;39(1):1-10.

22. Murphy TL, Murphy KM. Dendritic cells in cancer immunology. Cell Mol Immunol. 2022;19(1):3-13.

23. Bates JP, Derakhshandeh R, Jones L, Webb TJ. Mechanisms of immune evasion in breast cancer. BMC Cancer. 2018;18(1):556.

24. Gil Del Alcazar CR, Aleckovic M, Polyak K. Immune Escape during Breast Tumor Progression. Cancer Immunol Res. 2020;8(4):422-7.

25. Wculek SK, Cueto FJ, Mujal AM, Melero I, Krummel MF, Sancho D. Dendritic cells in cancer immunology and immunotherapy. Nat Rev Immunol. 2020;20(1):7-24.

26. Finn OJ. Cancer immunology. N Engl J Med. 2008;358(25):2704-15.

27. Liao D, Luo Y, Markowitz D, Xiang R, Reisfeld RA. Cancer associated fibroblasts promote tumor growth and metastasis by modulating the tumor immune microenvironment in a 4T1 murine breast cancer model. PLoS One. 2009;4(11):e7965.

28. Garner H, de Visser KE. Immune crosstalk in cancer progression and metastatic spread: a complex conversation. Nat Rev Immunol. 2020.

29. Garcia-Gomez A, Rodriguez-Ubreva J, Ballestar E. Epigenetic interplay between immune, stromal and cancer cells in the tumor microenvironment. Clin Immunol. 2018;196:64-71.

30. Klymenko Y, Nephew KP. Epigenetic Crosstalk between the Tumor Microenvironment and Ovarian Cancer Cells: A Therapeutic Road Less Traveled. Cancers (Basel). 2018;10(9).

31. Maekita T, Nakazawa K, Mihara M, Nakajima T, Yanaoka K, Iguchi M, et al. High levels of aberrant DNA methylation in Helicobacter pylori-infected gastric mucosae and its possible association with gastric cancer risk. Clin Cancer Res. 2006;12(3 Pt 1):989-95.

32. Li CJ, Liao WT, Wu MY, Chu PY. New Insights into the Role of Autophagy in Tumor Immune Microenvironment. Int J Mol Sci. 2017;18(7).

33. Xu Z, Sandler DP, Taylor JA. Blood DNA Methylation and Breast Cancer: A Prospective Case-Cohort Analysis in the Sister Study. J Natl Cancer Inst. 2020;112(1):87-94.

34. Mutirangura A. Is global hypomethylation a nidus for molecular pathogenesis of age-related noncommunicable diseases? Epigenomics. 2019;11(6):577-9.

35. Lopez-Otin C, Blasco MA, Partridge L, Serrano M, Kroemer G. The hallmarks of aging. Cell. 2013;153(6):1194-217.

36. Lee JW, Ong EBB. Genomic Instability and Cellular Senescence: Lessons From the Budding Yeast. Front Cell Dev Biol. 2020;8:619126.

37. Tubbs A, Nussenzweig A. Endogenous DNA Damage as a Source of Genomic Instability in Cancer. Cell. 2017;168(4):644-56.

38. Jintaridth P, Mutirangura A. Distinctive patterns of age-dependent hypomethylation in interspersed repetitive sequences. Physiol Genomics. 2010;41(2):194-200.

39. Ramos RB, Fabris V, Lecke SB, Maturana MA, Spritzer PM. Association between global leukocyte DNA methylation and cardiovascular risk in postmenopausal women. BMC Med Genet. 2016;17(1):71.

40. Thongsroy J, Patchsung M, Mutirangura A. The association between Alu hypomethylation and severity of type 2 diabetes mellitus. Clin Epigenetics. 2017;9:93.

41. Patchsung M, Settayanon S, Pongpanich M, Mutirangura D, Jintarith P, Mutirangura A. Alu siRNA to increase Alu element methylation and prevent DNA damage. Epigenomics. 2018;10(2):175-85.

42. Liu X, Hartman CL, Li L, Albert CJ, Si F, Gao A, et al. Reprogramming lipid metabolism prevents effector T cell senescence and enhances tumor immunotherapy. Sci Transl Med. 2021;13(587).

43. Gruber IV, El Yousfi S, Durr-Storzer S, Wallwiener D, Solomayer EF, Fehm T. Down-regulation of CD28, TCR-zeta (zeta) and up-regulation of FAS in peripheral cytotoxic T-cells of primary breast cancer patients. Anticancer Res. 2008;28(2A):779-84.

44. Fessler J, Fasching P, Raicht A, Hammerl S, Weber J, Lackner A, et al. Lymphopenia in primary Sjogren's syndrome is associated with premature aging of naive CD4+ T cells. Rheumatology (Oxford). 2021;60(2):588-97.

45. Tsukishiro T, Donnenberg AD, Whiteside TL. Rapid turnover of the CD8(+)CD28(-) T-cell subset of effector cells in the circulation of patients with head and neck cancer. Cancer Immunol Immunother. 2003;52(10):599-607.

46. Crespo J, Sun H, Welling TH, Tian Z, Zou W. T cell anergy, exhaustion, senescence, and stemness in the tumor microenvironment. Curr Opin Immunol. 2013;25(2):214-21.

47. Barzilai N, Crandall JP, Kritchevsky SB, Espeland MA. Metformin as a Tool to Target Aging. Cell Metab. 2016;23(6):1060-5.

48. Weichhart T. mTOR as Regulator of Lifespan, Aging, and Cellular Senescence: A Mini-Review. Gerontology. 2018;64(2):127-34.

49. Campisi J, Kapahi P, Lithgow GJ, Melov S, Newman JC, Verdin E. From discoveries in ageing research to therapeutics for healthy ageing. Nature. 2019;571(7764):183-92.

50. Gonzalez-Freire M, Diaz-Ruiz A, Hauser D, Martinez-Romero J, Ferrucci L, Bernier M, et al. The road ahead for health and lifespan interventions. Ageing Res Rev. 2020;59:101037.

51. Schneider U, Schwenk HU, Bornkamm G. Characterization of EBV-genome negative "null" and "T" cell lines derived from children with acute lymphoblastic leukemia and leukemic transformed non-Hodgkin lymphoma. Int J Cancer. 1977;19(5):621-6.

52. Yu S, Kim T, Yoo KH, Kang K. The T47D cell line is an ideal experimental model to elucidate the progesterone-specific effects of a luminal A subtype of breast cancer. Biochem Biophys Res Commun. 2017;486(3):752-8.

53. Woolf DK, Padhani AR, Makris A. Assessing response to treatment of bone metastases from breast cancer: what should be the standard of care? Ann Oncol. 2015;26(6):1048-57.

54. Gennari A, Andre F, Barrios CH, Cortes J, de Azambuja E, DeMichele A, et al. ESMO Clinical Practice Guideline for the diagnosis, staging and treatment of patients with metastatic breast cancer. Ann Oncol. 2021;32(12):1475-95.

55. Skvortsova K, Iovino N, Bogdanovic O. Functions and mechanisms of epigenetic inheritance in animals. Nat Rev Mol Cell Biol. 2018;19(12):774-90.

56. Moore LD, Le T, Fan G. DNA methylation and its basic function. Neuropsychopharmacology. 2013;38(1):23-38.

57. Hermann A, Goyal R, Jeltsch A. The Dnmt1 DNA-(cytosine-C5)-methyltransferase methylates DNA processively with high preference for hemimethylated target sites. J Biol Chem. 2004;279(46):48350-9.

58. Lyko F. The DNA methyltransferase family: a versatile toolkit for epigenetic regulation. Nat Rev Genet. 2018;19(2):81-92.

59. Rhee I, Jair KW, Yen RW, Lengauer C, Herman JG, Kinzler KW, et al. CpG methylation is maintained in human cancer cells lacking DNMT1. Nature. 2000;404(6781):1003-7.

60. Bird A. DNA methylation de novo. Science. 1999;286(5448):2287-8.

61. Ghoneim HE, Fan Y, Moustaki A, Abdelsamed HA, Dash P, Dogra P, et al. De Novo Epigenetic Programs Inhibit PD-1 Blockade-Mediated T Cell Rejuvenation. Cell. 2017;170(1):142-57 e19.

62. Allis CD, Jenuwein T. The molecular hallmarks of epigenetic control. Nat Rev Genet. 2016;17(8):487-500.

63. Elbarbary RA, Lucas BA, Maquat LE. Retrotransposons as regulators of gene expression. Science. 2016;351(6274):aac7247.

64. Kitkumthorn N, Mutirangura A. Long interspersed nuclear element-1 hypomethylation in cancer: biology and clinical applications. Clin Epigenetics. 2011;2(2):315-30.

65. Deininger P. Alu elements: know the SINEs. Genome Biol. 2011;12(12):236.

66. Yang AS, Estecio MR, Doshi K, Kondo Y, Tajara EH, Issa JP. A simple method for estimating global DNA methylation using bisulfite PCR of repetitive DNA elements. Nucleic Acids Res. 2004;32(3):e38.

67. Cho YH, Yazici H, Wu HC, Terry MB, Gonzalez K, Qu M, et al. Aberrant promoter hypermethylation and genomic hypomethylation in tumor, adjacent normal tissues and blood from breast cancer patients. Anticancer Res. 2010;30(7):2489-96.

68. Bodelon C, Ambatipudi S, Dugue PA, Johansson A, Sampson JN, Hicks B, et al. Blood DNA methylation and breast cancer risk: a meta-analysis of four prospective cohort studies. Breast Cancer Res. 2019;21(1):62.

69. Hou L, Wang H, Sartori S, Gawron A, Lissowska J, Bollati V, et al. Blood leukocyte DNA hypomethylation and gastric cancer risk in a high-risk Polish population. Int J Cancer. 2010;127(8):1866-74.

70. Woo HD, Kim J. Global DNA hypomethylation in peripheral blood leukocytes as a biomarker for cancer risk: a meta-analysis. PLoS One. 2012;7(4):e34615.

71. Ye D, Jiang D, Zhang X, Mao Y. Alu Methylation and Risk of Cancer: A Meta-analysis. Am J Med Sci. 2020;359(5):271-80.

72. Choi JY, James SR, Link PA, McCann SE, Hong CC, Davis W, et al. Association between global DNA hypomethylation in leukocytes and risk of breast cancer. Carcinogenesis. 2009;30(11):1889-97.

73. Wu HC, Delgado-Cruzata L, Flom JD, Perrin M, Liao Y, Ferris JS, et al. Repetitive element DNA methylation levels in white blood cell DNA from sisters discordant for breast cancer from the New York site of the Breast Cancer Family Registry. Carcinogenesis. 2012;33(10):1946-52.

74. Joyce BT, Gao T, Zheng Y, Liu L, Zhang W, Dai Q, et al. Prospective changes in global DNA methylation and cancer incidence and mortality. Br J Cancer. 2016;115(4):465-72.

75. Parashar S, Cheishvili D, Mahmood N, Arakelian A, Tanvir I, Khan HA, et al. DNA methylation signatures of breast cancer in peripheral T-cells. BMC Cancer. 2018;18(1):574.

76. Xu X, Gammon MD, Hernandez-Vargas H, Herceg Z, Wetmur JG, Teitelbaum SL, et al. DNA methylation in peripheral blood measured by LUMA is associated with breast cancer in a population-based study. FASEB J. 2012;26(6):2657-66.

77. Severi G, Southey MC, English DR, Jung CH, Lonie A, McLean C, et al. Epigenome-wide methylation in DNA from peripheral blood as a marker of risk for breast cancer. Breast Cancer Res Treat. 2014;148(3):665-73.

78. van Veldhoven K, Polidoro S, Baglietto L, Severi G, Sacerdote C, Panico S, et al. Epigenome-wide association study reveals decreased average methylation levels years before breast cancer diagnosis. Clin Epigenetics. 2015;7(1):67.

79. Manoochehri M, Hielscher T, Borhani N, Gerhauser C, Fletcher O, Swerdlow AJ, et al. Epigenetic quantification of circulating immune cells in peripheral blood of triple-negative breast cancer patients. Clin Epigenetics. 2021;13(1):207.

80. Boonsongserm P, Angsuwatcharakon P, Puttipanyalears C, Aporntewan C, Kongruttanachok N, Aksornkitti V, et al. Tumor-induced DNA methylation in the white blood cells of patients with colorectal cancer. Oncol Lett. 2019;18(3):3039-48.

81. Puttipanyalears C, Kitkumthorn N, Buranapraditkun S, Keelawat S, Mutirangura A. Breast cancer upregulating genes in stromal cells by LINE-1 hypermethylation and micrometastatic detection. Epigenomics. 2016;8(4):475-86.

82. Kitkumthorn N, Tuangsintanakul T, Rattanatanyong P, Tiwawech D, Mutirangura A. LINE-1 methylation in the peripheral blood mononuclear cells of cancer patients. Clin Chim Acta. 2012;413(9-10):869-74.

83. Kuchiba A, Iwasaki M, Ono H, Kasuga Y, Yokoyama S, Onuma H, et al. Global methylation levels in peripheral blood leukocyte DNA by LUMA and breast cancer: a case-control study in Japanese women. Br J Cancer. 2014;110(11):2765-71.

84. Brennan K, Garcia-Closas M, Orr N, Fletcher O, Jones M, Ashworth A, et al. Intragenic ATM methylation in peripheral blood DNA as a biomarker of breast cancer risk. Cancer Res. 2012;72(9):2304-13.

85. Delgado-Cruzata L, Wu HC, Perrin M, Liao Y, Kappil MA, Ferris JS, et al. Global DNA methylation levels in white blood cell DNA from sisters discordant for breast cancer from the New York site of the Breast Cancer Family Registry. Epigenetics. 2012;7(8):868-74.

86. Deroo LA, Bolick SC, Xu Z, Umbach DM, Shore D, Weinberg CR, et al. Global DNA methylation and one-carbon metabolism gene polymorphisms and the risk of breast cancer in the Sister Study. Carcinogenesis. 2014;35(2):333-8.

87. Omilusik KD, Goldrath AW. The origins of memory T cells. Nature. 2017;552(7685):337-9.

88. Schreiber RD, Old LJ, Smyth MJ. Cancer immunoediting: integrating immunity's roles in cancer suppression and promotion. Science. 2011;331(6024):1565-70.

89. Gao Y, Baccarelli A, Shu XO, Ji BT, Yu K, Tarantini L, et al. Blood leukocyte Alu and LINE-1 methylation and gastric cancer risk in the Shanghai Women's Health Study. Br J Cancer. 2012;106(3):585-91.

90. Akers SN, Moysich K, Zhang W, Collamat Lai G, Miller A, Lele S, et al. LINE1 and Alu repetitive element DNA methylation in tumors and white blood cells from epithelial ovarian cancer patients. Gynecol Oncol. 2014;132(2):462-7.

91. Batlle E, Massague J. Transforming Growth Factor-beta Signaling in Immunity and Cancer. Immunity. 2019;50(4):924-40.

92. Lee C, Zhang Q, Zi X, Dash A, Soares MB, Rahmatpanah F, et al. TGF-beta mediated DNA methylation in prostate cancer. Transl Androl Urol. 2012;1(2):78-88.

93. Luo X, Zhang Q, Liu V, Xia Z, Pothoven KL, Lee C. Cutting edge: TGF-beta-induced expression of Foxp3 in T cells is mediated through inactivation of ERK. J Immunol. 2008;180(5):2757-61.

94. Gasche JA, Hoffmann J, Boland CR, Goel A. Interleukin-6 promotes tumorigenesis by altering DNA methylation in oral cancer cells. Int J Cancer. 2011;129(5):1053-63.

95. Kitkumthorn N, Keelawat S, Rattanatanyong P, Mutirangura A. LINE-1 and Alu methylation patterns in lymph node metastases of head and neck cancers. Asian Pac J Cancer Prev. 2012;13(9):4469-75.

96. Pobsook T, Subbalekha K, Sannikorn P, Mutirangura A. Improved measurement of LINE-1 sequence methylation for cancer detection. Clin Chim Acta. 2011;412(3-4):314-21.

97. Meevassana J, Serirodom S, Prabsattru P, Boonsongserm P, Kamolratanakul S, Siritientong T, et al. Alu repetitive sequence CpG methylation changes in burn scars. Burns. 2021.

98. Westrich JA, Warren CJ, Pyeon D. Evasion of host immune defenses by human papillomavirus. Virus Res. 2017;231:21-33.

99. Bauer M, Fink B, Thurmann L, Eszlinger M, Herberth G, Lehmann I. Tobacco smoking differently influences cell types of the innate and adaptive immune system-indications from CpG site methylation. Clin Epigenetics. 2015;7:83.

100. Jintaridth P, Tungtrongchitr R, Preutthipan S, Mutirangura A. Hypomethylation of Alu elements in post-menopausal women with osteoporosis. PLoS One. 2013;8(8):e70386.

101. Yuksel S, Kucukazman SO, Karatas GS, Ozturk MA, Prombhul S, Hirankarn N. Methylation Status of Alu and LINE-1 Interspersed Repetitive Sequences in Behcet's Disease Patients. Biomed Res Int. 2016;2016:1393089.

102. Lange NE, Sordillo J, Tarantini L, Bollati V, Sparrow D, Vokonas P, et al. Alu and LINE-1 methylation and lung function in the normative ageing study. BMJ Open. 2012;2(5).

103. Pangrazzi L, Weinberger B. T cells, aging and senescence. Exp Gerontol. 2020;134:110887.

104. Onyema OO, Njemini R, Forti LN, Bautmans I, Aerts JL, De Waele M, et al. Aging-associated subpopulations of human CD8+ T-lymphocytes identified by their CD28 and CD57 phenotypes. Arch Gerontol Geriatr. 2015;61(3):494-502.

105. Gao A, Liu X, Lin W, Wang J, Wang S, Si F, et al. Tumor-derived ILT4 induces T cell senescence and suppresses tumor immunity. J Immunother Cancer. 2021;9(3).

106. Guadagni F, Ferroni P, Carlini S, Mariotti S, Spila A, Aloe S, et al. A re-evaluation of carcinoembryonic antigen (CEA) as a serum marker for breast cancer: a prospective longitudinal study. Clin Cancer Res. 2001;7(8):2357-62.

107. van Dalum G, van der Stam GJ, Tibbe AG, Franken B, Mastboom WJ, Vermes I, et al. Circulating tumor cells before and during follow-up after breast cancer surgery. Int J Oncol. 2015;46(1):407-13.

108. Jones PA, Ohtani H, Chakravarthy A, De Carvalho DD. Epigenetic therapy in immune-oncology. Nat Rev Cancer. 2019;19(3):151-61.

109. Abbas AK, Lichtman AHH, Pillai S. Basic immunology : functions and disorders of the immune system [still image]. London: Elsevier Health Sciences,; 2015.

110. Yang Q, Jeremiah Bell J, Bhandoola A. T-cell lineage determination. Immunol Rev. 2010;238(1):12-22.

111. Klein L, Kyewski B, Allen PM, Hogquist KA. Positive and negative selection of the T cell repertoire: what thymocytes see (and don't see). Nat Rev Immunol. 2014;14(6):377-91.

112. Kumar BV, Connors TJ, Farber DL. Human T Cell Development, Localization, and Function throughout Life. Immunity. 2018;48(2):202-13.

113. Abbas AK, Lichtman AH, Pillai S. Cellular and molecular immunology. Philadelphia: Elsevier,; 2018.

114. Srinivasan J, Lancaster JN, Singarapu N, Hale LP, Ehrlich LIR, Richie ER. Age-Related Changes in Thymic Central Tolerance. Front Immunol. 2021;12:676236.

115. Haines CJ, Giffon TD, Lu LS, Lu X, Tessier-Lavigne M, Ross DT, et al. Human CD4+ T cell recent thymic emigrants are identified by protein tyrosine kinase 7 and have reduced immune function. J Exp Med. 2009;206(2):275-85.

116. Levy A, Rangel-Santos A, Torres LC, Silveira-Abreu G, Agena F, Carneiro-Sampaio M. T cell receptor excision circles as a tool for evaluating thymic function in young children. Braz J Med Biol Res. 2019;52(7):e8292.

117. Lewis DB, Haines C, Ross D. Protein tyrosine kinase 7: a novel surface marker for human recent thymic emigrants with potential clinical utility. J Perinatol. 2011;31 Suppl 1:S72-81.

118. Dutta A, Venkataganesh H, Love PE. New Insights into Epigenetic Regulation of T Cell Differentiation. Cells. 2021;10(12).

119. van den Broek T, Borghans JAM, van Wijk F. The full spectrum of human naive T cells. Nat Rev Immunol. 2018;18(6):363-73.

120. Zhu J, Paul WE. Peripheral CD4+ T-cell differentiation regulated by networks of cytokines and transcription factors. Immunol Rev. 2010;238(1):247-62.

121. Zhu J, Paul WE. CD4 T cells: fates, functions, and faults. Blood. 2008;112(5):1557-69.

122. Germain RN. T-cell development and the CD4-CD8 lineage decision. Nat Rev Immunol. 2002;2(5):309-22.

123. Saule P, Trauet J, Dutriez V, Lekeux V, Dessaint JP, Labalette M. Accumulation of memory T cells from childhood to old age: central and effector memory cells in CD4(+) versus effector memory and terminally differentiated memory cells in CD8(+) compartment. Mech Ageing Dev. 2006;127(3):274-81.

124. Sallusto F, Geginat J, Lanzavecchia A. Central memory and effector memory T cell subsets: function, generation, and maintenance. Annu Rev Immunol. 2004;22:745-63.

125. Graham N, Eisenhauer P, Diehl SA, Pierce KK, Whitehead SS, Durbin AP, et al. Rapid Induction and Maintenance of Virus-Specific CD8(+) TEMRA and CD4(+) TEM Cells Following Protective Vaccination Against Dengue Virus Challenge in Humans. Front Immunol. 2020;11:479.

126. Akondy RS, Monson ND, Miller JD, Edupuganti S, Teuwen D, Wu H, et al. The yellow fever virus vaccine induces a broad and polyfunctional human memory CD8+ T cell response. J Immunol. 2009;183(12):7919-30.

127. Xu W, Larbi A. Markers of T Cell Senescence in Humans. Int J Mol Sci. 2017;18(8).

128. Youngblood B, Hale JS, Kissick HT, Ahn E, Xu X, Wieland A, et al. Effector CD8 T cells dedifferentiate into long-lived memory cells. Nature. 2017;552(7685):404-9.

129. Martin MD, Badovinac VP. Defining Memory CD8 T Cell. Front Immunol. 2018;9:2692.

130. Joshi NS, Kaech SM. Effector CD8 T cell development: a balancing act between memory cell potential and terminal differentiation. J Immunol. 2008;180(3):1309-15.

131. Veiga-Fernandes H, Rocha B. High expression of active CDK6 in the cytoplasm of CD8 memory cells favors rapid division. Nat Immunol. 2004;5(1):31-7.

132. Brinkman CC, Peske JD, Engelhard VH. Peripheral tissue homing receptor control of naive, effector, and memory CD8 T cell localization in lymphoid and non-lymphoid tissues. Front Immunol. 2013;4:241.

133. Saeidi A, Zandi K, Cheok YY, Saeidi H, Wong WF, Lee CYQ, et al. T-Cell Exhaustion in Chronic Infections: Reversing the State of Exhaustion and Reinvigorating Optimal Protective Immune Responses. Front Immunol. 2018;9:2569.

134. McLane LM, Abdel-Hakeem MS, Wherry EJ. CD8 T Cell Exhaustion During Chronic Viral Infection and Cancer. Annu Rev Immunol. 2019;37:457-95.

135. Raskov H, Orhan A, Christensen JP, Gogenur I. Cytotoxic CD8(+) T cells in cancer and cancer immunotherapy. Br J Cancer. 2021;124(2):359-67.

136. Thallinger C, Fureder T, Preusser M, Heller G, Mullauer L, Holler C, et al. Review of cancer treatment with immune checkpoint inhibitors : Current concepts, expectations, limitations and pitfalls. Wien Klin Wochenschr. 2018;130(3-4):85-91.

137. Dolina JS, Van Braeckel-Budimir N, Thomas GD, Salek-Ardakani S. CD8(+) T Cell Exhaustion in Cancer. Front Immunol. 2021;12:715234.

138. Geginat J, Paroni M, Maglie S, Alfen JS, Kastirr I, Gruarin P, et al. Plasticity of human CD4 T cell subsets. Front Immunol. 2014;5:630.

139. Sakaguchi S, Yamaguchi T, Nomura T, Ono M. Regulatory T cells and immune tolerance. Cell. 2008;133(5):775-87.

140. Rocamora-Reverte L, Melzer FL, Wurzner R, Weinberger B. The Complex Role of Regulatory T Cells in Immunity and Aging. Front Immunol. 2020;11:616949.

141. Zheng SG, Wang J, Wang P, Gray JD, Horwitz DA. IL-2 is essential for TGF-beta to convert naive CD4+CD25- cells to CD25+Foxp3+ regulatory T cells and for expansion of these cells. J Immunol. 2007;178(4):2018-27.

142. Booth NJ, McQuaid AJ, Sobande T, Kissane S, Agius E, Jackson SE, et al. Different proliferative potential and migratory characteristics of human CD4+ regulatory T cells that express either CD45RA or CD45RO. J Immunol. 2010;184(8):4317-26.

143. Rosenblum MD, Way SS, Abbas AK. Regulatory T cell memory. Nat Rev Immunol. 2016;16(2):90-101.

144. Sprent J, Cho JH, Boyman O, Surh CD. T cell homeostasis. Immunol Cell Biol. 2008;86(4):312-9.

145. den Braber I, Mugwagwa T, Vrisekoop N, Westera L, Mogling R, de Boer AB, et al. Maintenance of peripheral naive T cells is sustained by thymus output in mice but not humans. Immunity. 2012;36(2):288-97.

146. Freitas AA, Rocha B. Population biology of lymphocytes: the flight for survival. Annu Rev Immunol. 2000;18:83-111.

147. Raeber ME, Zurbuchen Y, Impellizzieri D, Boyman O. The role of cytokines in T-cell memory in health and disease. Immunol Rev. 2018;283(1):176-93.

148. Ge Q, Rao VP, Cho BK, Eisen HN, Chen J. Dependence of lymphopenia-induced T cell proliferation on the abundance of peptide/ MHC epitopes and strength of their interaction with T cell receptors. Proc Natl Acad Sci U S A. 2001;98(4):1728-33.

149. Tuma RA, Pamer EG. Homeostasis of naive, effector and memory CD8 T cells. Curr Opin Immunol. 2002;14(3):348-53.

150. Fessler J, Ficjan A, Duftner C, Dejaco C. The impact of aging on regulatory T-cells. Front Immunol. 2013;4:231.

151. Ogrunc M, d'Adda di Fagagna F. Never-ageing cellular senescence. Eur J Cancer. 2011;47(11):1616-22.

152. Campisi J. Replicative senescence: an old lives' tale? Cell. 1996;84(4):497-500.

153. Chen JH, Hales CN, Ozanne SE. DNA damage, cellular senescence and organismal ageing: causal or correlative? Nucleic Acids Res. 2007;35(22):7417-28.

154. Herranz N, Gil J. Mechanisms and functions of cellular senescence. J Clin Invest. 2018;128(4):1238-46.

155. Akbar AN, Henson SM, Lanna A. Senescence of T Lymphocytes: Implications for Enhancing Human Immunity. Trends Immunol. 2016;37(12):866-76.

156. de Magalhaes JP, Curado J, Church GM. Meta-analysis of age-related gene expression profiles identifies common signatures of aging. Bioinformatics. 2009;25(7):875-81.

157. Dimri GP, Lee X, Basile G, Acosta M, Scott G, Roskelley C, et al. A biomarker that identifies senescent human cells in culture and in aging skin in vivo. Proc Natl Acad Sci U S A. 1995;92(20):9363-7.

158. Lee YI, Choi S, Roh WS, Lee JH, Kim TG. Cellular Senescence and Inflammaging in the Skin Microenvironment. Int J Mol Sci. 2021;22(8).

159. Goronzy JJ, Weyand CM. Mechanisms underlying T cell ageing. Nat Rev Immunol. 2019;19(9):573-83.

160. Goronzy JJ, Fang F, Cavanagh MM, Qi Q, Weyand CM. Naive T cell maintenance and function in human aging. J Immunol. 2015;194(9):4073-80.

161. Le Page A, Dupuis G, Larbi A, Witkowski JM, Fulop T. Signal transduction changes in CD4(+) and CD8(+) T cell subpopulations with aging. Exp Gerontol. 2018;105:128-39.

162. Ovadya Y, Landsberger T, Leins H, Vadai E, Gal H, Biran A, et al. Impaired immune surveillance accelerates accumulation of senescent cells and aging. Nat Commun. 2018;9(1):5435.

163. Lioulios G, Fylaktou A, Papagianni A, Stangou M. T cell markers recount the course of immunosenescence in healthy individuals and chronic kidney disease. Clin Immunol. 2021;225:108685.

164. Strioga M, Pasukoniene V, Characiejus D. CD8+ CD28- and CD8+ CD57+ T cells and their role in health and disease. Immunology. 2011;134(1):17-32.

165. Booiman T, Wit FW, Girigorie AF, Maurer I, De Francesco D, Sabin CA, et al. Terminal differentiation of T cells is strongly associated with CMV infection and increased in HIV-positive individuals on ART and lifestyle matched controls. PLoS One. 2017;12(8):e0183357.

166. Rodriguez IJ, Lalinde Ruiz N, Llano Leon M, Martinez Enriquez L, Montilla Velasquez MDP, Ortiz Aguirre JP, et al. Immunosenescence Study of T Cells: A Systematic Review. Front Immunol. 2020;11:604591.

167. Merino J, Martinez-Gonzalez MA, Rubio M, Inoges S, Sanchez-Ibarrola A, Subira ML. Progressive decrease of CD8high+ CD28+ CD57- cells with ageing. Clin Exp Immunol. 1998;112(1):48-51.

168. Akbar AN, Fletcher JM. Memory T cell homeostasis and senescence during aging. Curr Opin Immunol. 2005;17(5):480-5.

169. Ferrando-Martinez S, Ruiz-Mateos E, Hernandez A, Gutierrez E, Rodriguez-Mendez Mdel M, Ordonez A, et al. Age-related deregulation of naive T cell homeostasis in elderly humans. Age (Dordr). 2011;33(2):197-207.

170. Yang JY, Park MJ, Park S, Lee ES. Increased senescent CD8+ T cells in the peripheral blood mononuclear cells of Behcet's disease patients. Arch Dermatol Res. 2018;310(2):127-38.

171. Weng NP, Akbar AN, Goronzy J. CD28(-) T cells: their role in the age-associated decline of immune function. Trends Immunol. 2009;30(7):306-12.

172. Kim C, Jin J, Weyand CM, Goronzy JJ. The Transcription Factor TCF1 in T Cell Differentiation and Aging. Int J Mol Sci. 2020;21(18).

173. Ron-Harel N, Sharpe AH, Haigis MC. Mitochondrial metabolism in T cell activation and senescence: a mini-review. Gerontology. 2015;61(2):131-8.

174. Zhang L, Romero P. Metabolic Control of CD8(+) T Cell Fate Decisions and Antitumor Immunity. Trends Mol Med. 2018;24(1):30-48.

175. Zhao Y, Shao Q, Peng G. Exhaustion and senescence: two crucial dysfunctional states of T cells in the tumor microenvironment. Cell Mol Immunol. 2020;17(1):27-35.

176. Philip M, Schietinger A. CD8(+) T cell differentiation and dysfunction in cancer. Nat Rev Immunol. 2022;22(4):209-23.

177. Chen L, Ashe S, Brady WA, Hellstrom I, Hellstrom KE, Ledbetter JA, et al. Costimulation of antitumor immunity by the B7 counterreceptor for the T lymphocyte molecules CD28 and CTLA-4. Cell. 1992;71(7):1093-102.

178. Hashimoto M, Kamphorst AO, Im SJ, Kissick HT, Pillai RN, Ramalingam SS, et al. CD8 T Cell Exhaustion in Chronic Infection and Cancer: Opportunities for Interventions. Annu Rev Med. 2018;69:301-18.

179. Roberts A, Bentley L, Tang T, Stewart F, Pallini C, Juvvanapudi J, et al. Ex vivo modelling of PD-1/PD-L1 immune checkpoint blockade under acute, chronic, and exhaustion-like conditions of T-cell stimulation. Sci Rep. 2021;11(1):4030.

180. Zhang J, He T, Xue L, Guo H. Senescent T cells: a potential biomarker and target for cancer therapy. EBioMedicine. 2021;68:103409.

181. Prieto LI, Baker DJ. Cellular Senescence and the Immune System in Cancer. Gerontology. 2019;65(5):505-12.

182. Huff WX, Kwon JH, Henriquez M, Fetcko K, Dey M. The Evolving Role of CD8(+)CD28(-) Immunosenescent T Cells in Cancer Immunology. Int J Mol Sci. 2019;20(11).

183. Montes CL, Chapoval AI, Nelson J, Orhue V, Zhang X, Schulze DH, et al. Tumor-induced senescent T cells with suppressor function: a potential form of tumor immune evasion. Cancer Res. 2008;68(3):870-9.

184. Moreira A, Gross S, Kirchberger MC, Erdmann M, Schuler G, Heinzerling L. Senescence markers: Predictive for response to checkpoint inhibitors. Int J Cancer. 2019;144(5):1147-50.

185. Fessler J, Raicht A, Husic R, Ficjan A, Duftner C, Schwinger W, et al. Premature senescence of T-cell subsets in axial spondyloarthritis. Ann Rheum Dis. 2016;75(4):748-54.

186. Hernandez-Segura A, Nehme J, Demaria M. Hallmarks of Cellular Senescence. Trends Cell Biol. 2018;28(6):436-53.

187. Liu X, Mo W, Ye J, Li L, Zhang Y, Hsueh EC, et al. Regulatory T cells trigger effector T cell DNA damage and senescence caused by metabolic competition. Nat Commun. 2018;9(1):249.

188. Sivakumar S, Abu-Shah E, Ahern DJ, Arbe-Barnes EH, Jainarayanan AK, Mangal N, et al. Activated Regulatory T-Cells, Dysfunctional and Senescent T-Cells Hinder the Immunity in Pancreatic Cancer. Cancers (Basel). 2021;13(8).

189. Ramello MC, Nunez NG, Tosello Boari J, Bossio SN, Canale FP, Abrate C, et al. Polyfunctional KLRG-1(+)CD57(+) Senescent CD4(+) T Cells Infiltrate Tumors and Are Expanded in Peripheral Blood From Breast Cancer Patients. Front Immunol. 2021;12:713132.

190. Song G, Wang X, Jia J, Yuan Y, Wan F, Zhou X, et al. Elevated level of peripheral CD8(+)CD28(-) T lymphocytes are an independent predictor of

progression-free survival in patients with metastatic breast cancer during the course of chemotherapy. Cancer Immunol Immunother. 2013;62(6):1123-30.

191. Goronzy JJ, Weyand CM. Aging, autoimmunity and arthritis: T-cell senescence and contraction of T-cell repertoire diversity - catalysts of autoimmunity and chronic inflammation. Arthritis Res Ther. 2003;5(5):225-34.

192. Onyema OO, Decoster L, Njemini R, Forti LN, Bautmans I, De Waele M, et al. Chemotherapy-induced changes and immunosenescence of CD8+ T-cells in patients with breast cancer. Anticancer Res. 2015;35(3):1481-9.

193. Trintinaglia L, Bandinelli LP, Grassi-Oliveira R, Petersen LE, Anzolin M, Correa BL, et al. Features of Immunosenescence in Women Newly Diagnosed With Breast Cancer. Front Immunol. 2018;9:1651.

194. Poschke I, De Boniface J, Mao Y, Kiessling R. Tumor-induced changes in the phenotype of blood-derived and tumor-associated T cells of early stage breast cancer patients. Int J Cancer. 2012;131(7):1611-20.

195. Biylgi O, Karagoz B, Turken O, Gultepe M, Ozgun A, Tuncel T, et al. CD4+CD25(high), CD8+CD28- cells and thyroid autoantibodies in breast cancer patients. Cent Eur J Immunol. 2014;39(3):338-44.

196. Li Y, Qian T, Zhao H, Zhang Z, Ming Y, Qiao G, et al. Decreased level of peripheral CD8(+)CD28(+) T cells is associated with lymph node metastasis in patients with breast cancer. Future Oncol. 2020;16(32):2611-7.

197. Schmid P, Rugo HS, Adams S, Schneeweiss A, Barrios CH, Iwata H, et al. Atezolizumab plus nab-paclitaxel as first-line treatment for unresectable, locally advanced or metastatic triple-negative breast cancer (IMpassion130): updated efficacy results from a randomised, double-blind, placebo-controlled, phase 3 trial. Lancet Oncol. 2020;21(1):44-59.

198. Ye J, Ma C, Hsueh EC, Eickhoff CS, Zhang Y, Varvares MA, et al. Tumor-derived gammadelta regulatory T cells suppress innate and adaptive immunity through the induction of immunosenescence. J Immunol. 2013;190(5):2403-14.

199. Ferrara R, Naigeon M, Auclin E, Duchemann B, Cassard L, Jouniaux JM, et al. Circulating T-cell Immunosenescence in Patients with Advanced Non-small Cell Lung Cancer Treated with Single-agent PD-1/PD-L1 Inhibitors or Platinum-based Chemotherapy. Clin Cancer Res. 2021;27(2):492-503.

200. Ramello MC, Tosello Boari J, Canale FP, Mena HA, Negrotto S, Gastman B, et al. Tumor-induced senescent T cells promote the secretion of pro-inflammatory cytokines and angiogenic factors by human monocytes/macrophages through a mechanism that involves Tim-3 and CD40L. Cell Death Dis. 2014;5:e1507.

201. Martinez-Zamudio RI, Dewald HK, Vasilopoulos T, Gittens-Williams L, Fitzgerald-Bocarsly P, Herbig U. Senescence-associated beta-galactosidase reveals the abundance of senescent CD8+ T cells in aging humans. Aging Cell. 2021;20(5):e13344.

202. Lee KA, Shin KS, Kim GY, Song YC, Bae EA, Kim IK, et al. Characterization of age-associated exhausted CD8(+) T cells defined by increased expression of Tim-3 and PD-1. Aging Cell. 2016;15(2):291-300.

203. Cortes J, Rugo HS, Cescon DW, Im SA, Yusof MM, Gallardo C, et al. Pembrolizumab plus Chemotherapy in Advanced Triple-Negative Breast Cancer. N Engl J Med. 2022;387(3):217-26.

204. Shirakawa K, Sano M. T Cell Immunosenescence in Aging, Obesity, and Cardiovascular Disease. Cells. 2021;10(9).

205. Mittelbrunn M, Kroemer G. Hallmarks of T cell aging. Nat Immunol. 2021;22(6):687-98.

206. Pangrazzi L, Reidla J, Carmona Arana JA, Naismith E, Miggitsch C, Meryk A, et al. CD28 and CD57 define four populations with distinct phenotypic properties within human CD8(+) T cells. Eur J Immunol. 2020;50(3):363-79.

207. Gregg R, Smith CM, Clark FJ, Dunnion D, Khan N, Chakraverty R, et al. The number of human peripheral blood CD4+ CD25high regulatory T cells increases with age. Clin Exp Immunol. 2005;140(3):540-6.

208. Falci C, Gianesin K, Sergi G, Giunco S, De Ronch I, Valpione S, et al. Immune senescence and cancer in elderly patients: results from an exploratory study. Exp Gerontol. 2013;48(12):1436-42.

209. Pawelec G. Hallmarks of human "immunosenescence": adaptation or dysregulation? Immun Ageing. 2012;9(1):15.

210. Huang B, Liu R, Wang P, Yuan Z, Yang J, Xiong H, et al. CD8(+)CD57(+) T cells exhibit distinct features in human non-small cell lung cancer. J Immunother Cancer. 2020;8(1).

211. Onyema OO, Decoster L, Njemini R, Forti LN, Bautmans I, De Waele M, et al. Shifts in subsets of CD8+ T-cells as evidence of immunosenescence in patients with cancers affecting the lungs: an observational case-control study. BMC Cancer. 2015;15:1016.

212. Lan B, Zhang J, Lu D, Li W. Generation of cancer-specific CD8(+) CD69(+) cells inhibits colon cancer growth. Immunobiology. 2016;221(1):1-5.

213. Kim HD, Jeong S, Park S, Lee YJ, Ju YS, Kim D, et al. Implication of CD69(+) CD103(+) tissue-resident-like CD8(+) T cells as a potential immunotherapeutic target for cholangiocarcinoma. Liver Int. 2021;41(4):764-76.

214. Agarwal A, Mohanti BK, Das SN. Ex vivo triggering of T-cell-mediated immune responses by autologous tumor cell vaccine in oral cancer patients. Immunopharmacol Immunotoxicol. 2007;29(1):95-104.

215. Caras I, Grigorescu A, Stavaru C, Radu DL, Mogos I, Szegli G, et al. Evidence for immune defects in breast and lung cancer patients. Cancer Immunol Immunother. 2004;53(12):1146-52.

216. Lee PP, Yee C, Savage PA, Fong L, Brockstedt D, Weber JS, et al. Characterization of circulating T cells specific for tumor-associated antigens in melanoma patients. Nat Med. 1999;5(6):677-85.

217. Zhang M, Liu ZZ, Aoshima K, Cai WL, Sun H, Xu T, et al. CECR2 drives breast cancer metastasis by promoting NF-kappaB signaling and macrophage-mediated immune suppression. Sci Transl Med. 2022;14(630):eabf5473.

218. Joseph R, Soundararajan R, Vasaikar S, Yang F, Allton KL, Tian L, et al. CD8(+) T cells inhibit metastasis and CXCL4 regulates its function. Br J Cancer. 2021;125(2):176-89.

219. Olkhanud PB, Baatar D, Bodogai M, Hakim F, Gress R, Anderson RL, et al. Breast cancer lung metastasis requires expression of chemokine receptor CCR4 and regulatory T cells. Cancer Res. 2009;69(14):5996-6004.

220. Liu X, Si F, Bagley D, Ma F, Zhang Y, Tao Y, et al. Blockades of effector T cell senescence and exhaustion synergistically enhance antitumor immunity and immunotherapy. J Immunother Cancer. 2022;10(10).

221. DeSantis CE, Ma J, Gaudet MM, Newman LA, Miller KD, Goding Sauer A, et al. Breast cancer statistics, 2019. CA Cancer J Clin. 2019;69(6):438-51.

222. Tran D, Bergholz J, Zhang H, He H, Wang Y, Zhang Y, et al. Insulin-like growth factor-1 regulates the SIRT1-p53 pathway in cellular senescence. Aging Cell. 2014;13(4):669-78.

223. Tatar M, Kopelman A, Epstein D, Tu MP, Yin CM, Garofalo RS. A mutant Drosophila insulin receptor homolog that extends life-span and impairs neuroendocrine function. Science. 2001;292(5514):107-10.

224. Salminen A, Kaarniranta K, Kauppinen A. Insulin/IGF-1 signaling promotes immunosuppression via the STAT3 pathway: impact on the aging process and age-related diseases. Inflamm Res. 2021;70(10-12):1043-61.

225. Wu QJ, Zhang TN, Chen HH, Yu XF, Lv JL, Liu YY, et al. The sirtuin family in health and disease. Signal Transduct Target Ther. 2022;7(1):402.

226. Longo VD, Kennedy BK. Sirtuins in aging and age-related disease. Cell. 2006;126(2):257-68.

227. Vang O, Ahmad N, Baile CA, Baur JA, Brown K, Csiszar A, et al. What is new for an old molecule? Systematic review and recommendations on the use of resveratrol. PLoS One. 2011;6(6):e19881.

228. Lu T, Finkel T. Free radicals and senescence. Exp Cell Res. 2008;314(9):1918-22.

229. Borras C, Gambini J, Lopez-Grueso R, Pallardo FV, Vina J. Direct antioxidant and protective effect of estradiol on isolated mitochondria. Biochim Biophys Acta. 2010;1802(1):205-11.

230. Selvarani R, Mohammed S, Richardson A. Effect of rapamycin on aging and age-related diseases-past and future. Geroscience. 2021;43(3):1135-58.

231. Mannick JB, Del Giudice G, Lattanzi M, Valiante NM, Praestgaard J, Huang B, et al. mTOR inhibition improves immune function in the elderly. Sci Transl Med. 2014;6(268):268ra179.

232. Kraig E, Linehan LA, Liang H, Romo TQ, Liu Q, Wu Y, et al. A randomized control trial to establish the feasibility and safety of rapamycin treatment in an older human cohort: Immunological, physical performance, and cognitive effects. Exp Gerontol. 2018;105:53-69.

233. Lang UE, Heger J, Willbring M, Domula M, Matschke K, Tugtekin SM. Immunosuppression using the mammalian target of rapamycin (mTOR) inhibitor

everolimus: pilot study shows significant cognitive and affective improvement. Transplant Proc. 2009;41(10):4285-8.

234. Semba RD, Ferrucci L, Bartali B, Urpi-Sarda M, Zamora-Ros R, Sun K, et al. Resveratrol levels and all-cause mortality in older community-dwelling adults. JAMA Intern Med. 2014;174(7):1077-84.

235. Wong RH, Thaung Zaw JJ, Xian CJ, Howe PR. Regular Supplementation With Resveratrol Improves Bone Mineral Density in Postmenopausal Women: A Randomized, Placebo-Controlled Trial. J Bone Miner Res. 2020;35(11):2121-31.

236. Thaung Zaw JJ, Howe PR, Wong RH. Long-term effects of resveratrol on cognition, cerebrovascular function and cardio-metabolic markers in postmenopausal women: A 24-month randomised, double-blind, placebo-controlled, crossover study. Clin Nutr. 2021;40(3):820-9.

237. Boscolo P, del Signore A, Sabbioni E, Di Gioacchino M, Di Giampaolo L, Reale M, et al. Effects of resveratrol on lymphocyte proliferation and cytokine release. Ann Clin Lab Sci. 2003;33(2):226-31.

238. Katsyuba E, Romani M, Hofer D, Auwerx J. NAD(+) homeostasis in health and disease. Nat Metab. 2020;2(1):9-31.

239. Zhao Y, Zhang J, Zheng Y, Zhang Y, Zhang XJ, Wang H, et al. NAD(+) improves cognitive function and reduces neuroinflammation by ameliorating mitochondrial damage and decreasing ROS production in chronic cerebral hypoperfusion models through Sirt1/PGC-1alpha pathway. J Neuroinflammation. 2021;18(1):207.

240. Hershberger KA, Martin AS, Hirschey MD. Role of NAD(+) and mitochondrial sirtuins in cardiac and renal diseases. Nat Rev Nephrol. 2017;13(4):213-25.

241. Martens CR, Denman BA, Mazzo MR, Armstrong ML, Reisdorph N, McQueen MB, et al. Chronic nicotinamide riboside supplementation is well-

tolerated and elevates NAD(+) in healthy middle-aged and older adults. Nat Commun. 2018;9(1):1286.

242. Brakedal B, Dolle C, Riemer F, Ma Y, Nido GS, Skeie GO, et al. The NADPARK study: A randomized phase I trial of nicotinamide riboside supplementation in Parkinson's disease. Cell Metab. 2022;34(3):396-407 e6.

243. Omran HM, Almaliki MS. Influence of NAD+ as an ageing-related immunomodulator on COVID 19 infection: A hypothesis. J Infect Public Health. 2020;13(9):1196-201.

244. Qiu Y, Zhou X, Liu Y, Tan S, Li Y. The Role of Sirtuin-1 in Immune Response and Systemic Lupus Erythematosus. Front Immunol. 2021;12:632383.

245. Kulkarni AS, Gubbi S, Barzilai N. Benefits of Metformin in Attenuating the Hallmarks of Aging. Cell Metab. 2020;32(1):15-30.

246. Mohammed I, Hollenberg MD, Ding H, Triggle CR. A Critical Review of the Evidence That Metformin Is a Putative Anti-Aging Drug That Enhances Healthspan and Extends Lifespan. Front Endocrinol (Lausanne). 2021;12:718942.

247. Martin DE, Cadar AN, Panier H, Torrance BL, Kuchel GA, Bartley JM. The effect of metformin on influenza vaccine responses in nondiabetic older adults: a pilot trial. Immun Ageing. 2023;20(1):18.

248. Benko AL, Olsen NJ, Kovacs WJ. Estrogen and telomerase in human peripheral blood mononuclear cells. Mol Cell Endocrinol. 2012;364(1-2):83-8.

249. Samaras N, Papadopoulou MA, Samaras D, Ongaro F. Off-label use of hormones as an antiaging strategy: a review. Clin Interv Aging. 2014;9:1175-86.

250. Gameiro C, Romao F. Changes in the immune system during menopause and aging. Front Biosci (Elite Ed). 2010;2(4):1299-303.

251. Yasar P, Ayaz G, User SD, Gupur G, Muyan M. Molecular mechanism of estrogen-estrogen receptor signaling. Reprod Med Biol. 2017;16(1):4-20.

252. Gruber CJ, Tschugguel W, Schneeberger C, Huber JC. Production and actions of estrogens. N Engl J Med. 2002;346(5):340-52.

253. Patel S, Homaei A, Raju AB, Meher BR. Estrogen: The necessary evil for human health, and ways to tame it. Biomed Pharmacother. 2018;102:403-11.

254. Fuentes N, Silveyra P. Estrogen receptor signaling mechanisms. Adv Protein Chem Struct Biol. 2019;116:135-70.

255. Kovats S. Estrogen receptors regulate innate immune cells and signaling pathways. Cell Immunol. 2015;294(2):63-9.

256. Monteiro C, Kasahara T, Sacramento PM, Dias A, Leite S, Silva VG, et al. Human pregnancy levels of estrogen and progesterone contribute to humoral immunity by activating TFH /B cell axis. Eur J Immunol. 2021;51(1):167-79.

257. Engelmann F, Rivera A, Park B, Messerle-Forbes M, Jensen JT, Messaoudi I. Impact of Estrogen Therapy on Lymphocyte Homeostasis and the Response to Seasonal Influenza Vaccine in Post-Menopausal Women. PLoS One. 2016;11(2):e0149045.

258. Phiel KL, Henderson RA, Adelman SJ, Elloso MM. Differential estrogen receptor gene expression in human peripheral blood mononuclear cell populations. Immunol Lett. 2005;97(1):107-13.

259. Savino W, Mendes-da-Cruz DA, Lepletier A, Dardenne M. Hormonal control of T-cell development in health and disease. Nat Rev Endocrinol. 2016;12(2):77-89.

260. Rosenzweig R, Gupta S, Kumar V, Gumina RJ, Bansal SS. Estrogenic bias in T-Lymphocyte biology: Implications for cardiovascular disease. Pharmacol Res. 2021;170:105606.

261. Walker SE. Estrogen and autoimmune disease. Clin Rev Allergy Immunol. 2011;40(1):60-5.

262. Kim YY, Kim H, Ku SY, Suh CS, Kim SH, Choi YM, et al. Effects of estrogen on intracellular calcium-related T-lymphocyte function. Tissue Eng Regen Med. 2016;13(3):270-3.

263. Ku LT, Gercel-Taylor C, Nakajima ST, Taylor DD. Alterations of T cell activation signalling and cytokine production by postmenopausal estrogen levels. Immun Ageing. 2009;6:1.

264. Papapavlou G, Hellberg S, Raffetseder J, Brynhildsen J, Gustafsson M, Jenmalm MC, et al. Differential effects of estradiol and progesterone on human T cell activation in vitro. Eur J Immunol. 2021;51(10):2430-40.

265. Bagri P, Ghasemi R, McGrath JJC, Thayaparan D, Yu E, Brooks AG, et al. Estradiol Enhances Antiviral CD4(+) Tissue-Resident Memory T Cell Responses following Mucosal Herpes Simplex Virus 2 Vaccination through an IL-17-Mediated Pathway. J Virol. 2020;95(1).

266. Parl FF, Dawling S, Roodi N, Crooke PS. Estrogen metabolism and breast cancer: a risk model. Ann N Y Acad Sci. 2009;1155:68-75.

267. Mobley JA, Brueggemeier RW. Estrogen receptor-mediated regulation of oxidative stress and DNA damage in breast cancer. Carcinogenesis. 2004;25(1):3-9.

268. Rajapakse N, Butterworth M, Kortenkamp A. Detection of DNA strand breaks and oxidized DNA bases at the single-cell level resulting from exposure to estradiol and hydroxylated metabolites. Environ Mol Mutagen. 2005;45(4):397-404.

269. Cavalieri E, Frenkel K, Liehr JG, Rogan E, Roy D. Estrogens as endogenous genotoxic agents--DNA adducts and mutations. J Natl Cancer Inst Monogr. 2000(27):75-93.

270. Pescatori S, Berardinelli F, Albanesi J, Ascenzi P, Marino M, Antoccia A, et al. A Tale of Ice and Fire: The Dual Role for 17beta-Estradiol in Balancing DNA Damage and Genome Integrity. Cancers (Basel). 2021;13(7).

271. Cohly HH, Graham-Evans B, Ndebele K, Jenkins JK, McMurray R, Yan J, et al. Effect of light irradiation and sex hormones on jurkat T cells: 17beta-estradiol but not testosterone enhances UVA-induced cytotoxicity in Jurkat lymphocytes. Int J Environ Res Public Health. 2005;2(1):156-63.

272. Williamson LM, Lees-Miller SP. Estrogen receptor alpha-mediated transcription induces cell cycle-dependent DNA double-strand breaks. Carcinogenesis. 2011;32(3):279-85.

273. Caldon CE. Estrogen signaling and the DNA damage response in hormone dependent breast cancers. Front Oncol. 2014;4:106.

274. Borras C, Ferrando M, Ingles M, Gambini J, Lopez-Grueso R, Edo R, et al. Estrogen Replacement Therapy Induces Antioxidant and Longevity-Related Genes in Women after Medically Induced Menopause. Oxid Med Cell Longev. 2021;2021:8101615.

275. Horstman AM, Dillon EL, Urban RJ, Sheffield-Moore M. The role of androgens and estrogens on healthy aging and longevity. J Gerontol A Biol Sci Med Sci. 2012;67(11):1140-52.

276. Xiang X, Huang J, Song S, Wang Y, Zeng Y, Wu S, et al. 17beta-estradiol inhibits H2O2-induced senescence in HUVEC cells through upregulating SIRT3 expression and promoting autophagy. Biogerontology. 2020;21(5):549-57.

277. Song S, Wu S, Wang Y, Wang Z, Ye C, Song R, et al. 17beta-estradiol inhibits human umbilical vascular endothelial cell senescence by regulating autophagy via p53. Exp Gerontol. 2018;114:57-66.

278. Zhu C, Zhang L, Zheng Y, Xu J, Song J, Rolfe BE, et al. Effects of estrogen on stress-induced premature senescence of vascular smooth muscle cells: a novel mechanism for the "time window theory" of menopausal hormone therapy. Atherosclerosis. 2011;215(2):294-300.

279. Stice JP, Chen L, Kim SC, Jung JS, Tran AL, Liu TT, et al. 17beta-Estradiol, aging, inflammation, and the stress response in the female heart. Endocrinology. 2011;152(4):1589-98.

280. Mann SN, Hadad N, Nelson Holte M, Rothman AR, Sathiaseelan R, Ali Mondal S, et al. Health benefits attributed to 17alpha-estradiol, a lifespan-extending compound, are mediated through estrogen receptor alpha. Elife. 2020;9.

281. King TL, Bryner BS, Underwood KB, Walters MR, Zimmerman SM, Johnson NK, et al. Estradiol-independent restoration of T-cell function in post-reproductive females. Front Endocrinol (Lausanne). 2023;14:1066356.

282. Kumru S, Godekmerdan A, Yilmaz B. Immune effects of surgical menopause and estrogen replacement therapy in peri-menopausal women. J Reprod Immunol. 2004;63(1):31-8.

283. Lin Z, Fillmore GC, Um TH, Elenitoba-Johnson KS, Lim MS. Comparative microarray analysis of gene expression during activation of human peripheral blood T cells and leukemic Jurkat T cells. Lab Invest. 2003;83(6):765-76.

284. Jenkins JK, Suwannaroj S, Elbourne KB, Ndebele K, McMurray RW. 17-beta-estradiol alters Jurkat lymphocyte cell cycling and induces apoptosis through suppression of Bcl-2 and cyclin A. Int Immunopharmacol. 2001;1(11):1897-911.

285. Abbas AA, Akbar AN. Induction of T Cell Senescence by Cytokine Induced Bystander Activation. Front Aging. 2021;2:714239.

286. Saluzzo J, Hallman KM, Aleck K, Dwyer B, Quigley M, Mladenovik V, et al. The regulation of tumor suppressor protein, p53, and estrogen receptor (ERalpha) by resveratrol in breast cancer cells. Genes Cancer. 2016;7(11-12):414-25.

287. Berger CE, Qian Y, Liu G, Chen H, Chen X. p53, a target of estrogen receptor (ER) alpha, modulates DNA damage-induced growth suppression in ER-positive breast cancer cells. J Biol Chem. 2012;287(36):30117-27.

288. Fernandez-Cuesta L, Anaganti S, Hainaut P, Olivier M. Estrogen levels act as a rheostat on p53 levels and modulate p53-dependent responses in breast cancer cell lines. Breast Cancer Res Treat. 2011;125(1):35-42.

289. Jimenez-Salazar JE, Damian-Ferrara R, Arteaga M, Batina N, Damian-Matsumura P. Non-Genomic Actions of Estrogens on the DNA Repair Pathways Are Associated With Chemotherapy Resistance in Breast Cancer. Front Oncol. 2021;11:631007.

290. Foster JS, Henley DC, Ahamed S, Wimalasena J. Estrogens and cell-cycle regulation in breast cancer. Trends Endocrinol Metab. 2001;12(7):320-7.

291. Khan M, Ullah R, Rehman SU, Shah SA, Saeed K, Muhammad T, et al. 17beta-Estradiol Modulates SIRT1 and Halts Oxidative Stress-Mediated Cognitive Impairment in a Male Aging Mouse Model. Cells. 2019;8(8).

292. Dai R, Edwards MR, Heid B, Ahmed SA. 17beta-Estradiol and 17alpha-Ethinyl Estradiol Exhibit Immunologic and Epigenetic Regulatory Effects in NZB/WF1 Female Mice. Endocrinology. 2019;160(1):101-18.

293. Luc JG, Paulin R, Zhao JY, Freed DH, Michelakis ED, Nagendran J. 2-Methoxyestradiol: A Hormonal Metabolite Modulates Stimulated T-Cells Function and proliferation. Transplant Proc. 2015;47(6):2057-66.